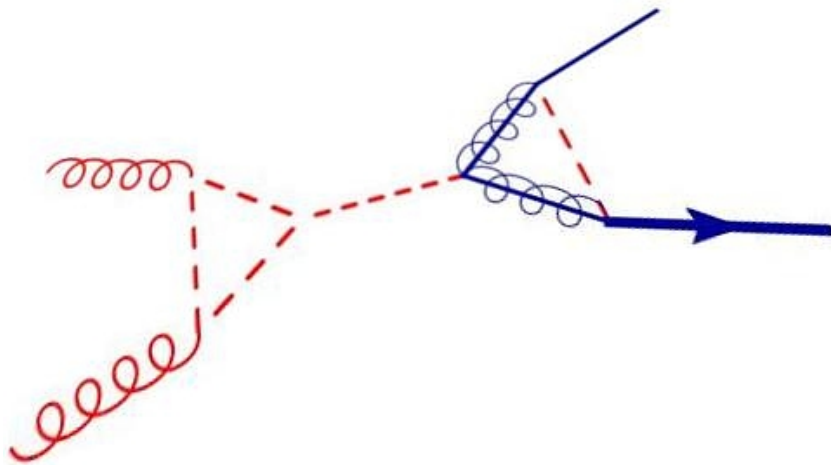


Master Thesis:

Supersymmetric Single Top Production with a $U(1)_R$ Symmetry

Robert Knegjens



Supervisor: Prof. Dr. Eric Laenen
Institute for Theoretical Physics, Utrecht University
Theory Group, Nikhef

November 26, 2009

Master's Thesis in Theoretical Physics

Author: Robert Knegjens

Supervisor: Prof. Dr. Eric Laenen

Institute for Theoretical Physics

Utrecht University



Universiteit Utrecht

The National Institute for Subatomic Physics (Nikhef)



Funded By:

Lord Rutherford Memorial Research Fellowship

Stichting voor Fundamenteel Onderzoek der Materie (FOM)



Abstract

The Standard Model extended with supersymmetry has particle couplings that violate baryon and lepton number conservation. Consequently, these models are vulnerable to predicting unobserved phenomena such as rapid proton decay. To forbid these couplings, a model with a $U(1)$ R-symmetry is assumed, specifically: the Minimal R-symmetric Supersymmetric Standard Model (MRSSM). We derive the particle spectrum and Feynman rules for the QCD sector of the MRSSM, which includes colour octet scalars (sgluons) and Dirac gluinos. Characteristic of the MRSSM is un-suppressed squark flavour mixing, allowing for the production of single top quarks at the one loop level. We consider the phenomenology of supersymmetric single top production at the LHC (14 TeV) using our own Monte Carlo simulation program. The analysis is performed at the parton level with irreducible Standard Model single top signals for the background. Sgluon mediated single top production is ruled out as a signal at the LHC. Production without a mediating sgluon is found to have the necessary signal strength and statistical significance for discovery at five of the six parameter points studied.

Acknowledgments

I would like to thank my supervisor Professor Eric Laenen for his support and guidance throughout the year. His support was not only limited to my thesis, but was also reflected through his interest and efforts in helping me look for PhD positions. Further, I am very grateful for his invitation for me to work within the Nikhef theory group, which proved to be a very stimulating environment. In terms of support and guidance, I would also like to thank Michele Herquet. I'm not sure what form this thesis would have taken if he had not pointed me towards an *exotic* article about continuous R symmetry.

I would like to express my gratitude to the PhD students in the theory group; namely Michelle, Reiner, Lisa, Sander, Gerben and Irene; for both their companionship throughout the year and for taking the time to look over various chapters of my thesis as it neared completion. Likewise, my fellow master's students at Nikhef, Ori and Maciek, deserve acknowledgment for many enlightening physics discussions as well as their good friendship over the last two years.

A special thanks is due to my girlfriend Meri who proofread my entire thesis as well as extended me much moral support and patience throughout the year. Also, although they were handicapped by an eleven hour time difference, I would like to thank my family for support: Brigit, Jan, Marry and Lucas.

Lastly, this master's degree would not have been possible without the financial support of the Lord Rutherford Memorial Research Fellowship granted to me by Canterbury University.

Contents

1	Introduction	1
2	Supersymmetry	3
2.1	The super-Poincaré Lie algebra	5
2.1.1	Spacetime symmetries	5
2.1.2	A graded Lie algebra	6
2.2	Superfields	8
2.2.1	Superfield formalism	8
2.2.2	SUSY transformations	9
2.2.3	Irreducible representations	10
2.3	Building a SUSY Lagrangian	12
2.3.1	D and F terms	12
2.3.2	Gauge theory	13
3	The Minimal Supersymmetric Standard Model	15
3.1	R-parity	16
3.2	Breaking of supersymmetry	17
3.3	Electroweak symmetry breaking	18
3.3.1	Neutralinos and charginos	20
3.3.2	Sfermion mixing	22
4	Strong SUSY Interactions	25
4.1	Feynman rules for supersymmetric $SU(3)_C$	26
4.2	Glino pair production (worked example)	28
4.2.1	Cross section calculation	28
4.2.2	Kinematic distributions	38
4.3	From partons to hadrons	40
4.4	Cascade decays	42
4.5	Technical aside: Majorana Feynman rules	43
4.5.1	Sample calculation	47

5	SUSY with a Continuous R-Symmetry	49
5.1	$U(1)_R$ symmetry	50
5.1.1	Superspace integration and spurions	51
5.2	The MRSSM	53
5.3	Squark flavour mixing	54
5.3.1	Squark masses	56
5.4	Scalar gluons and Dirac gluinos	57
5.5	Feynman Rules for $SU(3)_C \times U(1)_R$	62
5.5.1	Tree-level	63
5.5.2	Effective one-loop	64
5.6	Sgluon decays	73
5.7	Technical aside: scalar one-loop integrals	74
5.7.1	Two point function: $B_0(p; m_1, m_2)$	74
5.7.2	Three point function: $C_0(p_1, p_2; m_1, m_2, m_3)$	77
6	Numerical Methods	85
6.1	Phase space integration	85
6.2	Resonant Particles	87
6.2.1	Review: particle stability	87
6.2.2	Breit-Wigner factorization	90
6.2.3	Narrow width approximation	92
6.3	Multi-dimensional integration	93
6.3.1	The Monte Carlo integration method	94
6.3.2	Improving convergence	95
6.3.3	The VEGAS algorithm	97
6.4	Custom implementation	98
6.4.1	Validity check	100
7	MRSSM Single Top Phenomenology	103
7.1	Single top in the Standard Model	103
7.2	Single top in the MRSSM	105
7.2.1	Setting points in parameter space	105
7.2.2	Sgluon mediated single top	106
7.2.3	Non-sgluon mediated single top	111
7.3	Signals at the LHC	112
7.4	Signal exclusions from the Tevatron run	117
8	Conclusion	121
A	Notation and Conventions	123
B	Two Loop Calculation of α_s	127

Chapter 1

Introduction

In the field of high energy particle physics, theory has been leading experiment for more than half a century. One theory in particular, the Standard Model of particle physics, has withstood all attempts at falsification since its conception, while making numerous successful predictions. Only one of its major predictions remains to be observed: the existence of the Higgs boson, a particle the theory postulates to be responsible for mass. To this end, the high energy physics community have built the most audacious particle accelerator to date, the Large Hadron Collider (LHC) at CERN in Geneva. The LHC will collide protons at speeds close to the speed of light and with an energy of 14 TeV, seven times greater than the record currently set by the Tevatron in Chicago. By creating conditions this violent, the quarks and gluons that comprise the colliding protons should interact with sufficient energy to produce the massive Higgs boson.

Despite all its successes, the Standard Model also has a range of shortcomings. It does not predict the observed oscillations of neutrinos and the implication hereof that neutrinos have mass. The Higgs boson's mass in the Standard Model has quantum corrections that are infinite and as a result unnatural fine-tuning of the theory's parameters is needed to restore predictive power. The Standard Model gives no explanation for dark matter or dark energy that together are postulated to comprise 95% of the energy content of our universe. Finally, the Standard Model does not include gravity, the fourth force of nature. These shortcomings together suggest that the Standard Model is the low energy effective theory of a larger and possibly more natural theory.

A possible extension to the Standard Model that addresses a number of these shortcomings is supersymmetry, the topic of this thesis. Supersymmetry is a postulated new symmetry of spacetime that requires nature to be invariant under the interchange of paired bosonic and fermionic fields. The addition of this symmetry to the Standard model solves the fine-tuning problem by canceling the troublesome infinities in the Higgs boson's mass. Furthermore, specific extensions, such as the Minimal Supersymmetric Standard Model (MSSM), provide particles that could explain dark matter and also unify the coupling strengths of the three Standard Model

forces. For an introduction to supersymmetry as an extension to the Standard Model see Baer[1] or Martin[2].

The Standard Model extended with supersymmetry does come with a potential pitfall; it no longer conserves baryon and lepton number. As a consequence, such models are vulnerable to predicting unobserved phenomena such as rapid proton decay. The MSSM chooses a pragmatic solution by insisting on an additional \mathbb{Z}_2 symmetry, known as R parity, to forbid baryon and lepton number violating couplings. There is, however, an interesting alternative; a theory with one supersymmetric generator¹ naturally admits a continuous $U(1)$ symmetry that forbids baryon and lepton number violating couplings. This continuous symmetry, however, also forbids gaugino and higgsino Majorana masses. Because massless gaugino and higgsino particles have not been observed, many realistic supersymmetric models, including the MSSM, require that this continuous symmetry is broken.

In this thesis we consider a supersymmetric extension to the Standard Model with an unbroken global $U(1)$ R-symmetry, the Minimal R-symmetric Supersymmetric Standard Model (MRSSM) [3]. The gauginos and higgsinos in the MRSSM are constructed to be Dirac rather Majorana spinors and can thus have Dirac masses, which are not forbidden by the continuous R symmetry. We will focus in particular on the QCD sector of the MRSSM. Here a new colour octet scalar particle emerges, known as a scalar gluon or sgluon, which has interesting couplings to gluons and quarks at the one loop level. Due to the Dirac nature of the gluino, squark flavour mixing in the MRSSM is unsuppressed by meson mixing experiments, allowing for quark flavour mixing interactions at the one loop level. An interesting phenomenological test of the MRSSM is therefore supersymmetric single top quark production as this process can only proceed via flavour changing interactions. This is analogous to single top production in the Standard Model, which proceeds via electroweak flavour mixing interactions. An overview of the latter is given by Laenen[4].

The structure of this thesis is as follows. In the next, or second, chapter we introduce supersymmetry, which includes a derivation of the super-Poincaré algebra and an overview of the superfield formalism. Next, we review the MSSM, as all of its field content and many of its features are common to the MRSSM. In the fourth chapter we give the Feynman rules for QCD interactions in the MSSM and give a worked example of an analytic cross section calculation for gluino pair production. In chapter five the particle spectrum and Feynman rules for the QCD sector of the MRSSM are derived. A discussion of squark flavour mixing in the MRSSM and a list of the sgluon's various decay rates are also given. In chapter six we review the numerical methods needed to calculate cross sections and then proceed to present the Monte Carlo program we developed to perform these calculations. The LHC phenomenology of single top production in the MRSSM, taking Standard Model single top production as the background, is examined in the seventh chapter. Conclusions are drawn in chapter eight.

¹N=1 supersymmetry

Chapter 2

Supersymmetry

Supersymmetry (SUSY) is a postulated new symmetry of spacetime that has yet to be verified, or falsified, by experiment. The characteristic property of supersymmetry is that it transforms bosonic states into fermionic states and vice versa. That is, given a supersymmetric generator Q , we have

$$Q|\text{Boson}\rangle = |\text{Fermion}\rangle \quad \text{and} \quad Q|\text{Fermion}\rangle = |\text{Boson}\rangle.$$

Adding this new symmetry to our existing spacetime symmetries involves extending the Poincaré Algebra. This is discussed in detail in the following section. As we shall see, extending the Standard Model of particle physics with supersymmetry has many useful consequences.

The Standard Model suffers from what is known as the fine-tuning problem. Specifically, that the scalar masses of the theory, namely the Higgs boson mass, pick up their largest one-loop corrections to the tree level mass from the top quark loop, which is quadratically divergent. This means that the two biggest contributions to the Higgs boson mass

$$m_H^2 = m_{\text{tree}}^2 - \frac{\lambda_t^2}{8\pi^2} \Lambda_{\text{UV}}^2 + \dots \sim (200 \text{ GeV})^2, \quad (2.1)$$

are the positive tree level mass and a negative term dependent on the ultraviolet cut-off Λ_{UV} squared, where the minus sign is due to the closed fermion loop. This is thus the fine-tuning problem: two very large contributions must be precisely tuned so that their difference gives the much smaller value expected for the Higgs mass. Supersymmetry solves this problem by providing a bosonic superpartner to the top quark, the scalar top, that will have an identical but positive one-loop contribution to the Higgs mass, thereby exactly cancelling the quadratically divergent terms. The two cancelling loops are shown in figure 2.1.

Certain supersymmetric extensions to the Standard Model, particularly the Minimal Supersymmetric Standard Model (MSSM) to be introduced in chapter 3, have the property that the evolution of their gauge coupling constants, with respect to

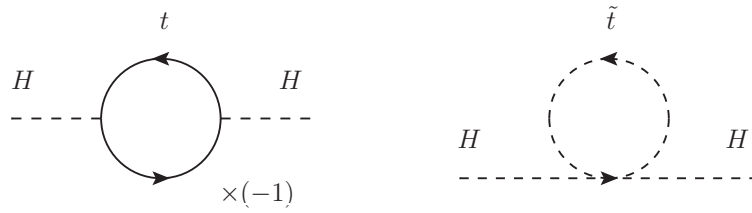


Figure 2.1: One loop contributions to the Higgs mass from the top quark (left) and its superpartner the scalar top quark (right).

the renormalization group equations, unify at some energy scale. For the MSSM this energy scale is 10^{16} GeV, as shown in figure 2.2. This scale is often referred to as the Grand Unified Theory (GUT) scale, as it could be the energy at which a larger GUT internal symmetry group breaks into the Standard Model symmetry group $SU(3)_C \times SU(2)_L \times U(1)_Y$.

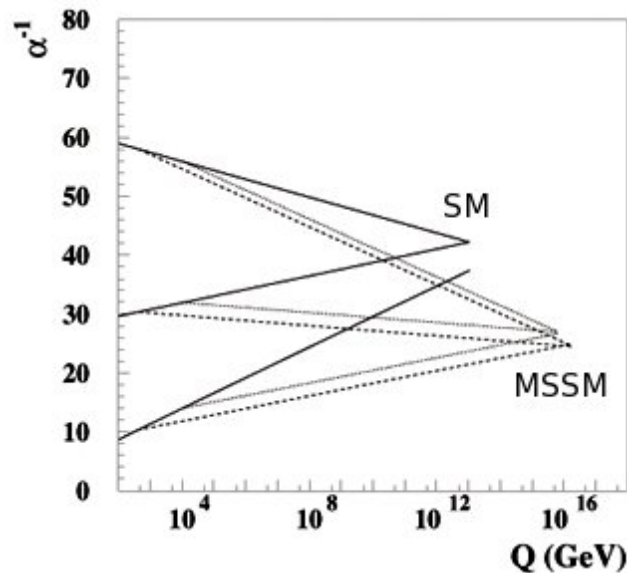


Figure 2.2: Evolution of $SU(3)_C \times SU(2)_L \times U(1)_Y$ gauge couplings for SM (solid) and MSSM (dashed).

In the field of cosmology, supersymmetry provides a number of compelling candidates to explain dark matter. By extending a supersymmetric model (such as the MSSM) with a symmetry that protects it against proton decay (in the case of the MSSM this is R-parity), it is possible for the lightest supersymmetric particle (LSP) to be stable. If the stable particle is also weakly interacting and electrically neutral, it classes as a weakly interacting massive particle (WIMP) that could have the required relic density to explain the perceived abundance of dark matter in the universe today. One such candidate is the neutralino appearing in the MSSM, which

we derive in section 3.3.1.

2.1 The super-Poincaré Lie algebra

2.1.1 Spacetime symmetries

The Poincaré group consists of all spacetime transformations, namely: translations, rotations and boosts. Translations are generated by the energy-momentum operators P_μ , rotations by the angular momentum operators J_i and boosts by the operators K_i . The generators J_i and K_i together give all proper orthochronous Lorentz transformations, thereby forming a subgroup of the Poincaré group, the Lorentz group, and obeying the sub-algebra

$$[J_i, J_j] = i\epsilon_{ijk}J_k, \quad [J_i, K_j] = i\epsilon_{ijk}K_k, \quad [K_i, K_j] = -i\epsilon_{ijk}J_k. \quad (2.2)$$

Often the rotation and boost generators are combined into an antisymmetric second rank tensor $M_{\mu\nu}$, where $M_{ij} = \epsilon_{ijk}J_k$ and $M_{0i} = -M_{i0} = -K_i$. The commutation relations of the Poincaré generators are

$$[P_\mu, P_\nu] = 0, \quad (2.3)$$

$$[M_{\mu\nu}, P_\lambda] = i(\eta_{\nu\lambda}P_\mu - \eta_{\mu\lambda}P_\nu), \quad (2.4)$$

$$[M_{\mu\nu}, M_{\rho\sigma}] = -i(\eta_{\mu\rho}M_{\nu\sigma} - \eta_{\mu\sigma}M_{\nu\rho} - \eta_{\nu\rho}M_{\mu\sigma} + \eta_{\nu\sigma}M_{\mu\rho}), \quad (2.5)$$

forming a *Lie algebra* known as the Poincaré algebra, with each of the generators satisfying the Jacobi identity.

The Lorentz group generators may also be rewritten as $A_i = \frac{1}{2}(J_i + iK_i)$ and $B_i = \frac{1}{2}(J_i - iK_i)$, in which case the algebra decomposes into two sub-algebras

$$[A_i, A_j] = i\epsilon_{ijk}A_k, \quad [B_i, B_j] = i\epsilon_{ijk}B_k, \quad [A_i, B_j] = 0, \quad (2.6)$$

with each isomorphic to the Lie group $SU(2)$. We can therefore find representations of the Lorentz group by taking those of the product group $SU(2) \times SU(2)$. The Casimir operators¹ of this group are A^2 and B^2 , and have as their (angular momentum) eigenvalues $j(j+1)$ and $j'(j'+1)$ respectively. A representation of the Lorentz group can thus be labelled as (j, j') . A Lorentz scalar transforms as the representation $(0, 0)$ and a four-vector as $(\frac{1}{2}, \frac{1}{2})$. The representations $(\frac{1}{2}, 0) \equiv \psi_L$ and $(0, \frac{1}{2}) \equiv \chi_R$ are equivalent to two component *Weyl* spinors, which transform independently under the action of the group $SL(2, \mathbb{C})$ [5]:

$$\psi_L \rightarrow \exp(i\sigma \cdot (\theta - i\phi))\psi_L = M\psi_L, \quad (2.7)$$

$$\chi_R \rightarrow \exp(i\sigma \cdot (\theta + i\phi))\chi_R = N\chi_R, \quad (2.8)$$

¹Operators that commute with every generator

for $M, N \in SL(2, \mathbb{C})$. Here θ and ϕ are the rotation and boost parameters of the operators J and K respectively. The four-component *Dirac* spinor transforms as the direct sum of these two representations $(\frac{1}{2}, 0) \oplus (0, \frac{1}{2})$ and may thus be written as

$$\psi_D = \begin{pmatrix} \psi_L \\ \chi_R \end{pmatrix}. \quad (2.9)$$

Similarly, by noting that the spinor $-i\sigma_2\psi_L^*$ transforms as $(0, \frac{1}{2})$, a four-component *Majorana* spinor satisfying the condition $\psi = \psi^c = C\bar{\psi}^T$ is written as

$$\psi_M = \begin{pmatrix} \psi_L \\ -i\sigma_2\psi_L^* \end{pmatrix}. \quad (2.10)$$

A Weyl spinor may therefore be written as a four-component Majorana spinor and vice versa.

2.1.2 A graded Lie algebra

A no-go theorem by Coleman and Mandula[6] states that the most general Lie algebra for symmetries of an S-matrix² can only have as generators those of the Poincaré group along with a finite number of Lorentz scalar generators belonging to the Lie algebra of a compact Lie group (the generators of the internal symmetry group $SU(3)_c \times SU(2)_L \times U(1)_Y$ for example). In other words, we cannot add additional spacetime symmetries to our Lie algebra in a realistic quantum field theory.

This restriction can, however, be bypassed if we generalize the Lie algebra to a *graded Lie algebra*. A graded Lie algebra consists of commuting *even* generators X and anti-commuting *odd* generators Q , satisfying

$$\{Q, Q'\} = X, \quad [X, X'] = X'', \quad [Q, X] = Q'. \quad (2.11)$$

The even generators X are those of the original Poincaré algebra, namely P_μ and $M_{\mu\nu}$, which satisfy the (even) commutation relations given in (2.5). To find valid odd generators we consider irreducible representations of the Lorentz group, (j, j') , with spin $j + j'$. Such representations may be written with spinor components as linear combinations of the construct $Q_{\alpha_1 \dots \alpha_{2j}; \dot{\beta}_1 \dots \dot{\beta}_{2j'}}$, where the undotted and dotted spinor indices denote transformation as left and right Weyl spinors respectively. Consider the anti-commutator of Q with its hermitian conjugate Q^\dagger

$$\{Q_{\alpha_1 \dots \alpha_{2j}; \dot{\beta}_1 \dots \dot{\beta}_{2j'}}, Q_{\dot{\gamma}_1 \dots \dot{\gamma}_{2j}; \delta_1 \dots \delta_{2j'}}\}. \quad (2.12)$$

By choosing all the spinor indices equal $\alpha = \beta = \gamma = \delta = 1$ (to simplify the Clebsch Gordon coefficients), the resulting components of the commutator become

$$\{Q_{\underbrace{1 \dots 1}_{2j}; \underbrace{\dot{1} \dots \dot{1}}_{2j'}}, Q_{\underbrace{\dot{1} \dots \dot{1}}_{2j}; \underbrace{1 \dots 1}_{2j'}}\} = X_{\underbrace{1 \dots 1}_{2(j+j')}} \underbrace{\dot{1} \dots \dot{1}}_{2(j+j')} \quad (2.13)$$

²Specifically, for the S-matrix of a local relativistic quantum field theory in four dimensional spacetime.

and therefore transform as a $(j + j', j + j')$ representation. Because Q and Q^\dagger are anti-commuting (odd) generators, their spin $j + j'$ must be half integer. Therefore the spin of the resulting $2(j + j')$ representation must be integer, and we can conclude that it belongs to the commuting (even) generators X .

From the no-go theorem we know that the only valid non-scalar generators of the even Lie algebra are those of the Poincaré group, such that

$$\{Q, Q^\dagger\} = P + M, \quad (2.14)$$

where indices have been suppressed to maintain generality. The four vector P_μ transforms as the representation $(\frac{1}{2}, \frac{1}{2})$ and $M_{\mu\nu}$ as an anti-symmetric second rank tensor transforms as a combination of $(1, 0)$ and $(0, 1)$.

Considering first the odd generators Q that commute with translations

$$[Q, P_\mu] = 0, \quad (2.15)$$

we find that

$$[P, \{Q, Q^\dagger\}] = [P, P] + [P, M] = 0, \quad (2.16)$$

implying that $[P, M] = 0$, which is in contradiction with (2.4). We conclude that (2.14) can not have M dependence. Hence the only valid candidate for $(j + j', j + j')$ is $(\frac{1}{2}, \frac{1}{2})$ representing the energy-momentum generator of the Poincaré group. This implies that Q must be a Weyl spinor, and we may associate

$$Q_\alpha \equiv (\frac{1}{2}, 0), \quad Q_\alpha^\dagger \equiv (0, \frac{1}{2}). \quad (2.17)$$

With a suitable choice of normalization, we arrive at the anti-commutation relation

$$\{Q_\alpha, (Q_\beta)^\dagger\} = P_{\alpha\beta} = \sigma_{\alpha\beta}^\mu P_\mu \quad (2.18)$$

where σ^i are the standard Pauli matrices, $\sigma^0 = -1$ and P_μ is the energy-momentum four vector of the Poincaré group.

The possibility of odd generators Q that do not commute with translations is considered in the original paper of Haag *et al.* [7], which concludes that there are in general no such new generators.

In four-component spinor notation, the supersymmetry extension to the Poincaré algebra, known as the *super-Poincaré* algebra, is given by

$$[P_\mu, Q_a] = 0, \quad (2.19)$$

$$[M_{\mu\nu}, Q_a] = -(\frac{1}{2}\sigma_{\mu\nu})_{ab}Q_b, \quad (2.20)$$

$$\{Q_a, \bar{Q}_b\} = 2(\gamma^\mu)_{ab}P_\mu. \quad (2.21)$$

Using the property that the charge is a Majorana spinor satisfying the condition $Q = Q^c = CQ^T$, the following (anti-)commutators also follow

$$[P_\mu, \bar{Q}_a] = 0, \quad (2.22)$$

$$[M_{\mu\nu}, \bar{Q}_a] = \bar{Q}_b \left(\frac{1}{2} \sigma_{\mu\nu} \right)_{ba}, \quad (2.23)$$

$$\{Q_a, Q_b\} = -2(\gamma^\mu C)_{ab} P_\mu, \quad (2.24)$$

$$\{\bar{Q}_a, \bar{Q}_b\} = 2(C^{-1} \gamma^\mu)_{ab} P_\mu. \quad (2.25)$$

From relation (2.19) we see that P^2 is a Casimir of the algebra. This means that a state ψ and its superpartner state $Q\psi$ must have the same mass

$$Q(P^2\psi) = Q(m_\psi^2\psi) \Rightarrow P^2(Q\psi) = m_\psi^2(Q\psi). \quad (2.26)$$

The W^2 Casimir of the original Poincaré algebra constructed from the Pauli-Lubanski four-vector $W_\mu = \frac{1}{2} \epsilon_{\mu\nu\rho\sigma} P^\nu M^{\rho\sigma}$ is no longer a Casimir of the super-Poincaré algebra, as is evident from (2.20). Consequently, a state and its superpartner state will have different spin.

2.2 Superfields

2.2.1 Superfield formalism

In the previous section it was found that a supersymmetry transformation on a field alters its spin. It would thus be useful to combine fields with different spin (bosonic and fermionic), which transform into one another under supersymmetry, into one all encompassing *superfield*. This superfield would then conveniently transform non-trivially into itself under supersymmetry transformations. However, we cannot simply add bosonic and fermionic fields together as they differ in their commutation and Lorentz transformation properties. To be able to add a fermionic field ψ to scalar (bosonic) fields, we need to contract the spinor into a scalar. We introduce a Majorana spinor θ whose components $\theta_1, \theta_2, \theta_3$ and θ_4 are anti-commuting Grassmann numbers, satisfying

$$\{\theta_a, \theta_b\} = 0. \quad (2.27)$$

By requiring that

$$\{\theta_a, \psi_b\} = 0, \quad (2.28)$$

we can construct scalar terms for a spinor ψ , such as $\bar{\theta}\psi$. These scalar contractions behave identically to ordinary bosonic scalar fields \mathcal{S} and hence expressions such as $\bar{\theta}\psi + \mathcal{S}$ are now possible. For a more detailed discussion see [8][1].

Superfields are thus defined to exist in an extension of ordinary four-dimensional spacetime known as *superspace*, which is labeled by the spacetime coordinates x^μ and the four spinor coordinates θ_a . Because of the anti-commuting nature of the

θ components, it is possible to expand a superfield into a finite number of linearly independent θ -terms. A convenient basis for this expansion is given by Baer *et al.* [1]

$$\begin{aligned} \hat{\Phi}(x, \theta) = & \mathcal{S} - i\sqrt{2}\bar{\theta}\gamma_5\psi - \frac{i}{2}(\bar{\theta}\gamma_5\theta)\mathcal{M} + \frac{1}{2}(\bar{\theta}\theta)\mathcal{N} + \frac{1}{2}(\bar{\theta}\gamma_5\gamma_\mu\theta)V^\mu \\ & + i(\bar{\theta}\gamma_5\theta)\left[\bar{\theta}\left(\lambda + \frac{1}{\sqrt{2}}\not{\theta}\psi\right)\right] - \frac{1}{4}(\bar{\theta}\gamma_5\theta)^2\left[\mathcal{D} - \frac{1}{2}\square\mathcal{S}\right] \end{aligned} \quad (2.29)$$

giving 8 fermionic and 8 bosonic complex component fields $\{\psi_a, \lambda_b\}$ and $\{\mathcal{S}, \mathcal{M}, \mathcal{N}, V^\mu, \mathcal{D}\}$ respectively. We will refer to this basis as the canonical basis. Certain operations, such as the product of two superfields or a symmetry transformation, may give a superfield with different θ terms, but it will always be possible to rewrite these in the canonical basis.

2.2.2 SUSY transformations

Now that we have a general superfield, we consider how it transforms under an infinitesimal global supersymmetry transformation. In-order to construct a unitary transformation operator we require a scalar operator. The supersymmetry generator Q however is a Majorana spinor, therefore the infinitesimal transformation parameter α is chosen to also be a Majorana spinor, so that the contraction $\bar{\alpha}Q$ gives a scalar. The transformation is then given by

$$\begin{aligned} \hat{\Phi}' &= e^{i\bar{\alpha}Q}\hat{\Phi}e^{-i\bar{\alpha}Q} \\ &= \hat{\Phi} + i[\bar{\alpha}Q, \hat{\Phi}], \end{aligned} \quad (2.30)$$

where in the second line we have assumed that the parameter α is infinitesimal.

Recall that the spacetime generator P_μ generates infinitesimal spacetime translations

$$\delta_a\phi = a^\mu[iP_\mu, \phi] = a^\mu\partial_\mu\phi, \quad (2.31)$$

so that it may be represented by a differential operator $P_\mu \equiv -i\partial_\mu$ in spacetime. Similarly, we can expect Q to be represented by a differential operator in superspace. To derive this representation, first observe that Q as a spinorial operator will change the Lorentz transformation properties of the superfield by either removing or adding a θ , so that

$$[Q_m, \hat{\Phi}(x, \theta)] = \left(M_{mn} \frac{\partial}{\partial\theta_n} + N_{mn}\theta_n \right) \hat{\Phi}(x, \theta) \quad (2.32)$$

where the matrices M_{mn} and N_{mn} must still be determined. Next consider two successive SUSY transformations

$$[[\bar{\alpha}_1Q, \bar{\alpha}_2Q], \hat{\Phi}] = [\bar{\alpha}_1Q, [\bar{\alpha}_2Q, \hat{\Phi}]] - [\bar{\alpha}_2Q, [\bar{\alpha}_1Q, \hat{\Phi}]]. \quad (2.33)$$

The right hand side is found to reduce to an expression involving the unknown matrices, whereas the left hand side contains the commutation relation

$$\{Q, Q\} = -2\gamma^\mu CP_\mu \equiv 2i\gamma^\mu C\partial_\mu, \quad (2.34)$$

and therefore contributes a spacetime derivative of the superfield. The equation is solved by setting $M = 1$ and $N = i\partial$, thereby giving the supersymmetric transformation of the superfield

$$\delta_\alpha \hat{\Phi} = i[\bar{\alpha}Q, \hat{\Phi}] = (-\bar{\alpha}\frac{\partial}{\partial\theta} - i\bar{\alpha}\partial\theta)\hat{\Phi}, \quad (2.35)$$

equivalent to a derivative in superspace.

By rewriting the transformed superfield $\delta_\alpha \hat{\Phi}$ in the canonical basis, the components are found to transform supersymmetrically as

$$\delta\mathcal{S} = i\sqrt{2}\bar{\alpha}\gamma_5\psi, \quad (2.36)$$

$$\delta\psi = -\frac{\alpha\mathcal{M}}{\sqrt{2}} - i\frac{\gamma_5\alpha\mathcal{N}}{\sqrt{2}} - i\frac{\gamma_\mu\alpha V^\mu}{\sqrt{2}} - \frac{\gamma_5\partial\mathcal{S}\alpha}{\sqrt{2}}, \quad (2.37)$$

$$\delta\mathcal{M} = \bar{\alpha}(\lambda + i\sqrt{2}\partial\psi), \quad (2.38)$$

$$\delta\mathcal{N} = i\bar{\alpha}\gamma_5(\lambda + i\sqrt{2}\partial\psi), \quad (2.39)$$

$$\delta V^\mu = -i\bar{\alpha}\gamma^\mu\lambda + \sqrt{2}\bar{\alpha}\partial^\mu\psi, \quad (2.40)$$

$$\delta\lambda = -i\gamma_5\alpha\mathcal{D} - \frac{1}{2}[\partial, \gamma_\mu]V^\mu\alpha, \quad (2.41)$$

$$\delta\mathcal{D} = \bar{\alpha}\partial_\mu(\gamma^\mu\gamma_5\lambda). \quad (2.42)$$

2.2.3 Irreducible representations

Irreducible representations (irreps) of the superfield formulated above are the smallest possible collections of component fields that transform only into themselves. This effectively allows us to set the component fields not occurring in this collection permanently to zero as they will not be regenerated by a supersymmetry transformation. Here we present the irreps of global supersymmetry that are needed to construct the MSSM.

We construct our first irrep by observing that the component fields λ and \mathcal{D} transform into one another up to the term $[\partial, \gamma_\mu]V^\mu$ in the λ transformation. As this term is anti-symmetric, we can take $V_\mu = \delta_\mu\zeta$ to set it to zero, and subsequently safely set $\lambda = \mathcal{D} = 0$. The remaining components can be further reduced into two distinct irreps. One of these is obtained by setting $V^\mu = i\partial^\mu\mathcal{S}$, $\psi_R = 0$ and $\mathcal{M} = -i\mathcal{N} \equiv \mathcal{F}$. The components $\hat{\mathcal{S}} \equiv \{\mathcal{S}, \psi_L, \mathcal{F}\}$ are then collectively known as the chiral scalar superfield and transform as

$$\delta\mathcal{S} = -i\sqrt{2}\bar{\alpha}\psi_L, \quad (2.43)$$

$$\delta\psi_L = -\sqrt{2}\mathcal{F}\alpha_{L\mathcal{S}} + \sqrt{2}\partial\mathcal{S}\alpha_{R\mathcal{S}}, \quad (2.44)$$

$$\delta\mathcal{F} = i\sqrt{2}\bar{\alpha}\partial_\mu(\gamma^\mu\psi_L). \quad (2.45)$$

The other irrep is obtained by setting $V^\mu = -i\partial^\mu \mathcal{S}$, $\psi_L = 0$ and $\mathcal{M} = i\mathcal{N} \equiv i\mathcal{F}$ and is known as the anti-chiral scalar superfield. Conjugating a chiral scalar superfield gives an anti-chiral scalar superfield

$$\begin{aligned}\hat{\mathcal{S}}^\dagger &= \left(\mathcal{S} + i\sqrt{2}\bar{\theta}\psi_L + i\bar{\theta}\theta_L\mathcal{F} + \frac{i}{2}(\bar{\theta}\gamma_5\gamma_\mu\theta)\partial^\mu\mathcal{S} - \frac{1}{\sqrt{2}}(\bar{\theta}\gamma_5\theta) \cdot \bar{\theta}\not{\partial}\psi_L + \frac{1}{8}(\bar{\theta}\gamma_5\theta)^2\Box\mathcal{S} \right)^\dagger \\ &= \mathcal{S}^\dagger - i\sqrt{2}\bar{\theta}\psi_R - i\bar{\theta}\theta_R\mathcal{F}^\dagger - \frac{i}{2}(\bar{\theta}\gamma_5\gamma_\mu\theta)\partial^\mu\mathcal{S}^\dagger - \frac{1}{\sqrt{2}}(\bar{\theta}\gamma_5\theta) \cdot \bar{\theta}\not{\partial}\psi_R + \frac{1}{8}(\bar{\theta}\gamma_5\theta)^2\Box\mathcal{S}^\dagger.\end{aligned}\tag{2.46}$$

The product of two chiral scalar superfields gives another scalar superfield, whereas the product of a chiral scalar superfield with an anti-chiral scalar superfield returns a general superfield

$$\begin{aligned}\hat{\mathcal{S}}_1\hat{\mathcal{S}}_2 &= \hat{\mathcal{S}}_3, \\ \hat{\mathcal{S}}_1\hat{\mathcal{S}}_2^\dagger &= \hat{\Phi}.\end{aligned}\tag{2.47}$$

To simplify the superfield superspace expansion of a chiral superfield we can introduce a superspace coordinate

$$\hat{x}_\mu \equiv x_\mu + \frac{i}{2}\bar{\theta}\gamma_5\gamma_\mu\theta,\tag{2.48}$$

defined so that the terms containing derivatives in the original expansion arise from a Taylor series expansion of the non-derivative terms around $\hat{x} \simeq x$. The chiral superfield may thus be written in the more convenient form

$$\hat{\mathcal{S}}(\hat{x}, \theta) = \mathcal{S}(\hat{x}) + i\sqrt{2}\bar{\theta}\psi_L(\hat{x}) + i\bar{\theta}\theta_L\mathcal{F}(\hat{x}).\tag{2.49}$$

By setting $F^{\mu\nu} \equiv \partial^\mu V^\nu - \partial^\nu V^\mu$ we also find that

$$\delta F^{\mu\nu} = -i\bar{\alpha}[\gamma^\nu\partial^\mu - \gamma^\mu\partial^\nu]\lambda,\tag{2.50}$$

$$\delta\lambda = -i\gamma_5\alpha\mathcal{D} + \frac{1}{4}[\gamma^\nu, \gamma^\mu]F^{\mu\nu}\alpha,\tag{2.51}$$

$$\delta\mathcal{D} = \bar{\alpha}\not{\partial}\gamma_5\lambda.\tag{2.52}$$

We cannot in general, however, set the component fields \mathcal{S} , ψ , \mathcal{M} and \mathcal{N} to zero, as they will be regenerated by supersymmetry transformations. In order to successfully form an irrep from these components we require gauge theory, which allows the components \mathcal{S} , ψ , \mathcal{M} and \mathcal{N} to be set to zero by a condition known as the *Wess-Zumino gauge*. This gives the irrep $\hat{V}_A := \{V_A^\mu, \lambda_A, \mathcal{D}_A\}$, satisfying $\hat{V}_A^\dagger = \hat{V}_A$ and known as the real vector potential superfield. It has the superspace expansion:

$$\hat{V}_A(x, \theta) = \frac{1}{2}(\bar{\theta}\gamma_5\gamma_\mu\theta)V_A^\mu(x) + i(\bar{\theta}\gamma_5\theta)\bar{\theta}\lambda_{AR}(x) - \frac{1}{4}(\bar{\theta}\gamma_5\theta)^2\mathcal{D}_A(x).\tag{2.53}$$

2.3 Building a SUSY Lagrangian

The Lagrangian of a global supersymmetric theory can be formulated as a density in spacetime or in superspace with the action integral following suite. Here we develop the former formulation as an ordinary spacetime density. We assume our supersymmetric theory has provided us with a collection of irreps, in our case chiral scalar superfields \hat{S} and real vector superfields \hat{V} . The Lagrangian will then be made up of component fields (to remove the θ dependence) of combinations of these irrep superfields.

2.3.1 D and F terms

Before discussing supersymmetric gauge theory, we present the general principles of building a Lagrangian using chiral scalar superfields. Recall from (2.47) that only the product of two scalar chiral superfields gives back a scalar chiral superfield. A mixture of scalar chiral and anti-scalar chiral superfields will give a general superfield. From (2.42) and (2.45) we see that none of the component fields are invariant under a supersymmetry transformation, which means it will be impossible to build a Lagrangian invariant under supersymmetry (at least by the method prescribed above). Fortunately, it is not the Lagrangian density, but rather the action that must be invariant under supersymmetry transformations for supersymmetry to be realized as a symmetry of nature. Component fields transforming as total derivatives are therefore valid candidates from which to build a Lagrangian:

$$\delta S = \int d^4x \delta \mathcal{L} = 0 \quad \Rightarrow \quad \begin{cases} \delta \mathcal{L} = 0 \\ \delta \mathcal{L} = \partial_\mu(\dots) \end{cases} \quad (2.54)$$

For a general superfield $\hat{\Phi}$, the only component field transforming as a total derivative is the \mathcal{D} field: $\delta \mathcal{D} = \not{\partial}(\dots)$. Thus for some function of superfields $F(\hat{\Phi}_i)$, the \mathcal{D} field component (i.e. the coefficient of the $-\frac{1}{4}(\bar{\theta}\gamma_5\theta)^2$ term) is a valid candidate for the Lagrangian (granted it is also renormalizable)

$$F(\hat{\Phi}_i) \Big|_{\mathcal{D}\text{-term}} \in \mathcal{L}. \quad (2.55)$$

As an example, consider the Kähler potential $K(\hat{S}, \hat{S}^\dagger) = \hat{S}^\dagger \hat{S}$, which after some calculation, yields the kinetic terms of the component fields for the chiral scalar superfield

$$\hat{S}^\dagger \hat{S} \Big|_{\mathcal{D}\text{-term}} = \partial_\mu S^\dagger \partial^\mu S + \frac{i}{2} \bar{\psi} \not{\partial} \psi + \mathcal{F}^\dagger \mathcal{F} \in \mathcal{L}. \quad (2.56)$$

Note that the F field here has no derivative terms, which means it is an auxillary field with algebraic equations of motion (giving constraints on the system).

For a chiral scalar superfield \hat{S} , the only component field transforming as a total derivative is the \mathcal{F} field: $\delta \mathcal{F} = \not{\partial}(\dots)$. To ensure the F component yields a total

derivative, we define a function made up of *only* chiral scalar superfields as the superpotential $\hat{f}(\hat{S})$, such that

$$\hat{f}(\hat{S}) \Big|_{\mathcal{F}\text{-term}} \in \mathcal{L}. \quad (2.57)$$

2.3.2 Gauge theory

Following the usual gauge theory prescription, we would like to add local gauge transformations to our component fields as

$$\psi(x) \rightarrow e^{igt_A \omega_A(x)} \psi(x), \quad (2.58)$$

and insist that the Lagrangian density be invariant under them. Our Lagrangian density is, however, constructed using the superfield formalism, making it necessary to extend the notion of local gauge transformations to superfields. Because the transformation is local, we wish to avoid derivatives in the superspace expansion, and therefore use the \hat{x}_μ expansion of the chiral scalar superfield given in (2.49). We cannot simply apply the operator $\exp(igt_A \omega_A(x))$ to the entire chiral superfield \hat{S} , for it is not itself a chiral superfield (having only a scalar component) and the product of the two will therefore not be one either (see equation 2.47). The solution is to define the transformation parameter as a chiral superfield $\hat{\Omega}_A(\hat{x})$, whose components are strictly complex or Grassmann valued functions of x (as opposed to component fields). A supersymmetric gauge transformation in this formalism is then

$$\hat{S} \rightarrow e^{igt_A \hat{\Omega}_A(\hat{x})} \hat{S}. \quad (2.59)$$

We can now check how this gauge transformation affects the construction of the Lagrangian density. The superpotential \hat{f} defined above is a polynomial of chiral scalar superfields, containing no derivatives. Its invariance under global supersymmetry also implies it is locally so, and therefore all F terms are unaffected by the gauge transformations. The Kähler potential, responsible for the kinetic terms of the component fields of \hat{S} , is not invariant

$$\hat{S}^\dagger \hat{S} \rightarrow \hat{S}^\dagger e^{-igt_A \hat{\Omega}_A^\dagger(\hat{x})} e^{igt_B \hat{\Omega}_B(\hat{x})} \hat{S}. \quad (2.60)$$

It is therefore necessary to modify the Kähler potential to

$$\hat{S}^\dagger e^{-2gt_A \hat{V}_A} \hat{S}, \quad (2.61)$$

and impose the *gauge condition*

$$e^{-igt_C \hat{\Omega}_C^\dagger(\hat{x})} \left(e^{-2gt_A \hat{V}_A} \right) e^{igt_D \hat{\Omega}_D(\hat{x})} = e^{-2gt_B \hat{V}_B}. \quad (2.62)$$

The superfield \hat{V}_A is exactly the real vector potential superfield introduced in section 2.2.3. This modified Kähler potential is responsible for giving gauge interactions

with the matter chiral superfields, analogous to replacing derivatives with covariant derivatives in a standard gauge theory.

The field components of the real vector potential superfield \hat{V}_A can also be expressed in terms of a chiral *spinor* superfield:

$$\hat{W}_A(\hat{x}, \theta) = \lambda_{AL} + \frac{1}{2}\gamma^\mu\gamma^\nu(\partial_\mu V_{A\nu} - \partial_\nu V_{A\mu})\theta_L - i\bar{\theta}\theta_L(\not{D}\lambda_{AR}) - i\mathcal{D}_A\theta_L, \quad (2.63)$$

for which the gauge condition can be rewritten as

$$e^{igt_C\hat{\Omega}_C(\hat{x})}\left(t_A\hat{W}_A\right)e^{-igt_D\hat{\Omega}_D(\hat{x})} = t_B\hat{W}_B. \quad (2.64)$$

Just as for the chiral scalar superfield, the product of two of these superfields remains a chiral spinor superfield. We may thus take the F -term component (more correctly the $\bar{\theta}\theta_L$ component, as this field does not have an \mathcal{F} field) just as we did for the superpotential. A gauge and Lorentz invariant combination of these gauge superfields that is also renormalizable is

$$\overline{\hat{W}_A^c}\hat{W}_A\Big|_{\mathcal{F}\text{-term}} = \frac{i}{2}\bar{\lambda}_A\not{D}_{AB}\lambda_B - \frac{1}{4}F_{\mu\nu A}F_A^{\mu\nu} + \frac{1}{2}\mathcal{D}_A\mathcal{D}_A, \quad (2.65)$$

which is seen to yield the kinetic terms of the gauge component fields. The \mathcal{D} fields, just like the \mathcal{F} fields, are seen to have no derivative terms and are therefore auxiliary fields with algebraic equations of motion.

The master supersymmetric Lagrangian of a gauge theory with chiral scalar superfields \hat{S}_i and real vector superfields \hat{V}_A , obtained by including all possible renormalizable contributions from these superfields, is

$$\begin{aligned} \mathcal{L} = & \sum_i (D_\mu \mathcal{S}_i)^\dagger (D^\mu \mathcal{S}_i) + \frac{i}{2} \sum_i \bar{\psi}_i \not{D} \psi_i + \sum_A \left[\frac{i}{2} \bar{\lambda}_A (\not{D}\lambda)_A - \frac{1}{4} F_{\mu\nu A} F_A^{\mu\nu} \right] \\ & - \sqrt{2} \sum_{i,A} \left(\mathcal{S}_i^\dagger g_A t_A \bar{\lambda}_A \psi_{Li} + \text{h.c.} \right) \\ & - \frac{1}{2} \sum_A \left[\sum_i \mathcal{S}_i^\dagger g_A t_A \mathcal{S}_i + \xi_A \right]^2 - \sum_i \left| \frac{\partial \hat{f}}{\partial \hat{S}_i} \right|_{\hat{S}=S}^2 \\ & - \frac{1}{2} \sum_{i,j} \bar{\psi}_i \left[\left(\frac{\partial^2 \hat{f}}{\partial \hat{S}_i \partial \hat{S}_j} \right)_{\hat{S}=S} P_L + \left(\frac{\partial^2 \hat{f}}{\partial \hat{S}_i \partial \hat{S}_j} \right)_{\hat{S}=S}^\dagger P_R \right] \psi_j. \end{aligned} \quad (2.66)$$

Notice that the F and D fields have been substituted by their algebraic equations of motion. The only remaining freedom any supersymmetric theory of this type has after specifying the irreps is a choice for the superpotential \hat{f} . The term in the second line gives interactions between a particle, its superpartner and a gauge fermion.

Chapter 3

The Minimal Supersymmetric Standard Model

With the master supersymmetric Lagrangian template given in (2.66) it is straightforward to construct a supersymmetric extension to the Standard Model. We keep the same internal symmetry group $SU(3)_c \times SU(2)_L \times U(1)_Y$, and promote each Standard Model gauge field to a real vector superfield:

$$\begin{aligned} B_\mu &\rightarrow \hat{B} \ni (B_\mu, \lambda_0, \mathcal{D}_B), \\ W_{a\mu} &\rightarrow \hat{W}_a \ni (W_{a\mu}, \lambda_a, \mathcal{D}_{W_a}), \\ g_{A\mu} &\rightarrow \hat{g}_A \ni (G_{A\mu}, \tilde{g}_A, \mathcal{D}_{g_A}), \end{aligned} \quad (3.1)$$

where $a = 1, 2, 3$ and $A = 1, \dots, 8$ are the index the $SU(2)_L$ and $SU(3)_c$ generators respectively.

Every fermion field in the Standard Model is likewise promoted to a chiral scalar superfield

$$\begin{aligned} \begin{pmatrix} \nu_{iL} \\ e_{iL} \end{pmatrix} &\rightarrow \begin{pmatrix} \hat{\nu}_i \\ \hat{e}_i \end{pmatrix} \equiv \hat{L}_i, & \begin{pmatrix} u_{iL} \\ d_{iL} \end{pmatrix} &\rightarrow \begin{pmatrix} \hat{u}_i \\ \hat{d}_i \end{pmatrix} \equiv \hat{Q}_i, \\ (e_{iR})^c &\rightarrow \hat{E}_i^c, & (u_{iR})^c &\rightarrow \hat{U}_i^c, \\ & & (d_{iR})^c &\rightarrow \hat{D}_i^c, \end{aligned} \quad (3.2)$$

where $i = 1, 2, 3$ is the flavour (family) index. In order to cast the right-handed fermion fields into chiral scalar superfields (as opposed to anti-chiral superfields) we have taken their conjugates. These conjugated spinor fields now transform in the conjugate representations of their respective internal symmetries. Consider, for example, the up quark, whose degrees of freedom exist in the superfields

$$\hat{u} \ni (\tilde{u}_L, \psi_{uL}, \mathcal{F}_u), \quad (3.3)$$

$$\hat{U}^c \ni (\tilde{u}_R^\dagger, \psi_{U^cL}, \mathcal{F}_{U^c}). \quad (3.4)$$

The Majorana field $\psi_{U^c L}$ transforms in the respective conjugate representations and so has opposite charges to ψ_{uL} . We must therefore use its conjugate $\psi_{U^c R}$ to construct the full Dirac spinor field for the up quark:

$$u = P_L \psi_u + P_R \psi_{U^c}. \quad (3.5)$$

The Higgs potential must enter via the superpotential $\hat{f}(\hat{S})$, as this is the only freedom we have for adding new terms into the Lagrangian. The Higgs fields are therefore promoted to chiral scalar superfields

$$\phi = \begin{pmatrix} \phi^+ \\ \phi^0 \end{pmatrix} \rightarrow \hat{H}_u = \begin{pmatrix} \hat{h}_u^+ \\ \hat{h}_u^0 \end{pmatrix}. \quad (3.6)$$

Allowing \hat{H}_u to have hypercharge $Y = 1$ so that it may couple to up-type quarks in the superpotential, we realise that we also need a Higgs field with hypercharge $Y = -1$ to couple to the down-type quarks. In the Standard Model this would be achieved simply by taking the conjugate of the Higgs field. In the superfield formalism, however, taking the conjugate would give us an anti-chiral scalar field, which is not allowed to enter in the superpotential (see section 2.3 of the previous chapter). We are thus forced to introduce a second Higgs doublet superfield with hypercharge $Y = -1$:

$$\hat{H}_d = \begin{pmatrix} \hat{h}_d^- \\ \hat{h}_d^0 \end{pmatrix} \quad (3.7)$$

The minimal superpotential of the Minimal Supersymmetric Standard Model (MSSM) is then

$$\hat{f} = \mu \hat{H}_u \hat{H}_d + \mathbf{f}_u \epsilon_{ab} \underbrace{\hat{Q}^a}_{\frac{1}{3}} \underbrace{\hat{H}_u^b}_{1} \underbrace{\hat{U}^c}_{-\frac{4}{3}} + \mathbf{f}_d \underbrace{\hat{Q}}_{\frac{1}{3}} \cdot \underbrace{\hat{H}_d}_{-1} \underbrace{\hat{D}^c}_{\frac{2}{3}} + \mathbf{f}_e \hat{L} \cdot \hat{H}_d \hat{E}^c \quad (3.8)$$

with hypercharge conservation indicated. The \mathbf{f} matrices here are analogous to the Yukawa coupling matrices from the Standard Model. A list of all the MSSM particle fields before electroweak breaking is given in table 3.1.

3.1 R-parity

The Standard Model naturally conserves baryon number B and lepton number L for all gauge invariant and renormalizable terms. This is not true for the MSSM, where it is possible to add gauge invariant and renormalizable terms to the superpotential that violate baryon and lepton number. To see this, note that quark superfields have baryon number $B = 1/3(-1/3)$ and lepton superfields have lepton number $L = 1(-1)$. Examples of baryon and lepton number violating superpotential terms

SM Particles		Superpartners	
Fermions		Scalar Fermions	
Quarks:	u, c, t, d, s, b	Squarks:	$\tilde{u}, \tilde{c}, \tilde{t}, \tilde{d}, \tilde{s}, \tilde{b}$
Leptons:	$e, \mu, \tau, \nu_e, \nu_\mu, \nu_\tau$	Sleptons:	$\tilde{e}, \tilde{\mu}, \tilde{\tau}, \tilde{\nu}_e, \tilde{\nu}_\mu, \tilde{\nu}_\tau$
Gauge Bosons		Gauginos	
Photon:	A_μ	Photino:	$\sin \theta_w \lambda_3 + \cos \theta_w \lambda_0$
W,Z Bosons:	W^\pm_μ	W-ino:	$\frac{1}{\sqrt{2}}(\lambda_1 \mp i\lambda_2)$
	Z_μ	Z-ino	$-\cos \theta_w \lambda_3 + \sin \theta_w \lambda_0$
Gluon:	G_μ	Gluino:	\tilde{g}
Higgs Bosons		Higgsinos	
	$h_u^+, h_u^0, (h_d^-, h_d^0)$		$\tilde{h}_u^+, \tilde{h}_u^0, \tilde{h}_d^-, \tilde{h}_d^0$

Table 3.1: The particle fields of the MSSM before electroweak breaking.

are then

$$\hat{f}_{\Delta L=1} \ni \epsilon \hat{L} \hat{Q} \hat{D}^c + \epsilon \hat{L} \hat{L} \hat{E}^c + \epsilon \hat{L} \hat{H}_u, \quad (3.9)$$

$$\hat{f}_{\Delta B=1} \ni \hat{U}^c \hat{U}^c \hat{D}^c, \quad (3.10)$$

$$\hat{f}_{\Delta B=\Delta L=1} \ni \epsilon \hat{Q} \hat{L} \hat{Q} \cdot \hat{Q} + \hat{U}^c \hat{U}^c \hat{D}^c \hat{E}^c. \quad (3.11)$$

These terms are of concern, because we do not observe baryon or lepton number violation in experiment. In particular, if both B and L numbers are violated rapid proton decay is possible, a phenomena that has been experimentally ruled out. To ensure the absence of these baryon and lepton violating terms in the MSSM superpotential, a new symmetry named R-parity is often introduced. R-parity is defined as

$$R = (-1)^{3(B-L)+2s}, \quad (3.12)$$

where s is the particles spin. Conservation of R-parity implies conservation of baryon and lepton numbers. It turns out that all superpartners have R-parity -1 whereas the Standard Model particles and the Higgs doublets have R parity +1. The MSSM with R-parity thus requires all superpartners to occur in pairs. This leads to an interesting implication for cosmology: because the lightest superpartner cannot decay, it is stable and could have a sizable relic density, making it a potential dark matter candidate if it is also electrically neutral, massive and weakly interacting¹.

3.2 Breaking of supersymmetry

From relation (2.19) it is clear that particles and their superpartners must have the same mass. We do not, however, observe particles such as scalar electrons in

¹Such Weakly Interacting Massive Particles are known as WIMPs

nature nor any of the other superpartners. Therefore, if supersymmetry truly is a symmetry of nature, it must be broken. How it must be broken is not known, but possible mechanisms include spontaneously (like the electroweak symmetry), explicitly or dynamically. Breaking of supersymmetry will in general add additional non-supersymmetric *breaking terms* to the supersymmetric Lagrangian. Some of these breaking terms could re-introduce the quadratic divergences that supersymmetry so vitally helped eliminate, this is known as hard breaking. To protect the scalar masses of the theory, which was one of the primary motivations for extending the Standard Model with supersymmetry, we assume that supersymmetry is broken softly i.e. that the breaking terms do not re-introduce quadratic divergences. Due to our ignorance of how supersymmetry is broken, we must add all possible soft breaking terms to our MSSM Lagrangian:

$$\mathcal{L}_{\text{soft}} = \left[\tilde{L}_i^\dagger \mathbf{m}_{Lij}^2 \tilde{L}_j + \dots + m_{H_u}^2 |H_u|^2 + \dots \right] \quad (3.13)$$

$$- \frac{1}{2} [M_1 \bar{\lambda}_0 \lambda_0 + \dots] + \left[(\mathbf{a}_e)_{ij} \epsilon_{ab} \tilde{L}_i H_d \tilde{e}_{Rj}^\dagger + \dots \right] \quad (3.14)$$

$$+ \left[(\mathbf{c}_e)_{ij} \epsilon_{ab} \tilde{L}_i H_d^* \tilde{e}_{Rj}^\dagger + \dots \right] + [B\mu H_u H_d + h.c.] \quad (3.15)$$

The terms on the first line are the mass terms for the scalar fields in the theory. The terms in the square brackets on the second line are the mass terms of the gauginos. The \mathbf{a} and \mathbf{c} matrices describe trilinear scalar interactions and the terms in the last square brackets give the mixing of the scalar Higgs fields. The total number of free parameters of the MSSM including the soft breaking terms is 178.

A model with such a large parameter space is clearly quite unmanageable and has almost no predictive power. To make the MSSM a more reasonable theory to work with in practice, a series of phenomenological assumption are made to simplify the parameter space. These assumptions include removing sources of CP violation and flavour mixing and considering only the heaviest family of Standard Model particles². A model of this type usually has between 5 – 10 free parameters and is often referred to as the Constrained MSSM (CMSSM).

Besides from the CMSSM, another popular supersymmetric extension to the Standard Model with only four free parameters is minimal supergravity (mSUGRA). This model has local rather than global supersymmetry, and devolves its small set of parameters from the GUT scale via the renormalization group equations to fix parameters at the electroweak breaking scale.

3.3 Electroweak symmetry breaking

In the Standard Model, the electroweak symmetry group $SU(2)_L \times U(1)_Y$ is spontaneously broken by the presence of a scalar $SU(2)_L$ doublet field known as the

²For a detailed discussion of these assumptions and SUSY breaking in general please refer to Baer *et al.* [1].

Higgs. The breaking occurs because the potential for the Higgs has its groundstates at points where the Higgs has a non-zero vacuum expectation value (VEV). Consequently, three of the four electroweak generators no longer leave the groundstate invariant, which implies that their respective symmetries are broken. The unbroken generator Q , a combination of both $SU(2)_L$ and $U(1)_Y$ generators, belongs to the gauge group $U(1)_Q$ that is responsible for electromagnetic interactions. The degrees of freedom remaining from the broken generators are absorbed (or as some say: *eaten*) by the gauge bosons they were coupled to, giving them mass. This is known as the Higgs mechanism. As the Standard Model gauge bosons and fermions in the MSSM do not yet have mass, we would like it to employ a similar mechanism. The scalar potential in the MSSM is a combination of F-terms, D-terms and soft breaking terms

$$V_{\text{scalar}} = \sum_i \left| \frac{\partial \hat{f}}{\partial \hat{\mathcal{S}}_i} \right|_{\hat{\mathcal{S}}=S}^2 + \frac{1}{2} \sum_{\alpha} \left[\sum_i \mathcal{S}_i^{\dagger} g_{\alpha} t_{\alpha} \mathcal{S}_i \right]^2 + V_{\text{soft}}, \quad (3.16)$$

where

$$V_{\text{soft}} = \left[\tilde{L}_i^{\dagger} \mathbf{m}_{Lij}^2 \tilde{L}_j + \dots + m_{H_u}^2 |H_u|^2 + \dots \right] + [bH_u H_d + h.c.] \\ + \left[(\mathbf{a}_e)_{ij} \epsilon_{ab} \tilde{L}_i H_d \tilde{e}_{Rj}^{\dagger} + \dots \right] + \left[(\mathbf{c}_e)_{ij} \epsilon_{ab} \tilde{L}_i H_d^* \tilde{e}_{Rj}^{\dagger} + \dots \right], \quad (3.17)$$

are all the scalar terms from (3.15). To simplify matters we may first use the $SU(2)_L$ gauge symmetry to rotate (gauge-fix) the two scalar Higgs doublet fields to their lower neutral components h_u^0 and h_d^0 . The relevant potential then becomes

$$V_0 = (m_{H_u}^2 + \mu^2) |h_u^0|^2 + (m_{H_d}^2 + \mu^2) |h_d^0|^2 \\ - B\mu(h_u^0 h_d^0 + \text{h.c.}) + \frac{1}{8}(g^2 + g'^2) \left(|h_u^0|^2 - |h_d^0|^2 \right)^2, \quad (3.18)$$

with the critical points of this potential given by

$$\frac{\partial V_0}{\partial h_u^0} = 0 \quad \text{and} \quad \frac{\partial V_0}{\partial h_d^0} = 0. \quad (3.19)$$

To avoid the solution $\langle h_u^0 \rangle = \langle h_d^0 \rangle = 0$ forming a local minimum, we insist it is a local maximum (by insisting the second derivatives of the potential there are negative). Furthermore, to ensure the local minimum is stable we insist that the potential be positive when the quartic terms vanish at $|h_u^0| = |h_d^0|$. With these two conditions in place a minimum should develop away from the origin at the vacuum expectation values (VEVs) $\langle h_u^0 \rangle \equiv v_u$ and $\langle h_d^0 \rangle \equiv v_d$, related by the commonly defined parameter $\tan \beta \equiv v_u/v_d$.

The gauge bosons W^{\pm} and Z pick up their masses through the standard Higgs mechanism but now with an extra Higgs doublet field:

$$|D_{\mu} H_u|^2 + |D_{\mu} H_d|^2 \in \mathcal{L}, \quad (3.20)$$

where

$$\langle H_u \rangle = \begin{pmatrix} 0 \\ v_u \end{pmatrix} \quad \text{and} \quad \langle H_d \rangle = \begin{pmatrix} 0 \\ v_d \end{pmatrix}, \quad (3.21)$$

and the covariant derivative is given by

$$D_\mu = \partial_\mu + ig t_a W_{a\mu} + ig' \frac{Y}{2} B_\mu. \quad (3.22)$$

The mass of the W bosons is thus

$$M_W^2 = \frac{g^2}{2} (v_u^2 + v_d^2), \quad (3.23)$$

and the Z bosons follow suite with $M_Z = M_W \sec \theta_W$, where θ_W is the Weinberg weak mixing angle.

The Standard Model fermions acquire their masses via the master Lagrangian term

$$-\frac{1}{2} \sum_{i,j} \bar{\psi}_i \left(\frac{\partial^2 \hat{f}}{\partial \hat{\mathcal{S}}_i \partial \hat{\mathcal{S}}_j} \right)_{\hat{\mathcal{S}}=S} P_L \psi_j + \text{h.c.}, \quad (3.24)$$

specifically, from the f matrices in the superpotential, often referred to as Yukawa matrices in analogue to the Standard Model. Consider, for example, the up quark u with Majorana component fields belonging to the superfields \hat{u} and \hat{U}^c . Then

$$\left(\frac{\partial^2 \hat{f}}{\partial \hat{u} \partial \hat{U}^c} \right)_{\hat{\mathcal{S}}=S} = (\mathbf{f}_u)_{11} h_u^0 \xrightarrow{\text{EW}} f_u v_u, \quad (3.25)$$

and thus we have the mass term

$$-m_u \bar{u} u \in \mathcal{L}. \quad (3.26)$$

where the up quark mass has been defined as $m_u \equiv f_u v_u$.

The electroweak breaking of the Higgs boson fields is non-trivial. As we are not concerned with Higgs fields in this thesis we simply note that the physical states that develop are two charged scalars H^\pm , two neutral scalars h and H and a neutral pseudo-scalar A .

3.3.1 Neutralinos and charginos

Recall from the master Lagrangian (2.66) that the first term on the second line gave a trilinear interaction between a particle, its superpartner and a gaugino. When the MSSM undergoes electroweak breaking, similar to that of the Standard Model, the trilinear terms involving a Higgs scalar and its superpartner higgsino will be

reduced to bilinear terms as the Higgs scalar takes its constant vacuum expectation value:

$$\begin{aligned} \mathcal{L} &\ni -\sqrt{2}g\mathcal{S}_i^\dagger gt_A\bar{\lambda}_A\psi_{Li} \\ \xrightarrow{\text{EW}} &\ni g\underbrace{\langle h_u^0 \rangle}_{v_u}\bar{\lambda}_3\tilde{h}_u^0 + \dots \end{aligned} \quad (3.27)$$

These bilinear terms mix the higgsino and gaugino states. The true physical particles of the higgsino and gaugino states after electroweak breaking will then be the eigenstates of the total mass matrix. The physical eigenstates of the mass matrix of the neutral (charged) higgsino and gaugino fermion states will be called neutralinos (charginos).

We proceed to derive the neutralino states, noting that the chargino derivation is analogous³. Besides from the mixing terms of the electroweak breaking, mass term contributions also come from the Higgs superfield mixing in the superpotential $\hat{f} \ni \mu\hat{H}_u\hat{H}_d$ and from the soft breaking gaugino mass terms

$$\mathcal{L}_{\text{soft}} \ni -\frac{1}{2}M_1\bar{\lambda}_0\lambda_0 - \frac{1}{2}M_2\bar{\lambda}_3\lambda_3. \quad (3.28)$$

All mass term contributions of the neutral fermions may thus be written as

$$-\frac{1}{2} \begin{pmatrix} \bar{h}_u^0 & \bar{h}_d^0 & \bar{\lambda}_3 & \bar{\lambda}_0 \end{pmatrix} \begin{pmatrix} 0 & \mu & -\frac{gv_u}{\sqrt{2}} & \frac{g'v_u}{\sqrt{2}} \\ \mu & 0 & \frac{gv_d}{\sqrt{2}} & -\frac{g'v_d}{\sqrt{2}} \\ -\frac{gv_u}{\sqrt{2}} & \frac{gv_d}{\sqrt{2}} & M_2 & 0 \\ \frac{g'v_u}{\sqrt{2}} & -\frac{g'v_d}{\sqrt{2}} & 0 & M_1 \end{pmatrix} \begin{pmatrix} \tilde{h}_u^0 \\ \tilde{h}_d^0 \\ \lambda_3 \\ \lambda_0 \end{pmatrix}. \quad (3.29)$$

The mass matrix can be diagonalized by a unitary matrix $\mathcal{M}_D = V^\dagger \mathcal{M}_{\text{neutral}} V$, giving the neutralino eigenstates

$$\begin{pmatrix} \chi_1 \\ \chi_2 \\ \chi_3 \\ \chi_4 \end{pmatrix} = V^\dagger \begin{pmatrix} \tilde{h}_u^0 \\ \tilde{h}_d^0 \\ \lambda_3 \equiv \tilde{W}^3 \\ \lambda_0 \equiv \tilde{B} \end{pmatrix}. \quad (3.30)$$

From the master supersymmetric lagrangian given in equation (2.66), we see that the gaugino components (the wino and bino) couple electroweakly to matter (chiral) superfield pairs through the term

$$-\sqrt{2}g\mathcal{S}_i^\dagger gt_A\bar{\lambda}_A\psi_{Li} \in \mathcal{L}. \quad (3.31)$$

³The chargino mass matrix is not symmetric, causing the chiral projection operators to introduce γ_5 matrices into the mass terms that must be handled carefully.

Therefore quark-neutralino scattering is possible via the exchange of a scalar quark. The higgsino components can couple electroweakly to superfield pairs via the Yukawa couplings present in the term

$$-\frac{1}{2} \sum_{i,j} \bar{\psi}_i \left(\frac{\partial^2 \hat{f}}{\partial \hat{\mathcal{S}}_i \partial \hat{\mathcal{S}}_j} \right)_{\hat{\mathcal{S}}=S} P_L \psi_j + h.c. \in \mathcal{L} \quad (3.32)$$

Finally, the term

$$\frac{i}{2} \sum_i \bar{\psi}_i \not{D} \psi_i \in \mathcal{L} \quad (3.33)$$

gives couplings between neutralinos and the electroweak gauge bosons. Neutralinos, as well as charginos, therefore only couple electroweakly.

The neutralino

We call the lightest neutralino eigenstate *the neutralino* and denote it by χ_0 (i.e. the index i for which χ_i is the lightest is replaced by 0). The neutralino may be written as a linear combination of higgsinos and gauginos

$$\chi_0 = V_{10}^* \tilde{h}_u^0 + V_{20}^* \tilde{h}_d^0 + V_{30}^* \tilde{W}^3 + V_{40}^* \tilde{B}. \quad (3.34)$$

It is common to define a quantity such as the gaugino fraction $f_g := |V_{30}|^2 + |V_{40}|^2$ to measure if the neutralino is primarily gaugino $f_g > 0.5$ or higgsino < 0.5 .

The neutralino is a massive, electrically neutral and weakly interacting particle. If it is the lightest supersymmetric particle in a theory with R-parity conservation, which it is in many realistic models, then it is also protected against decay and must exist today in some quantity (provided it was ever produced). The neutralino may therefore be classified as a stable weakly interacting massive particle (WIMP), a candidate class for explaining cosmological dark matter. Whether the neutralino has a weak enough annihilation cross section to give the correct relic density is dependent on the SUSY parameter space.

3.3.2 Sfermion mixing

Apart from the scalar masses coming directly from the soft breaking terms, the scalar fermions also pick up additional mass contributions from the master Lagrangian D -terms, the superpotential and from soft scalar trilinear terms after electroweak symmetry breaking. The D -term contribution, like the original soft scalar masses, does not mix left and right handed sfermions. However, part of the superpotential contribution and all of the soft trilinear terms do.

Consider a fermion field t with corresponding superfields \hat{t} and \hat{T}^c . The relevant master Lagrangian term that gives the superpotential contribution is

$$\mathcal{L} \ni - \sum_i \left| \frac{\partial \hat{f}}{\partial \hat{\mathcal{S}}_i} \right|_{\hat{\mathcal{S}}=S}^2, \quad (3.35)$$

with

$$\hat{f} \ni \mu \hat{h}_u^0 \hat{h}_d^0 + f_t \hat{t} \hat{h}_u^0 \hat{I}^c. \quad (3.36)$$

After electroweak breaking we find

$$\mathcal{L} \ni -m_t^2 \left(\tilde{t}_L^\dagger \tilde{t}_L + \tilde{t}_R^\dagger \tilde{t}_R \right) - \mu m_t \cot \beta \left(\tilde{t}_L^\dagger \tilde{t}_R + \tilde{t}_R^\dagger \tilde{t}_L \right) \quad (3.37)$$

Likewise, the relevant soft trilinear terms are

$$(\mathbf{a}_u)_{ij} \epsilon_{ab} \tilde{Q}_i H_u \tilde{u}_{Rj}^\dagger + \text{h.c.} \quad (3.38)$$

By rewriting the matrix \mathbf{a}_u in terms of the superpotential Yukawa matrix \mathbf{f}_u as

$$(\mathbf{a}_u)_{ij} = A_{ij} (\mathbf{f}_u)_{ij}, \quad (3.39)$$

the trilinear terms give

$$\begin{aligned} & A_t f_t \tilde{t}_L h_u^0 \tilde{t}_R^\dagger + \text{h.c} \\ & \xrightarrow{\text{EW}} A_t m_t \left(\tilde{t}_L^\dagger \tilde{t}_R + \tilde{t}_R^\dagger \tilde{t}_L \right). \end{aligned} \quad (3.40)$$

All together, the sfermion mass matrix is

$$\mathcal{L} \ni - \begin{pmatrix} \tilde{t}_L^\dagger & \tilde{t}_R^\dagger \end{pmatrix} \begin{pmatrix} m_{\tilde{t}_L}^2 + m_t^2 + D(\tilde{t}_L) & m_t(-A_t + \mu \cot \beta) \\ m_t(-A_t + \mu \cot \beta) & m_{\tilde{t}_R}^2 + m_t^2 + D(\tilde{t}_R) \end{pmatrix} \begin{pmatrix} \tilde{t}_L \\ \tilde{t}_R \end{pmatrix}, \quad (3.41)$$

where $D(\tilde{t}_\sigma)$ are the D -term contributions. We thus see that sfermion mixing will occur if the corresponding fermion mass is similar in size to the soft breaking sfermion mass. This will generally only be the case for the third generation of sfermions. Therefore the mass eigenstates of the stop after electroweak breaking, for example, are given by

$$\begin{pmatrix} \tilde{t}_1 \\ \tilde{t}_2 \end{pmatrix} = \begin{pmatrix} \cos \theta_t & -\sin \theta_t \\ \sin \theta_t & \cos \theta_t \end{pmatrix} \begin{pmatrix} \tilde{t}_L \\ \tilde{t}_R \end{pmatrix}, \quad (3.42)$$

where θ_t is the stop mixing angle. Similarly the sbottom and stau have mass eigenstates $\tilde{b}_{1/2}$ and $\tilde{\tau}_{1/2}$. Neutrinos are assumed to be massless in the MSSM, therefore tau sneutrinos do not have mixed handed eigenstates.

Chapter 4

Strong SUSY Interactions

In this chapter we discuss the effects of supersymmetry on strong interactions. The term strong here refers to the strong force, as described by the $SU(3)_C$ gauge field theory of the Standard Model; better known as Quantum Chromodynamics (QCD). In standard QCD, the particles that interact strongly are quarks and gluons, which each carry a discrete internal degree of freedom known as colour. The quark, transforming in the fundamental representation of the gauge symmetry group, can have three such colours, whereas the gluon, transforming in the adjoint representation, has eight. Supersymmetry enlarges this sector by adding two strongly interacting superpartners, the squark and gluino, corresponding to the quark and gluon respectively. The squark, denoted by \tilde{q} , is a massive complex scalar field that transforms in the fundamental representation similar to the quark. Likewise, the gluino, denoted by \tilde{g} , is a massive Majorana fermion transforming in the adjoint representation. The addition of these particles contributes new strong interactions, whose Feynman rules we present in the following section.

A characteristic property of the strong force is that its strength is inversely proportional to the energy scale of the interaction, as we will discuss in section 4.3. At low energies the strong force is so powerful that it is impossible to isolate a single particle carrying colour charge. This phenomena is known as *confinement*, and implies that we may only indirectly observe colour charged particles through colour neutral bound states called *hadrons*. On the contrary, at high enough energies the strong coupling constant weakens to the point where we may treat it using perturbation theory, analogous to how we treat the electromagnetic and the weak forces. Interactions occurring at this energy range are referred to as hard scattering. Because we are interested in interactions occurring in highly energetic hadron colliders such as the LHC and Tevatron, we assume only hard scattering for strongly interacting particles throughout this thesis.

4.1 Feynman rules for supersymmetric $SU(3)_C$

From the master SUSY Lagrangian given in 2.66, the Lagrangian interaction terms that couple strongly in the MSSM are

$$\begin{aligned} \mathcal{L}_{\text{QCD}} = & \sum_{\sigma,i} (D_\mu \tilde{q}_{\sigma i})^\dagger (D^\mu \tilde{q}_{\sigma i}) + i \sum_i \bar{q}_i \not{D} q_i \\ & + \frac{i}{2} \bar{g}_A \not{D}_{AB} \tilde{g}_B - \frac{1}{4} (\partial_\mu G_{\nu A} - \partial_\nu G_{\mu A} - g_S f_{ABC} G_{B\mu} G_{C\nu})^2 \\ & - \left(\sqrt{2} g_S \sum_{\sigma,i} (-1)^\sigma \tilde{q}_{\sigma i}^\dagger t_A^F \bar{g}_A P_\sigma q_i + \text{h.c.} \right) - \frac{g_S^2}{2} \left(\sum_{\sigma,i} \tilde{q}_{\sigma i}^\dagger t_A^F \tilde{q}_{\sigma i} \right)^2 \end{aligned} \quad (4.1)$$

where

$$q = P_L \psi_q + P_R \psi_{Q^c}, \quad (4.2)$$

is the quark Dirac spinor with $q \in \{u, d\}$. The index i is used to sum over the three quark flavours and $\sigma \in \{L, R\}$ sums over the left and right-handed squark labels. The standard chiral projection operators have thus been denoted by

$$P_\sigma \equiv \begin{cases} P_L = \frac{1-\gamma_5}{2} & : \quad \sigma = L, \\ P_R = \frac{1+\gamma_5}{2} & : \quad \sigma = R. \end{cases} \quad (4.3)$$

Further, we define

$$\bar{\sigma} = \sigma(L \leftrightarrow R) \quad (4.4)$$

and

$$(-1)^\sigma \equiv \begin{cases} 1 & : \quad \sigma = L, \\ -1 & : \quad \sigma = R. \end{cases} \quad (4.5)$$

The covariant derivative acting on the quarks and squarks is defined as

$$(D_\mu)_{mn} = \delta_{mn} \partial_\mu + i g_S (t_A^F)_{mn} G_{\mu A}, \quad (4.6)$$



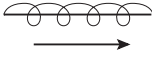
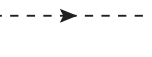
where m and n are colour indices in the fundamental representation. Likewise, the covariant derivative acting on the gluino is defined as

$$(D_\mu)_{AB} = \delta_{AB} \partial_\mu + i g_S \left(t_C^{\text{adj}} G_{C\mu} \right)_{AB}. \quad (4.7)$$

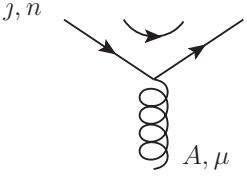
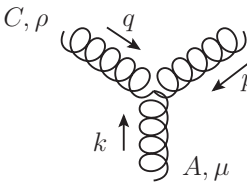
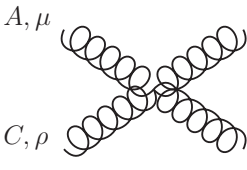
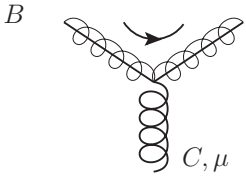
where A, B and C are colour indices in the adjoint representation.

Due to the presence of Majorana fermions, namely the gluinos, care must be taken when writing down and using the Feynman rules for the Lagrangian given above. In the last section of this chapter we present the Majorana Feynman rules that we use throughout this thesis. A noticeable feature of these rules is the concept of fermion flow, denoted by a separate arrow following any fermion chain. We must also be careful to account for the identical nature of Majorana fermions when considering the combinatorial factor of a vertex. Besides from these extra considerations, the Feynman rules are calculated in the standard way.

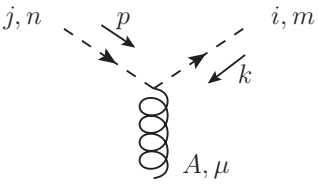
Propagators

Quark:		\vec{p}	=	$\frac{i(\not{p} + m)}{p^2 - m^2 + i\epsilon}$
Gluon:		\vec{p}	=	$\frac{-ig_{\mu\nu}}{p^2 + i\epsilon}$
Gluino:		\vec{p}	=	$\frac{i(\not{p} + m)}{p^2 - m_{\tilde{g}}^2 + i\epsilon}$
Squark:		\vec{p}	=	$\frac{i}{p^2 - m_{\tilde{q}\sigma}^2 + i\epsilon}$

Vertices

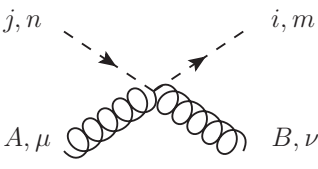
Gluon-quark-quark:		=	$-ig_S \delta_{ij} (t_A)_{mn} \gamma^\mu$
Gluon-gluon-gluon:		=	$g_S f_{ABC} [g^{\mu\nu} (k - p)^\rho + g^{\nu\rho} (p - q)^\mu + g^{\rho\mu} (q - k)^\nu]$
Four Gluon:		=	$-ig_S^2 [f_{ABE} f_{CDE} (g^{\mu\rho} g^{\nu\tau} - g^{\mu\tau} g^{\nu\rho}) + f_{ACE} f_{BDE} (g^{\mu\nu} g^{\rho\tau} - g^{\mu\tau} g^{\nu\rho}) + f_{ADE} f_{BCE} (g^{\mu\nu} g^{\rho\tau} - g^{\mu\rho} g^{\nu\tau})]$
Gluon-gluino-gluino:		=	$g_S \gamma^\mu f_{ABC}$

Gluon-squark-squark:



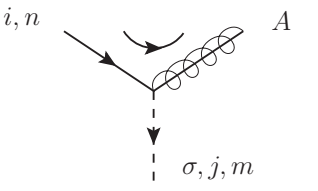
$$= -ig_S \delta_{ij} (t_A)_{mn} (p - k)^\mu$$

Gluon-gluon-squark-squark:



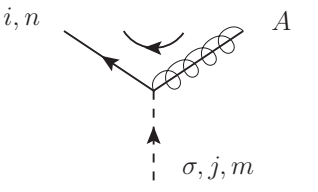
$$= ig_S^2 \delta_{ij} \{t_A, t_B\}_{mn} g^{\mu\nu}$$

Gluino-quark-squark:



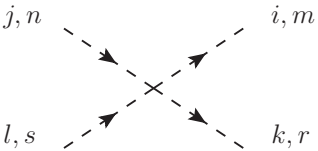
$$= -(-1)^\sigma i\sqrt{2} g_S \delta_{ij} (t_A)_{mn} P_\sigma$$

Gluino-quark-squark:



$$= -(-1)^\sigma i\sqrt{2} g_S \delta_{ij} (t_A)_{mn} P_{\bar{\sigma}}$$

Four squark:



$$= \frac{i}{2} g_S^2 \delta_{ij} \delta_{kl} (t_A)_{nm} (t_A)_{rs}$$

4.2 Gluino pair production (worked example)

4.2.1 Cross section calculation

Quark-anti-quark annihilation

What follows is a detailed calculation of the cross section for gluino pair production via quark-anti-quark annihilation. Figure 4.1 gives the labeling conventions used for the external particles. Indices relating to transformations under the $SU(3)$ colour gauge group are kept explicit, with lowercase indices m, n, \dots denoting the fundamental representation and uppercase indices A, B, \dots the adjoint representation. All $SU(3)$ group generators t_A appearing in this section are in the fundamental representation.

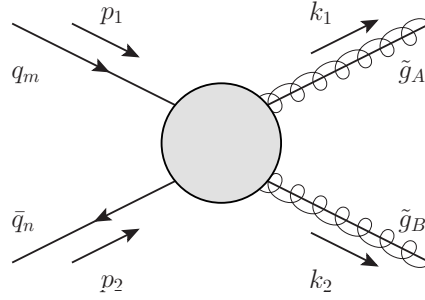


Figure 4.1: Labeling conventions for the process of gluino pair production via quark-anti-quark annihilation. With quarks and gluinos carrying colour labels in the fundamental and adjoint representations respectively.

For simplicity we group the scalar quarks \tilde{q}_L and \tilde{q}_R together as one particle, so that the process in question can be described by three Feynman diagrams, which are given in figure 4.2. Diagrams two and three are related by a cross channel symmetry.

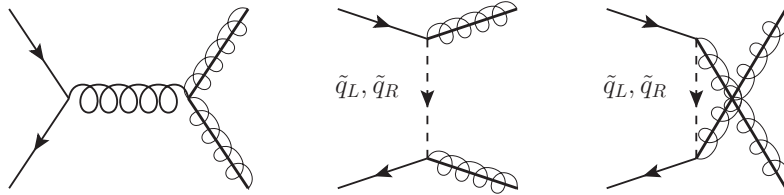


Figure 4.2: The three tree level diagrams for quark-anti-quark annihilation to gluino production, where the scalar quarks \tilde{q}_L and \tilde{q}_R have been grouped together for simplicity (but their distinction has not been forgotten).

We begin by calculating the amplitude for the first diagram

$$\begin{aligned} \mathcal{M}_1 &= ig_s \bar{v}_n(p_2) \gamma^\mu (t_D)_{nm} u_m(p_1) \left(\frac{-i\delta^{DC}}{(p_1 + p_2)^2} g_{\mu\nu} \right) g_s f_{ABC} \bar{u}_A(k_1) \gamma^\nu v_B(k_2) \\ &= -i \frac{g_s^2}{(p_1 + p_2)^2} \bar{v}(p_2) \gamma^\mu u(p_1) \bar{u}(k_1) \gamma_\nu v(k_2) \{if_{ABC}(t_D)_{nm}\} \end{aligned} \quad (4.8)$$

where we may use the Lie group generator relation $[t_A, t_B] = if_{ABC} t_C$ to write the amplitude as

$$\mathcal{M}_1 = -\frac{g_s^2}{\hat{s}} \bar{v}_n(p_2) \gamma^\mu u_m(p_1) \bar{u}_A(k_1) \gamma_\mu v_B(k_2) [t_A, t_B]_{nm}. \quad (4.9)$$

with $\hat{s} \equiv (p_1 + p_2)^2$ the Mandelstam variable¹.

¹Mandelstam variables with a hat correspond to partonic external momenta, as discussed in section 4.3.

In using the Feynman diagram prescription to write down the invariant amplitude \mathcal{M}_1 , a possible overall sign has been overlooked. To see this, recall that the invariant amplitude is a matrix element of the scattering matrix S ,

$$\langle \tilde{g}_B \tilde{g}_A | S | q_m \bar{q}_n \rangle = i(2\pi)^4 \delta^4(k_2 + k_1 - p_2 - p_1) \mathcal{M}(q_m \bar{q}_n \rightarrow \tilde{g}_B \tilde{g}_A). \quad (4.10)$$

A formal evaluation of the invariant amplitude in the canonical quantization formalism would therefore involve the reduction of the initial and final states on the lefthand side, using the definition of the scattering matrix

$$S = \exp \left[-i \int d^4x \mathcal{H}_{\text{int}} \right]. \quad (4.11)$$

There is, therefore, a possible overall sign arising from the anti-commutation of fermion operators in the reduction process that has not been accounted for by the Feynman diagram rules.

To account for this possible minus sign, we can choose an arbitrary order for the reduction process i.e. q_m , \bar{q}_n , \tilde{g}_A and lastly \tilde{g}_B . Then, for each spinor appearing in the invariant amplitude, we consider in the same order their respective anti-commuting reduction operators between initial and final states. For example

$$\begin{aligned} \mathcal{M} &\propto \bar{v}_n \gamma^\mu u_m \bar{u}_A \gamma_\mu v_B \\ &\rightarrow \langle \tilde{g}_B \tilde{g}_A | \bar{q}_n q_m \tilde{g}_A \tilde{g}_B | q_m \bar{q}_n \rangle \\ &\rightarrow +1. \end{aligned} \quad (4.12)$$

The operators q_m and \bar{q}_n each anti-commute twice and the gluino operators do not need to be commuted. There is thus no overall minus sign for this process (which is \mathcal{M}_1). As we will soon see, only \mathcal{M}_2 picks up a relative minus sign in this way. This is equivalent to counting the number of commutations required (which is equal to the number of minus signs) to order the spinor terms appearing in a given amplitude in the same way as an arbitrarily chosen reference amplitude.

To calculate the invariant amplitude \mathcal{M}_2 , we consider simultaneously the exchange of the scalar \tilde{q}_L and \tilde{q}_R fields

$$\begin{aligned} \mathcal{M}_2 \Big|_{(\tilde{q}_L/\tilde{q}_R)} &= - \frac{(\pm i)}{\sqrt{2}} g_s (\mp i)^\theta \bar{u}_A(k_1) (1 \mp \gamma_5) (t_A)_{km} u_m(p_1) \left(\frac{i\delta^{kl}}{(p_1 - k_1)^2 - m_{\tilde{q}}^2} \right) \\ &\quad \times \frac{(\pm i)}{\sqrt{2}} g_s (\pm i)^\theta \bar{v}_n(p_2) (1 \pm \gamma_5) (t_B)_{nl} v_B(k_2), \end{aligned} \quad (4.13)$$

such that

$$\mathcal{M}_2 \Big|_{(\tilde{q}_L/\tilde{q}_R)} = \frac{ig_s^2}{2(\hat{t} - m_{\tilde{q}}^2)} \bar{u}_A(k_1) (1 \mp \gamma_5) u_m(p_1) \bar{v}_n(p_2) (1 \pm \gamma_5) v_B(k_2) \{ (t_B t_A)_{mn} \}, \quad (4.14)$$

where the initial overall minus sign comes from the reduction process just mentioned and $m_{\tilde{q}}$ is the mass of the scalar quark.

\mathcal{M}_3 may be obtained by interchanging the outgoing colour indices $A \leftrightarrow B$ and momenta $k_1 \leftrightarrow k_2$, where this time there is no overall minus sign from the reduction operators

$$\mathcal{M}_3 \Big|_{(\tilde{q}_L/\tilde{q}_R)} = -\frac{ig_s^2}{2(\hat{u} - m_{\tilde{q}}^2)} \bar{u}_B(k_2)(1 \mp \gamma_5)u_m(p_1)\bar{v}_n(p_2)(1 \pm \gamma_5)v_A(k_1) \{(t_A t_B)_{mn}\} \quad (4.15)$$

Now that we have amplitude expressions for the three diagrams shown in figure 4.2, we proceed to calculate the various parts of spin averaged squared amplitude. Consider first

$$\begin{aligned} \sum_{\text{spins}} \mathcal{M}_1^\dagger \mathcal{M}_1 &= \sum_{s_1, s_2, r_1, r_2} \frac{-g_s^2}{\hat{s}} (-1)\bar{u}_m(p_1, s_1)\gamma^\nu v_n(p_2, s_2)(-1)\bar{v}_B(k_2, r_2)\gamma_\nu u_A(k_1, r_1)[t_A, t_B]_{mn} \\ &\quad \times \frac{-g_s^2}{\hat{s}} \bar{v}_n(p_2, s_2)\gamma^\mu u_m(p_1, s_1)\bar{u}_A(k_1, r_1)\gamma_\mu v_B(k_2, r_2)[t_B, t_A]_{nm}, \end{aligned} \quad (4.16)$$

using the spinor spin sum relations (A.13) gives

$$\sum_{\text{spins}} |\mathcal{M}_1|^2 = \frac{g_s^4}{\hat{s}^2} \text{Tr}(p_2 \gamma^\mu p_1 \gamma^\nu) \text{Tr}((k_2 - m_{\tilde{g}})\gamma_\nu(k_1 + m_{\tilde{g}})\gamma_\mu) \{ \text{Tr}([t_B, t_A][t_A, t_B]) \}, \quad (4.17)$$

where $m_{\tilde{g}}$ is the gluino mass. The factor containing colour generators can be evaluated using the Lie algebra relations $t_A t_A = C_2(r) \cdot \mathbf{1}$ and $t_A t_B t_A = [C_2(r) - \frac{1}{2}C_2(G)] t_B$, where for $SU(3)$ the Casimir $C_2(r)$ is $4/3$ and 3 in the fundamental and adjoint representations respectively. Thus

$$\begin{aligned} \text{Tr}([t_B, t_A][t_A, t_B]) &= 2 \{ \text{Tr}(t_B t_A t_A t_B) - \text{Tr}(t_B t_A t_B t_A) \} \\ &= 2 \left\{ C_2(r)^2 \text{Tr}(\mathbf{1}) - \left(C_2(r) - \frac{1}{2}C_2(G) \right) C_2(r) \text{Tr}(\mathbf{1}) \right\} \\ &= 12. \end{aligned} \quad (4.18)$$

Using standard gamma matrix trace relations to compute the helicity terms we find

$$\begin{aligned} \sum_{\text{spins}} |\mathcal{M}_1|^2 &= 12 \frac{g_s^4}{\hat{s}^2} 4(p_1^\nu p_2^\mu - p_1 \cdot p_2 g^{\mu\nu} + p_1^\mu p_2^\nu) 4(k_{1\mu} k_{2\nu} - k_1 \cdot k_2 g_{\mu\nu} + k_{1\nu} k_{2\mu} - m_{\tilde{g}}^2 g_{\mu\nu}) \\ &= 32 \cdot 3 \frac{g_s^4}{\hat{s}^2} [2(p_2 \cdot k_1)2(p_1 \cdot k_2) + 2(p_2 \cdot k_2)2(p_1 \cdot k_1) + 2m_{\tilde{g}}^2 2(p_1 \cdot p_2)]. \end{aligned} \quad (4.19)$$

Substituting the external momenta for Mandelstam variables

$$\hat{s} = (p_1 + p_2)^2 = 2p_1 \cdot p_2, \quad (4.20)$$

$$\hat{t} = (p_1 - k_1)^2 = -2p_1 \cdot k_1 + m_{\tilde{g}}^2, \quad (4.21)$$

$$\hat{u} = (p_1 - k_2)^2 = -2p_1 \cdot k_2 + m_{\tilde{g}}^2, \quad (4.22)$$

gives

$$\sum_{\text{spins}} |\mathcal{M}_1|^2 = 32g_s^4 \cdot 3 \left[\frac{(m_{\tilde{g}}^2 - \hat{u})^2 + (m_{\tilde{g}}^2 - \hat{t})^2 + 2m_{\tilde{g}}^2 \hat{s}}{\hat{s}^2} \right]. \quad (4.23)$$

Similarly, we now compute the squared amplitude for \mathcal{M}_2 . As $\mathcal{M}_2|_{(\tilde{q}_L/\tilde{q}_R)}$ represents two distinct diagrams, there are four possible combinations. The two diagrams that attempt to mix helicities vanish. To see this, consider

$$\begin{aligned} \mathcal{M}_2^\dagger|_{\tilde{q}_L} \mathcal{M}_2|_{\tilde{q}_R} &= \frac{g_s^4}{4(\hat{t} - m_{\tilde{q}}^2)^2} \text{Tr}(\not{p}_1(1 + \gamma_5)(\not{k}_1 + m_{\tilde{g}})(1 + \gamma_5)) \\ &\quad \times \text{Tr}(\not{p}_2(1 - \gamma_5)(\not{k}_2 - m_{\tilde{g}})(1 - \gamma_5)) \cdot \text{Tr}(t_B t_A t_A t_B) \end{aligned} \quad (4.24)$$

$$\propto \dots \text{Tr}(\not{p}_1(1 + \gamma_5)(1 - \gamma_5)(\not{k}_1)) \dots = 0, \quad (4.25)$$

using the relation $\{\gamma_5, \gamma_\mu\} = 0$. The squared amplitudes of the two remaining squared amplitudes may be computed by keeping \mathcal{M}_2 in its general form:

$$\begin{aligned} \sum_{\text{spins}} |\mathcal{M}_2|^2|_{(\tilde{q}_L/\tilde{q}_R)} &= \frac{g_s^4}{4(\hat{t} - m_{\tilde{q}}^2)^2} \text{Tr}(\not{p}_1(1 \mp \gamma_5)(\not{k}_1 + m_{\tilde{g}})(1 \pm \gamma_5)) \\ &\quad \times \text{Tr}(\not{p}_2(1 \pm \gamma_5)(\not{k}_2 - m_{\tilde{g}})(1 \mp \gamma_5)) \cdot \text{Tr}(t_B t_A t_A t_B). \end{aligned} \quad (4.26)$$

The colour factor can be evaluated using the same relations as before and gives $16/3$. As the trace of an odd number of gamma matrices is zero, the mass term in both helicity traces goes to zero. Furthermore, we may use the relation $\text{Tr}(\gamma_5 \gamma_\mu \gamma_\nu) = 0$ and again that $\gamma_5^2 = 1$ to simplify the expression to

$$\begin{aligned} \sum_{\text{spins}} |\mathcal{M}_2|^2|_{(\tilde{q}_L/\tilde{q}_R)} &= \frac{4g_s^4}{3(\hat{t} - m_{\tilde{q}}^2)^2} [2\text{Tr}(\not{p}_1 \not{k}_1) 2\text{Tr}(\not{p}_2 \not{k}_2)] \\ &= 16g_s^4 \frac{4}{3(\hat{t} - m_{\tilde{q}}^2)^2} [2(p_1 \cdot k_1) 2(p_2 \cdot k_2)]. \end{aligned} \quad (4.27)$$

Substituting Mandelstam variables for the external momenta and adding the diagram contributions for \tilde{q}_L and \tilde{q}_R together gives

$$\sum_{\text{spins}} |\mathcal{M}_2|^2 = 32g_s^4 \cdot \frac{4}{3} \left[\left(\frac{m_{\tilde{g}}^2 - \hat{t}}{m_{\tilde{q}}^2 - \hat{t}} \right)^2 \right]. \quad (4.28)$$

By applying crossing symmetries of the Mandelstam variables, namely $\hat{t} \leftrightarrow \hat{u}$, we automatically also have the squared amplitude for the invariant amplitude \mathcal{M}_3 :

$$\sum_{\text{spins}} |\mathcal{M}_3|^2 = 32g_s^4 \cdot \frac{4}{3} \left[\left(\frac{m_{\tilde{g}}^2 - \hat{u}}{m_{\tilde{q}}^2 - \hat{u}} \right)^2 \right]. \quad (4.29)$$

Now consider the squared amplitude obtained by combining diagrams one and two, keeping the expression for \mathcal{M}_2 in its general form (so that it describes the exchange of both types of scalar quark). We have

$$\begin{aligned} \sum_{\text{spins}} \mathcal{M}_1^\dagger \mathcal{M}_2 \Big|_{(\tilde{q}_L/\tilde{q}_R)} &= \sum_{\text{spins}} \frac{-g_s^4}{2\hat{s}(\hat{t} - m_{\tilde{q}}^2)} (-1)\bar{u}(p_1)\gamma_\mu v(p_2)(-1)\bar{v}(k_2)\gamma^\mu u(k_1) \\ &\quad \times \bar{u}(k_1)(1 \mp \gamma_5)u(p_1)\bar{v}(p_2)(1 \pm \gamma_5)v(k_2) \cdot \{\text{Tr}([t_B, t_A]t_B t_A)\}, \end{aligned} \quad (4.30)$$

the colour factor evaluates to give -6 , and by the spinor spin sum relations

$$\begin{aligned} \sum_{\text{spins}} \mathcal{M}_1^\dagger \mathcal{M}_2 \Big|_{(\tilde{q}_L/\tilde{q}_R)} &= \frac{6g_s^4}{2\hat{s}(\hat{t} - m_{\tilde{q}}^2)} \text{Tr}(\not{p}_2(1 \pm \gamma_5)(\not{k}_2 - m_{\tilde{g}})\gamma^\mu(\not{k}_1 + m_{\tilde{g}})(1 \mp \gamma_5)\not{p}_1\gamma_\mu) \\ &= \frac{24g_s^4}{\hat{s}(\hat{t} - m_{\tilde{q}}^2)} [2(k_1 \cdot p_1)2(p_2 \cdot k_2) + m_{\tilde{g}}^2 2(p_1 \cdot p_2)] \\ &= \frac{24g_s^4}{\hat{s}(\hat{t} - m_{\tilde{q}}^2)} [(m_{\tilde{g}}^2 - \hat{t})^2 + m_{\tilde{g}}^2 \hat{s}]. \end{aligned} \quad (4.31)$$

This squared amplitude is invariant with respect to the type of scalar quark exchanged in diagram \mathcal{M}_2 , therefore we may double it to include both contributions. By also adding the hermitian conjugate, we get

$$\sum_{\text{spins}} \mathcal{M}_1^\dagger \mathcal{M}_2 + \text{h.c.} = 32g_s^4 \cdot (-3) \left[\frac{(m_{\tilde{g}}^2 - \hat{t})^2 + m_{\tilde{g}}^2 \hat{s}}{\hat{s}(m_{\tilde{q}}^2 - \hat{t})} \right], \quad (4.32)$$

where the minus sign has come from the denominator. By again applying the crossing symmetry $\hat{t} \leftrightarrow \hat{u}$ we also find

$$\sum_{\text{spins}} \mathcal{M}_1^\dagger \mathcal{M}_3 + \text{h.c.} = 32g_s^4 \cdot (-3) \left[\frac{(m_{\tilde{g}}^2 - \hat{u})^2 + m_{\tilde{g}}^2 \hat{s}}{\hat{s}(m_{\tilde{q}}^2 - \hat{u})} \right]. \quad (4.33)$$

Lastly, we consider the squared amplitude $\mathcal{M}_2^\dagger \mathcal{M}_3$. As both of these amplitudes corresponds to two distinct diagrams, in order to distinguish the four possible combinations we introduce the phase factors ϕ_2 and ϕ_3 that we define as

$$\phi_i = \begin{cases} 1 & : \mathcal{M}_i | \tilde{q}_L \\ -1 & : \mathcal{M}_i | \tilde{q}_R \end{cases}, \quad (4.34)$$

for $i = 2, 3$. A general expression for this squared amplitude is then

$$\begin{aligned} \sum_{\text{spins}} \mathcal{M}_2^\dagger \mathcal{M}_3 \Big|_{(\phi_2, \phi_3)} &= \frac{-g_s^4}{4(\hat{t} - m_{\tilde{q}}^2)(\hat{u} - m_{\tilde{q}}^2)} \bar{u}(p_1)(1 + \phi_2 \gamma_5)u(k_1)\bar{v}(k_2)(1 - \phi_2 \gamma_5)v(p_2) \\ &\quad \times \bar{u}(k_2)(1 - \phi_3 \gamma_5)u(p_1)\bar{v}(p_2)(1 + \phi_3 \gamma_5)v(k_1) \cdot \{\text{Tr}(t_A t_B t_A t_B)\}, \end{aligned} \quad (4.35)$$

where the colour indices of spinors have been suppressed. The colour factor evaluates to $-6/9$. To be able to proceed using standard gamma matrix trace technology and the spinor sum relations, we need to rewrite the anti-fermion spinors in terms of fermion spinors. For this we use the spinor identities $u = C\bar{v}^T$ and $v = C\bar{u}^T$, where $C \equiv -i\gamma^2\gamma^0$ is the charge conjugation matrix satisfying $C^2 = -1$ and $[C, \gamma_5] = 0$. This gives the relation

$$\begin{aligned}\bar{v}(p)(1 \pm \phi_i\gamma_5)v(k) &= u^T(p)(-C)(1 \pm \phi_i\gamma_5)^T C\bar{u}^T(k) \\ &= (\bar{u}(k)(1 \pm \phi_i\gamma_5)(-C^2)u(p))^T \\ &= \bar{u}(k)(1 \pm \phi_i\gamma_5)u(p).\end{aligned}\tag{4.36}$$

Using the above relation to eliminate the anti-fermion spinors in equation (4.35) and then summing over spins, we have

$$\begin{aligned}\sum_{\text{spins}} \mathcal{M}_2^\dagger \mathcal{M}_3 \Big|_{(\phi_2, \phi_3)} &= \frac{3g_s^4}{18(\hat{t} - m_{\tilde{q}}^2)(\hat{u} - m_{\tilde{q}}^2)} \cdot \text{Tr}\left((\mathcal{K}_1 + m_{\tilde{g}})(1 + \phi_3\gamma_5)\not{p}_2(1 - \phi_2\gamma_5)\right. \\ &\quad \left. \times (\mathcal{K}_2 + m_{\tilde{g}})(1 - \phi_3\gamma_5)\not{p}_1(1 + \phi_2\gamma_5)\right).\end{aligned}\tag{4.37}$$

By commuting the terms containing γ_5 's together,

$$\begin{aligned}\sum_{\text{spins}} \mathcal{M}_2^\dagger \mathcal{M}_3 \Big|_{(\phi_2, \phi_3)} &= \frac{3g_s^4}{18(\hat{t} - m_{\tilde{q}}^2)(\hat{u} - m_{\tilde{q}}^2)} \cdot \text{Tr}\left((\mathcal{K}_1 + m_{\tilde{g}})(1 + \phi_3\gamma_5)(1 + \phi_2\gamma_5)\not{p}_2\right. \\ &\quad \left. \times (\mathcal{K}_2 + m_{\tilde{g}})(1 - \phi_3\gamma_5)(1 - \phi_2\gamma_5)\not{p}_1\right),\end{aligned}\tag{4.38}$$

we see that we must require $\phi_2 = \phi_3$ for this term not to go to zero. Therefore

$$\begin{aligned}\sum_{\text{spins}} \mathcal{M}_2^\dagger \mathcal{M}_3 \Big|_{\phi_2=\phi_3} &= \frac{3g_s^4}{18(\hat{t} - m_{\tilde{q}}^2)(\hat{u} - m_{\tilde{q}}^2)} \cdot 4 \left[\text{Tr}\left((\mathcal{K}_1 + m_{\tilde{g}})(1 + \phi_i\gamma_5)\not{p}_2\right.\right. \\ &\quad \left. \times (\mathcal{K}_2 + m_{\tilde{g}})(1 - \phi_i\gamma_5)\not{p}_1\right) \\ &\quad \left. + m_{\tilde{g}}^2 \text{Tr}((1 + \phi_i\gamma_5)\not{p}_2(1 - \phi_i\gamma_5)\not{p}_1) \right] \\ &= \frac{3g_s^4}{18(\hat{t} - m_{\tilde{q}}^2)(\hat{u} - m_{\tilde{q}}^2)} \cdot 4 \left[0 + m_{\tilde{g}}^2 \text{Tr}(2(1 + \phi_i\gamma_5)\not{p}_2\not{p}_1) \right] \\ &= \frac{3g_s^4}{18(\hat{t} - m_{\tilde{q}}^2)(\hat{u} - m_{\tilde{q}}^2)} \cdot 16 \left[m_{\tilde{g}}^2 \hat{s} \right].\end{aligned}\tag{4.39}$$

The squared amplitude above is invariant to the ϕ_i factor introduced, so we simply double this result to account for both $\phi_2 = \phi_3$ combinations. Also including the hermitian conjugate term, the last squared amplitude term is then

$$\sum_{\text{spins}} \mathcal{M}_2^\dagger \mathcal{M}_3 + \text{h.c} = 32g_s^4 \cdot \frac{1}{3} \left[\frac{m_{\tilde{g}}^2 \hat{s}}{(m_{\tilde{q}}^2 - \hat{t})(m_{\tilde{q}}^2 - \hat{u})} \right].\tag{4.40}$$

The full squared amplitude is the sum of equations (4.23), (4.28), (4.29), (4.32), (4.33) and (4.40):

$$\begin{aligned} \sum_{\text{spins}} |\mathcal{M}|^2 = 32g_s^4 \left\{ 3 \left[\frac{(m_{\hat{g}}^2 - \hat{u})^2 + (m_{\hat{g}}^2 - \hat{t})^2 + 2m_{\hat{g}}^2 \hat{s}}{\hat{s}^2} \right] + \frac{4}{3} \left[\left(\frac{m_{\hat{g}}^2 - \hat{t}}{m_{\hat{q}}^2 - \hat{t}} \right)^2 \right] \right. \\ + \frac{4}{3} \left[\left(\frac{m_{\hat{g}}^2 - \hat{u}}{m_{\hat{q}}^2 - \hat{u}} \right)^2 \right] - 3 \left[\frac{(m_{\hat{g}}^2 - \hat{t})^2 + m^2 \hat{s}}{\hat{s}(m_{\hat{q}}^2 - \hat{t})} \right] \\ \left. - 3 \left[\frac{(m_{\hat{g}}^2 - \hat{u})^2 + m_{\hat{g}}^2 \hat{s}}{\hat{s}(m_{\hat{q}}^2 - \hat{u})} \right] + \frac{1}{3} \left[\frac{m_{\hat{g}}^2 \hat{s}}{(m_{\hat{q}}^2 - \hat{t})(m_{\hat{q}}^2 - \hat{u})} \right] \right\} \quad (4.41) \end{aligned}$$

The cross section for a process with two incoming and outgoing particles is given by

$$\sigma = \frac{1}{\mathcal{F}} \int dPS(2) \overline{\sum_{\text{spins}} |\mathcal{M}|^2} = \frac{1}{16\pi} \frac{1}{\lambda(\hat{s}, m_1^2, m_2^2)} \int d\hat{t} \overline{\sum_{\text{spins}} |\mathcal{M}|^2}. \quad (4.42)$$

The bar denotes spin and colour averaging, m_1 and m_2 are the masses of the incoming particles, in this case zero, and so for our purposes $\lambda(\hat{s}, 0, 0) = \hat{s}^2$. Note that if the two outgoing particles are indistinguishable, as is the case for two outgoing gluinos (Majorana fermions), we must include an extra factor of $1/2!$ to the total cross section. With the cross section given in this form, it is clear to see that the differential cross section with respect to the Mandelstam variable \hat{t} is

$$\frac{d\sigma}{d\hat{t}} = \frac{1}{16\pi} \frac{1}{\hat{s}^2} \overline{\sum_{\text{spins}} |\mathcal{M}|^2} \quad (4.43)$$

$$= \frac{1}{16\pi} \frac{1}{\hat{s}^2} \underbrace{\left(\frac{1}{3}\right)^2}_{\text{colour}} \underbrace{\left(\frac{1}{2}\right)^2}_{\text{spin}} \overline{\sum_{\text{spins}} |\mathcal{M}|^2} \quad (4.44)$$

$$= \left(\frac{g_s^2}{4\pi}\right)^2 \frac{\pi}{9} \frac{32}{4} \frac{1}{\hat{s}^2} \left\{ \dots \right\}, \quad (4.45)$$

where the Mandelstam variables satisfy the condition

$$\hat{s} + \hat{t} + \hat{u} = \sum_i m_i^2 = 2m_{\hat{g}}^2. \quad (4.46)$$

Making the substitution $\alpha_s = g_s^2/4\pi$, we finally arrive at the differential cross section

for gluino pair production via quark-anti-quark annihilation

$$\begin{aligned} \frac{d\sigma}{d\hat{t}} = \frac{8\pi}{9} \frac{\alpha_s^2}{\hat{s}^2} \left\{ 3 \left[\frac{(m_{\tilde{g}}^2 - \hat{u})^2 + (m_{\tilde{g}}^2 - \hat{t})^2 + 2m_{\tilde{g}}^2 \hat{s}}{\hat{s}^2} \right] + \frac{4}{3} \left[\left(\frac{m_{\tilde{g}}^2 - \hat{t}}{m_{\tilde{q}}^2 - \hat{t}} \right)^2 \right] \right. \\ \left. + \frac{4}{3} \left[\left(\frac{m_{\tilde{g}}^2 - \hat{u}}{m_{\tilde{q}}^2 - \hat{u}} \right)^2 \right] - 3 \left[\frac{(m_{\tilde{g}}^2 - \hat{t})^2 + m_{\tilde{g}}^2 \hat{s}}{\hat{s}(m_{\tilde{q}}^2 - \hat{t})} \right] \right. \\ \left. - 3 \left[\frac{(m_{\tilde{g}}^2 - \hat{u})^2 + m_{\tilde{g}}^2 \hat{s}}{\hat{s}(m_{\tilde{q}}^2 - \hat{u})} \right] + \frac{1}{3} \left[\frac{m_{\tilde{g}}^2 \hat{s}}{(m_{\tilde{q}}^2 - \hat{t})(m_{\tilde{q}}^2 - \hat{u})} \right] \right\}. \end{aligned} \quad (4.47)$$

To calculate the total cross section from (4.47) it is convenient to choose a specific reference frame. Here we take the centre of momentum frame, aligning the direction of the incoming particles with the \hat{z} axis. Thus

$$\begin{aligned} p_1 &= \frac{\sqrt{\hat{s}}}{2}(1, \hat{z}), & k_1 &= \frac{\sqrt{\hat{s}}}{2}(1, \beta \hat{n}), \\ p_2 &= \frac{\sqrt{\hat{s}}}{2}(1, -\hat{z}), & k_2 &= \frac{\sqrt{\hat{s}}}{2}(1, -\beta \hat{n}), \end{aligned} \quad (4.48)$$

where

$$\beta = \sqrt{1 - \frac{4m_{\tilde{g}}^2}{\hat{s}}}, \quad (4.49)$$

and \hat{n} is the direction of the outgoing particles, with $\hat{n} \cdot \hat{z} = \cos \theta$. In this frame

$$\hat{t} - m_{\tilde{g}}^2 = -2p_1 \cdot k_1 = -2(p_1^0 k_1^0 - \mathbf{p}_1 \cdot \mathbf{k}_1) = -\frac{\hat{s}}{2}(1 - \beta \cos \theta), \quad (4.50)$$

so that the domain of \hat{t} is given by

$$-\frac{\hat{s}}{2}(1 + \beta) + m_{\tilde{g}}^2 \leq \hat{t} \leq -\frac{\hat{s}}{2}(1 - \beta) + m_{\tilde{g}}^2. \quad (4.51)$$

The total cross section is thus given by

$$\sigma(q\bar{q} \rightarrow \tilde{g}\tilde{g}) = \frac{1}{2!} \int_{-\frac{\hat{s}}{2}(1+\beta)+m_{\tilde{g}}^2}^{-\frac{\hat{s}}{2}(1-\beta)+m_{\tilde{g}}^2} d\hat{t} \left(\frac{d\sigma}{d\hat{t}} \Big|_{\hat{s} + \hat{t} + \hat{u} = 2m_{\tilde{g}}^2} \right), \quad (4.52)$$

where a factor of $1/n!$ has been included to correct for the over counting of indistinguishable outgoing particles (in this case two gluino Majorana fermions). Performing the integral, we arrive at the following analytical result for the total cross

section of gluino production via quark anti-quark annihilation

$$\begin{aligned} \sigma(q\bar{q} \rightarrow \tilde{g}\tilde{g}) = & \frac{4\pi\alpha_s^2}{27\hat{s}^2} \theta(\hat{s} - 4m_{\tilde{g}}^2) \left\{ \right. \\ & \beta \cdot \left[\frac{-6(m_{\tilde{g}}^2 - 3m_{\tilde{q}}^2)(m_{\tilde{g}}^2 - m_{\tilde{q}}^2)^2 + (13m_{\tilde{g}}^4 - 32m_{\tilde{g}}^2m_{\tilde{q}}^2 + 31m_{\tilde{q}}^4)\hat{s} + 5m_{\tilde{q}}^2\hat{s}^2}{(m_{\tilde{g}}^2 - m_{\tilde{q}}^2)^2 + m_{\tilde{g}}^2\hat{s}} \right] \\ & - 2 \ln \left(\frac{2m_{\tilde{g}}^2 - 2m_{\tilde{q}}^2 - \hat{s}(1 - \beta)}{2m_{\tilde{g}}^2 - 2m_{\tilde{q}}^2 - \hat{s}(1 + \beta)} \right) \\ & \left. \times \left[\frac{18(m_{\tilde{g}}^2 - m_{\tilde{q}}^2)^3 - (7m_{\tilde{g}}^2 - 25m_{\tilde{q}}^2)(m_{\tilde{g}}^2 - m_{\tilde{q}}^2)\hat{s} - 8m_{\tilde{q}}^2\hat{s}^2}{\hat{s}(2m_{\tilde{q}}^2 - 2m_{\tilde{g}}^2 + \hat{s})} \right] \right\}. \quad (4.53) \end{aligned}$$

The step function θ ensures the process only occurs when the incoming energy $\sqrt{\hat{s}}$ is greater than two gluino masses.

Gluon fusion

Aside from quark-anti-quark annihilation, the only other tree level process by which a pair of gluinos can be produced from incoming Standard Model particles is gluon fusion $g + g \rightarrow \tilde{g} + \tilde{g}$. As we will explain in section 4.3, the cross sections for these two (partonic) processes can be combined to give hadronic cross sections for gluino production, such as proton-proton collisions. The Feynman diagrams are shown in figure 4.3. The differential cross section for gluon fusion producing two gluinos is

$$\begin{aligned} \frac{d\sigma}{d\hat{t}}(gg \rightarrow \tilde{g}\tilde{g}) = & \frac{9\pi}{4} \frac{\alpha_s^2}{\hat{s}^2} \left\{ \left[\frac{2(m_{\tilde{g}}^2 - \hat{t})(m_{\tilde{g}}^2 - \hat{u})}{\hat{s}^2} \right] + \left[\frac{(m_{\tilde{g}}^2 - \hat{t})(m_{\tilde{g}}^2 - \hat{u}) - 2m_{\tilde{g}}^2(m_{\tilde{g}}^2 + \hat{t})}{(m_{\tilde{g}}^2 - \hat{t})^2} \right] \right. \\ & + \left[\frac{(m_{\tilde{g}}^2 - \hat{t})(m_{\tilde{g}}^2 - \hat{u}) - 2m_{\tilde{g}}^2(m_{\tilde{g}}^2 + \hat{u})}{(m_{\tilde{g}}^2 - \hat{u})^2} \right] + \left[\frac{m_{\tilde{g}}^2(\hat{s} - 4m_{\tilde{g}}^2)}{(m_{\tilde{g}}^2 - \hat{t})(m_{\tilde{g}}^2 - \hat{u})} \right] \\ & \left. - \left[\frac{(m_{\tilde{g}}^2 - \hat{t})(m_{\tilde{g}}^2 - \hat{u}) + m_{\tilde{g}}^2(\hat{u} - \hat{t})}{\hat{s}(m_{\tilde{g}}^2 - \hat{t})^2} \right] - \left[\frac{(m_{\tilde{g}}^2 - \hat{t})(m_{\tilde{g}}^2 - \hat{u}) + m_{\tilde{g}}^2(\hat{t} - \hat{u})}{\hat{s}(m_{\tilde{g}}^2 - \hat{u})^2} \right] \right\}, \quad (4.54) \end{aligned}$$

giving a total cross section of

$$\begin{aligned} \sigma(gg \rightarrow \tilde{g}\tilde{g}) = & \frac{3\pi\alpha_s^2}{4\hat{s}^2} \theta(\hat{s} - 4m_{\tilde{g}}^2) \left\{ -\hat{s}\beta \cdot [17m_{\tilde{g}}^2 + 4\hat{s}] \right. \\ & \left. + 3 \ln \left(\frac{1 - \beta}{1 + \beta} \right) \cdot [4m_{\tilde{g}}^4 - 4m_{\tilde{g}}^2\hat{s} - \hat{s}^2] \right\}, \quad (4.55) \end{aligned}$$

with all variables and parameters as defined in the previous section.

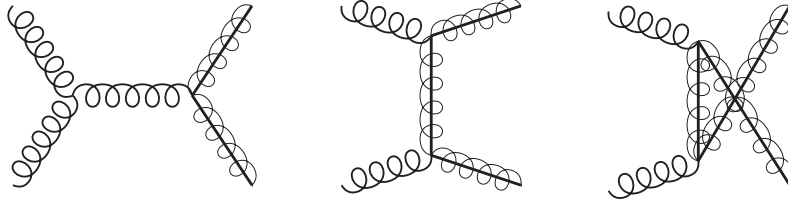


Figure 4.3: The tree level Feynman diagrams for gluon fusion to gluino production.

4.2.2 Kinematic distributions

The total cross section of a process, when combined with the luminosity of a given experiment, gives the probability of the event occurring. To see how this probability is distributed with respect to the kinematic properties of the outgoing particles, we can histogram the differential cross section against the kinematics. One typically chooses kinematical variables that are straight forward to measure in a particle detector, such as the transverse momentum, rapidity, pseudo-rapidity and azimuthal angle of a detected particle. Both the rapidity and pseudo-rapidity of a particle give a measure of the angle the particle makes with the beam pipe axis (\hat{z}). However, unlike the rapidity y , the pseudo-rapidity η does not depend on the energy of the particle:

$$\eta = \frac{1}{2} \ln \left(\frac{|\mathbf{k}| + k_L}{|\mathbf{k}| - k_L} \right), \quad (4.56)$$

where k_L is the longitudinal (as opposed to transverse) component of the momentum.

In the preceding section we derived the differential cross section (4.47) in terms of Lorentz invariant parameters, and switched to the centre of momentum frame to perform the total cross section integration. We may rewrite the differential cross section with respect to non-Lorentz invariant parameters such as the outgoing transverse momentum $|\mathbf{k}_1^T| = |\mathbf{k}_2^T|$ by simply applying the chain rule

$$\frac{d\sigma}{d|\mathbf{k}_1^T|} = \frac{dt}{d|\mathbf{k}_1^T|} \frac{d\sigma}{dt} \Big|_{t \rightarrow |\mathbf{k}_1^T|}. \quad (4.57)$$

To do this explicitly we switch to light-cone coordinates:

$$k_1^\pm = \frac{k_1^0 \pm k_1^3}{\sqrt{2}}, \quad (4.58)$$

$$\mathbf{k}_1^T = (k_1^1, k_1^2), \quad (4.59)$$

so that the Mandelstam variables may be written as

$$\hat{t} = (p_1 - k_1)^2 = m_{\tilde{g}}^2 - 2p_1 \cdot k_1 = m_{\tilde{g}}^2 - \sqrt{2\hat{s}} k_1^-, \quad (4.60)$$

$$\hat{u} = (p_1 - k_2)^2 = m_{\tilde{g}}^2 - 2p_1 \cdot k_2 = m_{\tilde{g}}^2 - \sqrt{2\hat{s}} k_1^+. \quad (4.61)$$

Using that

$$k_1^2 = m_{\tilde{g}}^2 = (k_1^0)^2 - \sum_{i=1}^2 (k_1^i)^2 - (k_1^3)^2 = 2k_1^+ k_1^- - |\mathbf{k}_1^T|^2, \quad (4.62)$$

together with equations (4.60) and (4.61), gives an expression relating the outgoing transverse momentum to the Mandelstam variables

$$\begin{aligned} |\mathbf{k}_1^T|^2 &= 2k_1^+ k_1^- - m_{\tilde{g}}^2 \\ &= \frac{(m_{\tilde{g}}^2 - \hat{t})(m_{\tilde{g}}^2 - \hat{u})}{\hat{s}} - m_{\tilde{g}}^2 \\ &= \frac{(m_{\tilde{g}}^2 - \hat{t})(\hat{s} + \hat{t} - m_{\tilde{g}}^2)}{\hat{s}} - m_{\tilde{g}}^2. \end{aligned} \quad (4.63)$$

Solving for \hat{t} in terms of the transverse momentum gives

$$\hat{t} = \frac{\hat{s}}{2} \left(-1 \pm \sqrt{1 - \frac{4}{\hat{s}} (m_{\tilde{g}}^2 + |\mathbf{k}_1^T|^2)} \right) + m_{\tilde{g}}^2, \quad (4.64)$$

and similarly the inverse is given by

$$|\mathbf{k}_1^T| = \sqrt{-\frac{1}{\hat{s}}(\hat{t} - m_{\tilde{g}}^2)^2 - \hat{t}}. \quad (4.65)$$

The maximum transverse momentum is $|\mathbf{k}_1^T|(\hat{t}_c) = (\sqrt{\hat{s}}/2)\beta$ at $\hat{t}_c = -\hat{s}/2 + m_{\tilde{g}}^2$. The Jacobian factor is computed as follows:

$$\begin{aligned} \frac{dt}{d|\mathbf{k}_1^T|} &= \pm \frac{\hat{s}}{4} \left(1 - \frac{4}{\hat{s}} (m_{\tilde{g}}^2 + |\mathbf{k}_1^T|^2) \right)^{-\frac{1}{2}} \cdot \frac{4}{\hat{s}} \cdot 2 |\mathbf{k}_1^T| \\ &= \frac{\sqrt{\hat{s}} |\mathbf{k}_1^T|}{\sqrt{\frac{1}{4}\hat{s} - m_{\tilde{g}}^2 - |\mathbf{k}_1^T|^2}}, \end{aligned} \quad (4.66)$$

giving the differential cross section with respect to the outgoing transverse momentum as

$$\frac{d\sigma}{d|\mathbf{k}_1^T|} = \frac{\sqrt{\hat{s}} |\mathbf{k}_1^T|}{\sqrt{\frac{1}{4}\hat{s} - m_{\tilde{g}}^2 - |\mathbf{k}_1^T|^2}} \cdot \frac{d\sigma}{dt} \Big|_{t \rightarrow |\mathbf{k}_1^T|}. \quad (4.67)$$

Rapidity in the centre of momentum frame can be treated in a similar way:

$$\begin{aligned} y_1 &= \frac{1}{2} \ln \left(\frac{k_1^0 + k_1^3}{k_1^0 - k_1^3} \right) = \frac{1}{2} \ln \left(\frac{k_1^+}{k_1^-} \right) \\ &= \frac{1}{2} \ln \left(\frac{\hat{s} + \hat{t} - m_{\tilde{g}}^2}{m_{\tilde{g}}^2 - \hat{u}} \right). \end{aligned} \quad (4.68)$$

Solving for \hat{t} gives

$$\hat{t} = -\frac{\hat{s}}{1 + (e^{y_1})^2} + m_{\hat{g}}^2. \quad (4.69)$$

Thus the Jacobian becomes

$$\frac{dt}{dy_1} = 2\hat{s} \left(\frac{e^{y_1}}{1 + (e^{y_1})^2} \right)^2, \quad (4.70)$$

and the differential cross section with respect to the rapidity of the first outgoing particle is

$$\frac{d\sigma}{dy_1} = 2\hat{s} \left(\frac{e^{y_1}}{1 + (e^{y_1})^2} \right)^2 \cdot \frac{d\sigma}{dt} \Big|_{t \rightarrow y_1}. \quad (4.71)$$

4.3 From partons to hadrons

The running of the strong coupling constant with respect to the renormalization parameter μ at the one loop level is given by

$$\alpha_s(\mu) = \frac{\alpha_s(\mu_0)}{(\alpha_s(\mu_0)\beta_0/2\pi) \ln\left(\frac{\mu}{\mu_0}\right) + 1}, \quad (4.72)$$

where μ_0 and $\alpha_s(\mu_0)$ specify a fixed renormalization point (see appendix B for a brief discussion and derivation of the strong coupling constant). The arbitrary parameter μ is typically set equal to an invariant energy scale Q of the process in question. The constant β_0 is dependent on the Casimirs of the gauge group to which α_s is a coupling (see equation B.5). In the case of strong interactions the gauge group is SU(3) colour, so that $\beta_0 = 11 - 2n_f/3$ and is therefore positive for the six known quark flavours. The positive sign of β_0 has an important implication for the running coupling behavior, as it implies that quarks and gluons are asymptotically free at high energies

$$\lim_{\mu \rightarrow \infty} \alpha_s(\mu) = 0, \quad (4.73)$$

and confined at low energies

$$\lim_{\mu \rightarrow \Lambda^+} \alpha_s(\mu) = \infty, \quad (4.74)$$

where Λ is the QCD mass scale (refer to appendix B). This confining behavior of strongly interacting particles at low energies means that they assemble into various bound states, known as hadrons. Detecting an isolated particle is not possible, as the energy required for its liberation is enough to create new particles from the vacuum for it to bind with.

A phenomenological means of dealing with the confinement of quarks and gluons is known as the *parton model*, with quarks and gluons collectively referred to

as partons. In this model, a hadron is thought of as both containing its defining bounded quarks as well as a sea of virtual quarks and gluons. A particle interacting with this hadron is presented with probabilities for encountering any given parton inside the hadron at some specific point in phase space. These probabilities can be determined empirically using deep inelastic scattering experiments and turn out to be process independent for each parton-hadron combination. Specifically, a particle scattering with a hadron h carrying momentum P has a probability $f_a^h(x, \mu_F)$ of scattering solely with a parton a carrying momentum $p = xP$ where $x \in [0, 1]$ is known as the momentum fraction. Here μ_F is the factorization scale and is typically set equal to the renormalization scale $\mu_F = \mu_R = Q$. These functions $f_a^h(x, \mu_F)$ are known as parton distribution functions (PDFs) and must sum to unity when integrated over the momentum fraction space x ,

$$\int_0^1 dx \left[\sum_q f_q^h(x) + \sum_{\bar{q}} f_{\bar{q}}^h(x) + f_g^h(x) \right] = 1, \quad (4.75)$$

where q, \bar{q} and g are all the partons assumed to be present in the hadron h .

In the case of gluino production at the LHC we are interested in proton-proton collisions. The two possible scenarios in the parton model are then a quark from one proton annihilating with an anti-quark from the other, or gluons from each proton fusing together. The parton level cross sections for both scenarios have already been worked out in the previous sections. Assigning the protons momenta P_1 and P_2 , the total invariant mass for this process is $S = (P_1 + P_2)^2$. The invariant mass for the parton level cross sections will depend on the momentum fractions of each parton, and is thus $\hat{s} = (x_1 P_1 + x_2 P_2)^2$. By integrating over the entire momentum fraction space and summing over all the possible parton combinations, the proton-proton cross section can be written in terms of the proton PDFs f as

$$\begin{aligned} \sigma(pp \rightarrow \tilde{g}\tilde{g}) = \int_0^1 dx_1 \int_0^1 dx_2 \left\{ \sum_{q, \bar{q}} f_{q, \bar{q}}(x_1, \mu_F) f_{\bar{q}, q}(x_2, \mu_F) \cdot \hat{\sigma}(q\bar{q} \rightarrow \tilde{g}\tilde{g}) \Big|_{\hat{s}} \right. \\ \left. + f_g(x_1, \mu_F) f_g(x_2, \mu_F) \cdot \hat{\sigma}(gg \rightarrow \tilde{g}\tilde{g}) \Big|_{\hat{s}} \right\}. \quad (4.76) \end{aligned}$$

Jets

Due to conservation of momentum, the hadrons formed from a highly energetic outgoing parton will continue to travel in mostly the same direction, forming a narrow cone-like structure of particles known as a *jet*. All processes involving outgoing partons in hadron colliders will result in the production of jets. By making careful measurements of these jets it is possible to deduce the original four momentum of the outgoing parton and thus learn more about the underlying hard scattering process. In section 7.1 we discuss the possibility of identifying whether a heavy parton, specifically a b -quark, spawned a given jet.

4.4 Cascade decays

The LHC is a hadron collider, therefore the dominant MSSM production processes will be from strong SUSY interactions. Specifically, the production of either a pair of gluinos or a pair of quarks will dominate. In the case of two gluinos being produced, most decays proceed via its quark-squark coupling, where the squark could be virtual (as may be necessary kinematically). Unlike the gluino, the squark also couples electroweakly, and so has many decay channels open to it, including to neutralinos and charginos. Neutralinos and charginos can decay to a variety of squarks and sleptons, which may in turn decay into lighter neutralino and chargino states. If R-parity (or a similar symmetry) is conserved, this decay chain of supersymmetric particles must terminate at the lightest supersymmetric particle (LSP) that in most realistic theories is the lightest neutralino state (see section 3.3.1). Because the neutralinos are electrically neutral and weakly interacting, a pair of them (deriving from the initial pair of gluinos or squarks) is expected to leave a hadron collider without direct detection for each supersymmetric process. Indirectly a pair of neutralinos can be detected by measuring high missing transverse energy corresponding to their sizable masses. An example of a MSSM cascade decay process is shown in figure 4.4. Typical signatures of such a process are thus high missing transverse energy as well as many jets and many leptons.

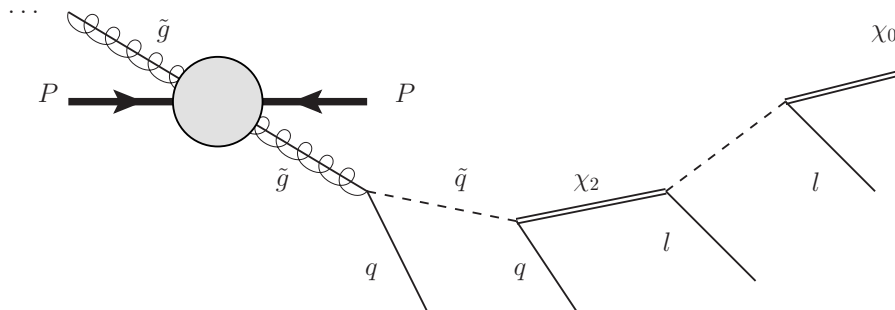


Figure 4.4: A typical MSSM cascade decay at the LHC starting from a strongly produced gluino pair.

The initial aim of this thesis was to consider what SUSY processes could have significant single top backgrounds. However, as discussed in chapter 7, Standard Model single top processes with missing transverse energy (from an escaping neutrino) characteristically emit just one lepton and very few jets (at least two, of which at least one is b-tagged). MSSM processes involving supersymmetric particles therefore have a negligible single top background. This shifted the focus of this thesis away from the MSSM and towards SUSY models that do have signals that mimic single top. One such model is discussed in the following chapter.

4.5 Technical aside: Majorana Feynman rules

A Majorana fermion is a Dirac fermion ψ that is self conjugate i.e. it satisfies the condition

$$\psi = \psi^c = C\bar{\psi}^T, \quad (4.77)$$

where C is the charge conjugation matrix (defined in equation (A.15)). Equivalently, a Majorana fermion is said to be its own anti-particle, and thereby does not have the same notion of fermion number (charge) conservation that Dirac fermions do. By naïve substitution of the above Majorana condition into the Dirac propagator $\langle 0 | T\psi(x)\bar{\psi}(y) | 0 \rangle = S(x-y)$, we see that the propagators $\langle 0 | T\bar{\psi}(x)\bar{\psi}(y) | 0 \rangle$ and $\langle 0 | T\psi(x)\psi(y) | 0 \rangle$, which both violate fermion number, no longer vanish as they do for the Dirac case.

There are various prescriptions given in the literature for dealing with Majorana fermions in Feynman diagrams. For convenience, most attempt to stay as close as possible to the well developed and familiar Dirac technology. One approach is given by Haber *et al.* [9], whose rules include three propagators and multiple vertex combinations, with C matrices appearing where fermion number is violated. In these rules, once a fermion chain has been written down, the C matrices present can be absorbed using the gamma matrix relations (A.17) and (A.18) and the spinor identities

$$u = C\bar{v}^T \quad \text{and} \quad v = C\bar{u}^T. \quad (4.78)$$

Having to commute and absorb C matrices in this way, however, is cumbersome. Furthermore, as it stands this method can give an ambiguous sign corresponding to the ambiguous choice of which end of the fermion chain one starts at (clearly the familiar convention of starting at an outgoing fermion no longer applies). To take care of this ambiguous sign, an arbitrary direction known as the fermion flow is introduced along the entire fermion chain, and a convention, such as beginning the rules from the outgoing end, is defined. The most elegant and compact example of Majorana Feynman rules with fermion flow that we found was by Denner *et al.* [10], whose rules avoid the explicit appearance of C matrices. We give the same prescription here in a slightly more compact form.

We write a generic Lagrangian interaction term between fermions χ and ψ (Dirac or Majorana) and a bosonic field Φ (easily generalized to multiple fields) as

$$\bar{\chi}\Gamma\psi \cdot \Phi = h_{abc}^i \bar{\chi}_a \Gamma_i \psi_b \Phi_c \quad (4.79)$$

where a, b and c label momentum and quantum numbers, $h_{abc}^i \in \mathbb{C}$ are the relevant prefactors and

$$\Gamma_i = 1, i\gamma_5, \gamma_\mu\gamma_5, \gamma_\mu, \sigma_{\mu\nu}. \quad (4.80)$$

The Γ_i have been defined in this way to satisfy the condition

$$\Gamma_i^\dagger = \gamma^0 \Gamma_i \gamma^0 \quad (4.81)$$

We further define

$$\Gamma' \equiv C\Gamma^T C^\dagger, \quad (4.82)$$

and observe that by relations (A.17) and (A.18) we may write $\Gamma' = h_{abc}^i \Gamma'_i$ with

$$\Gamma'_i = \eta_i \Gamma_i \quad (\text{no sum}), \quad \text{for} \quad \eta_i = \begin{cases} 1 & \Gamma_i = 1, i\gamma_5, \gamma_\mu\gamma_5 \\ -1 & \Gamma_i = \gamma_\mu, \sigma_{\mu\nu} \end{cases}. \quad (4.83)$$

Similarly, we write the momentum space (Dirac and Majorana) fermion propagator as

$$S(p) = \frac{i(\not{p} - m)}{p^2 - m^2 + i\epsilon}, \quad (4.84)$$

and observe that

$$CS(p)^T C^\dagger = S(-p). \quad (4.85)$$

To help compactify the Feynman rules, we introduce notation where a directed double line represents either a Dirac fermion with charge flow² along the same direction or a Majorana fermion carrying no fermion number (and hence undirected):

$$\begin{array}{c} \Rightarrow \\ \Rightarrow \\ \Rightarrow \end{array} \equiv \begin{cases} \begin{array}{c} \longrightarrow \\ \longrightarrow \end{array} & \text{Dirac} \\ \begin{array}{c} \longleftarrow \\ \longleftarrow \end{array} & \text{Majorana} \end{cases} \quad (4.86)$$

Fermion flow is an arbitrary direction chosen along an entire fermion chain, which we denote by a separate arrow moving alongside it. Every vertex on the chain will therefore have a charge flow direction (necessarily conserved if both the ingoing and outgoing fermions are Dirac) and a fermion flow direction. When the fermion flow and charge flow directions coincide, or where there is no charge flow present (i.e. only Majorana fermions), we assign the standard $i\Gamma$ term to the vertex. Whereas when fermion flow and charge flow are opposite in direction, we instead assign the $i\Gamma'$ term. Using the notation introduced above, we can write these fermion flow vertex rules compactly by the following three diagrams:

$$\begin{array}{c} \text{---} \\ \text{---} \end{array} \begin{array}{c} \longrightarrow \\ \longrightarrow \end{array} \begin{array}{c} \curvearrowright \\ \curvearrowright \end{array} i\Gamma, \quad \begin{array}{c} \text{---} \\ \text{---} \end{array} \begin{array}{c} \longrightarrow \\ \longrightarrow \end{array} \begin{array}{c} \curvearrowleft \\ \curvearrowleft \end{array} i\Gamma', \quad \begin{array}{c} \text{---} \\ \text{---} \end{array} \begin{array}{c} \longleftarrow \\ \longleftarrow \end{array} \begin{array}{c} \curvearrowleft \\ \curvearrowleft \end{array} i\Gamma' \quad (4.87)$$

In the same sense, there are two possible propagators, one for which fermion flow and charge flow (if present) align, and the other where they are in opposite direc-

²We refrain from using the equally valid term *fermion number* to avoid confusion with the newly introduced and independent notion of fermion flow.

tions:

$$\begin{array}{ccc}
 \begin{array}{c} \text{====>====} \\ \text{----->} \end{array} & S(p) & \xrightarrow{p} \\
 \begin{array}{c} \text{-----<} \\ \text{====<====} \end{array} & S(-p) &
 \end{array} \quad (4.88)$$

Lastly, spinors are assigned to external fermions based solely on the direction of fermion flow, completely independent of the type of fermion or its possible charge (we denote such general fermions here with single lines):

$$\begin{array}{ccc}
 \begin{array}{c} \bullet \text{-----} \\ \text{----->} \end{array} & \bar{u}(p) & \begin{array}{c} \text{-----} \bullet \\ \text{----->} \end{array} & u(p) & \xrightarrow{p} \\
 \begin{array}{c} \bullet \text{-----} \\ \text{-----<} \end{array} & v(p) & \begin{array}{c} \text{-----} \bullet \\ \text{-----<} \end{array} & \bar{v}(p) &
 \end{array} \quad (4.89)$$

Momentum in all these rules is taken to be flowing from left to right.

We thus state the Majorana Feynman rules:

1. Assign an arbitrary direction of fermion flow along the fermion chain (either direction gives an equivalent answer).
2. Starting opposite to the chosen direction of fermion flow, insert the relevant vertex, propagator and external spinor terms in accordance with the fermion flow direction.
3. Include a factor of -1 for every closed fermion loop in the diagram.
4. Include a combinatorial factor of $1/2$ for identical Majorana fermions occurring in closed self energy loop diagrams.

When calculating multiple diagrams in the construction of a total squared amplitude, a relative minus sign can arise between them from the operator reduction process (assuming here canonical quantization, but similarly in the path integral formalism). To see this, consider a two to two fermion process

$$\langle \chi_D \chi_C | S | \psi_A \bar{\psi}_B \rangle = i(2\pi)^4 \delta^4(k_D + k_C - p_B - p_A) \mathcal{M}(\psi_A \bar{\psi}_B \rightarrow \chi_C \chi_D). \quad (4.90)$$

where ψ and χ are Dirac and Majorana fermion fields respectively and

$$S = \exp \left[-i \int d^4x \mathcal{H}_{\text{int}} \right]. \quad (4.91)$$

is the scattering matrix. At tree level, the s and t-channel amplitudes for such a process take the generic form

$$\mathcal{M}_s \propto \bar{u}_C \Gamma v_D \bar{v}_B \Gamma u_A \quad \text{and} \quad \mathcal{M}_t \propto \bar{u}_C \Gamma u_A \bar{v}_B \Gamma v_D. \quad (4.92)$$

The corresponding S-matrix form of these amplitudes is

$$\mathcal{M}_s \rightarrow \langle \chi_D \chi_C | \chi_C \chi_D \bar{\psi}_B \psi_A | \psi_A \bar{\psi}_B \rangle \rightarrow +1, \quad (4.93)$$

$$\mathcal{M}_t \rightarrow \langle \chi_D \chi_C | \chi_C \psi_A \bar{\psi}_B \chi_D | \psi_A \bar{\psi}_B \rangle \rightarrow -1, \quad (4.94)$$

where we see a relative minus sign arise due to a difference in the number of anti-commutations required to perform the operator reduction. Clearly, the choice of initial and final states is arbitrary, so that the s-channel diagram could have just as easily acquired the minus sign. Because we are interested only in squared amplitudes, only the relative sign between diagrams is needed for computing interference terms. We therefore state one additional Feynman rule:

5. Where a given squared amplitude has more than one contributing diagrams, pick one diagram whose spinor ordering will serve as a reference. Then for all other contributing diagrams whose spinor ordering is an odd permutation of the reference order, include a factor of -1 .

Once the invariant amplitudes containing Majorana fermions have been computed using the Majorana Feynman rules above, they may be squared by the usual (Dirac) method (fermion flow is no longer needed). In some cases the calculation of interference terms may require a sum over spins for non-standard spinor combinations. The identities given in (4.78) can then be used to convert to the standard spinor sum expressions given in (A.13), modulo C matrices that must be eliminated in the standard way using relations (A.17) and (A.18). Alternatively, one could treat each term in the squared amplitude as one complete fermion chain and use the fermion flow formalism for the entire calculation, thereby avoiding any potential C matrix manipulations.

As a final consideration, given a Majorana interaction vertex of the form given in (4.79), its Hermitian conjugate is also a valid and typically distinct vertex for the theory. Specifically,

$$\begin{aligned} (\bar{\chi} \Gamma \psi)^\dagger &= [h_{abc}^i (\bar{\chi}_a)_\alpha (\Gamma_i)_{\alpha\beta} (\psi_b)_\beta \Phi_c]^\dagger \\ &= (h_{abc}^i)^* (\psi_b^\dagger)_\beta \left(\Gamma_i^\dagger \right)_{\beta\delta} \left(\gamma_0^\dagger \right)_{\delta\alpha} (\chi_a)_\alpha \Phi_c^*, \end{aligned} \quad (4.95)$$

where using the defining Γ_i condition given by equation (4.81),

$$\begin{aligned} (\bar{\chi} \Gamma \psi)^\dagger &= (h_{abc}^i)^* (\bar{\psi}_b)_\beta (\Gamma_i)_{\beta\alpha} (\chi_a)_\alpha \Phi_c^* \\ &= (h_{abc}^i)^* \bar{\psi}_b \Gamma_i^T \chi_a \Phi_c^* \end{aligned} \quad (4.96)$$

The Feynman rule for this Hermitian conjugate vertex, obtained by dropping the field terms and including a factor of i , is thus

$$(i\Gamma)^c = i(h_{abc}^i)^* \Gamma_i^T, \quad (4.97)$$

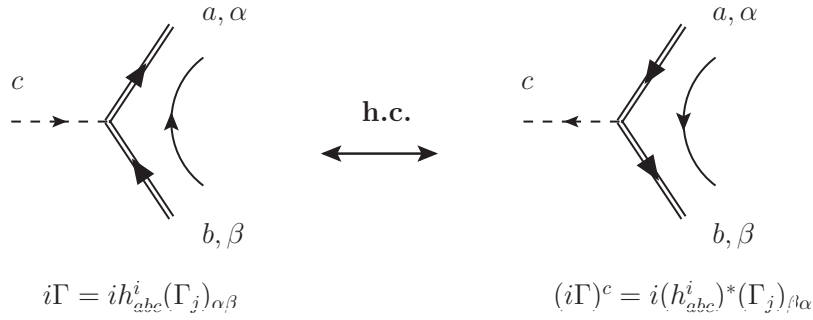


Figure 4.5: The relation between the Feynman rules for a generic Majorana vertex and its Hermitian conjugate.

as shown in figure 4.5. Note that taking the Hermitian conjugate of Γ in this way is strictly distinct from reversing the fermion flow of a vertex to obtain Γ' . Consider as an example the Feynman rule for a vertex containing a chiral projection operator

$$i\Gamma = ih_{abc}^i \Gamma_i = i\frac{1}{2}(1 \pm \gamma_5), \quad (4.98)$$

this has as its Hermitian conjugate vertex

$$\begin{aligned} (i\Gamma)^c &= i(h_{abc}^i)^* [\Gamma_i]^T = i\frac{1}{2}\{(1)^*[1]^T \pm (-i)^*[i\gamma_5]^T\} \\ &= i\frac{1}{2}(1 \mp \gamma_5). \end{aligned} \quad (4.99)$$

4.5.1 Sample calculation

To illustrate how our Majorana rules work, we calculate the invariant amplitude for the supersymmetric process of two incoming electrons (Dirac fermions) exchanging a photino (Majorana fermion) to give two left scalar electrons. The Feynman diagram is shown in figure 4.6, where we have picked an *arbitrary* direction of fermion flow. The two vertices of this diagram are the same, and we begin by labeling them with $i\Gamma$ (when fermion flow coincides with charge flow). Starting opposite to the direction of charge flow we use the rules (4.89), (4.87) and (4.88) to write the invariant amplitude as

$$i\mathcal{M} = \bar{v}(p_1) i\Gamma' S(k_1 - p_1) i\Gamma u(p_2) \quad (4.100)$$

$$= -i \bar{v}(p_1) h_{(\tilde{\gamma}, e^-, \tilde{e}_L^-)}^i \eta_i \Gamma_i \left(\frac{k_1 - p_1 + m_{\tilde{\gamma}}}{(k_1 - p_1)^2 - m_{\tilde{\gamma}}^2} \right) h_{(\tilde{\gamma}, e^-, \tilde{e}_L^-)}^j \Gamma_j u(p_2). \quad (4.101)$$

The vertex takes the form

$$ih_{(\tilde{\gamma}, e^-, \tilde{e}_L^-)}^i \Gamma_i = \frac{i}{\sqrt{2}} e(1 - \gamma_5) Q, \quad (4.102)$$

where we see that Γ_i is 1 or $i\gamma_5$, such that $\eta_i = 1$ in both cases. Thus the invariant amplitude becomes

$$\mathcal{M}(e^- e^- \rightarrow \tilde{e}_L^- \tilde{e}_L^-) = \frac{e^2 Q^2}{2} \bar{v}(p_1) (1 - \gamma_5) \left(\frac{\not{k}_1 - \not{p}_1 + m_{\tilde{\gamma}}}{(k_1 - p_1)^2 - m_{\tilde{\gamma}}^2} \right) (1 - \gamma_5) u(p_2). \quad (4.103)$$

To demonstrate that the direction of fermion flow is arbitrary, we compute again the general invariant amplitude, choosing now the reverse direction of fermion flow to show that we arrive at the same answer. The invariant amplitude is then

$$i\mathcal{M} = -\bar{v}(p_2) i\Gamma' S(p_1 - k_1) i\Gamma u(p_1), \quad (4.104)$$

where the minus arises from choosing the spinor reference order with respect to the first amplitude calculated. Taking the transpose of this term we find:

$$i\mathcal{M} = -u(p_1)^T i\Gamma^T S(p_1 - k_1)^T i\Gamma'^T \bar{v}(p_2)^T, \quad (4.105)$$

where using the spinor identities (4.78) and the propagator relation (4.85)

$$= -\bar{v}(p_1) iC^T \Gamma^T C^{-1} S(-(p_1 - k_1)) iC(C\Gamma^T C^{-1})^T C^{-1} u(p_2) \quad (4.106)$$

$$= -\bar{v}(p_1) (-1)iC\Gamma^T C^\dagger S(k_1 - p_1) iC(C^T)^{-1} \Gamma C^T C^{-1} u(p_2) \quad (4.107)$$

$$= \bar{v}(p_1) i\Gamma' S(k_1 - p_1) \Gamma u(p_2), \quad (4.108)$$

which is the same answer as above.

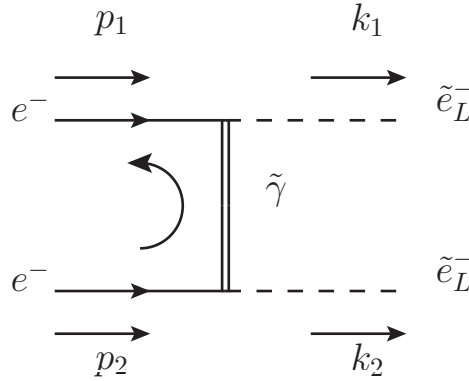


Figure 4.6: Feynman diagram for two incoming electrons exchanging a photino to give left scalar electrons.

Chapter 5

SUSY with a Continuous R-Symmetry

Aside from the familiar Standard Model symmetry group $SU(2)_c \times SU(2)_L \times U(1)_Y$, realistic supersymmetric theories require an additional internal symmetry to prevent terms appearing in the superpotential that give unobserved phenomena such as proton decay. The MSSM chooses the \mathbb{Z}_2 symmetry group, better known as R, or matter, parity. An equally effective choice is the $U(1)$ symmetry group, giving a continuous R symmetry, denoted by $U(1)_R$ [11]. A $U(1)_R$ symmetry with a Lorentz scalar generator R arises automatically in $N = 1$ supersymmetry. The generator R is the only scalar generator of the internal symmetry group that commutes non-trivially with the supersymmetric generators Q :

$$[Q_\alpha, R] = i (\gamma_5)_\alpha^\beta Q_\beta \quad (5.1)$$

As we will see shortly, a continuous R symmetry forbids gaugino and higgsino Majorana masses. Because massless superparticles are not observed, R symmetry is commonly assumed to be broken together with supersymmetry for this reason. In this chapter we discuss a model in which global R symmetry remains intact and no superparticles are massless.

The advantages of having an unbroken continuous global R symmetry include a restriction on the number of allowed soft-breaking terms and a natural suppression of the unobserved supersymmetric contributions to meson mixing experiments[3]. The latter implies that squark flavour mixing, the property of the model that gives these contributions, can be significantly larger than it is in the MSSM. Supersymmetric quark flavour mixing, although suppressed for meson mixing experiments, could therefore be observable through other flavour mixing processes such as single top production.

5.1 $U(1)_R$ symmetry

Working in superspace, the $U(1)_R$ symmetry charges of the superspace coordinates and superfields that ensure baryon and lepton number conservation are given in table 5.1. The charges of the superspace coordinates are a direct consequence of the non-trivial commutation relation between the scalar generator R and supersymmetric generator Q given by in (5.1).

Superspace Quantity	$U(1)_R$ charge	Description
θ_L	+1	LH Grassmann coordinate
θ_R	-1	RH Grassmann coordinate
\hat{S}	+1	Chiral scalar <i>matter</i> superfield
\hat{h}	0	Chiral scalar <i>Higgs</i> superfield
\hat{W}	+1	Chiral spinor <i>gauge</i> superfield
\hat{V}	0	Real vector <i>gauge</i> superfield

Table 5.1: Continuous R symmetry charges for superspace coordinates and superfields.

It is convenient to define an operator R_C that returns $U(1)_R$ charge of a field or superspace coordinate. For example, because $R_C[\theta_R^\dagger] = +1$, it follows that

$$R_C[\bar{\theta}P_L] = R_C[\theta_R^\dagger\gamma_0P_L] = +1, \quad (5.2)$$

and thus that

$$R_C[\bar{\theta}\theta_L] = +2. \quad (5.3)$$

The R charges of the component fields, denoted by bracketed superscripts, are given by the superspace expansions of their respective superfields (see section 2.2.3):

$$\hat{S}^{(1)}(\hat{x}, \theta) = \mathcal{S}^{(1)} + i\sqrt{2}\bar{\theta}^{(1)}\psi_L^{(0)} + i\bar{\theta}\theta_L^{(2)}\mathcal{F}^{(-1)}, \quad (5.4)$$

$$\hat{h}^{(0)}(\hat{x}, \theta) = h^{(0)} + i\sqrt{2}\bar{\theta}^{(1)}\psi_{hL}^{(-1)} + i\bar{\theta}\theta_L^{(2)}\mathcal{F}_h^{(-2)}, \quad (5.5)$$

$$\hat{W}_A^{(1)}(\hat{x}, \theta) = \lambda_{AL}^{(1)} + \frac{1}{2}\gamma^\mu\gamma^\nu \left(\partial_\mu V_{A\nu}^{(0)} - \partial_\nu V_{A\mu}^{(0)} \right) \theta_L^{(1)} - i\bar{\theta}\theta_L^{(2)} \left(\not{D}\lambda_{AR}^{(-1)} \right) - i\mathcal{D}_A^{(0)}\theta_L^{(1)}, \quad (5.6)$$

$$\hat{V}_A^{(0)}(x, \theta) = \frac{1}{2} (\bar{\theta}\gamma_5\gamma_\mu\theta)^{(0)} V_A^{\mu(0)} + i(\bar{\theta}\gamma_5\theta)^{(0)}\bar{\theta}^{(1)}\lambda_{AR}^{(-1)} - \frac{1}{4}(\bar{\theta}\gamma_5\theta)^2\mathcal{D}_A^{(0)}. \quad (5.7)$$

Component fields that are R-neutral are thus all matter fermions ψ_L , Higgs scalars h , gauge bosons $V_{A\mu}$ and auxillary D-term fields \mathcal{D}_A .

Because the Lagrangian is R-neutral by definition, the necessary continuous R charge of the superpotential \hat{f} can be read off from the master supersymmetric Lagrangian expression given in equation (2.66). Specifically, from the fourth line of

this expression:

$$R_C \left[-\frac{1}{2} \sum_{i,j} \bar{\psi}_i \left(\frac{\partial^2 \hat{f}}{\partial \hat{\mathcal{S}}_i \partial \hat{\mathcal{S}}_j} \right)_{\hat{s}=S} P_L \psi_j \right] = 0 \quad (5.8)$$

$$\Rightarrow R_C \left[\frac{\partial^2 \hat{f}}{\partial \hat{\mathcal{S}}_i \partial \hat{\mathcal{S}}_j} \right] = 0 \quad (5.9)$$

$$\Rightarrow R_C [\hat{f}] = +2. \quad (5.10)$$

Considering now the R-charge of the MSSM superpotential terms given in equation (3.8),

$$\hat{f}^{(2)} = \mu \hat{H}_u^{(0)} \hat{H}_d^{(0)} + \mathbf{f}_u \epsilon_{ab} \hat{Q}^{(1)a} \hat{H}_u^{(0)a} \hat{U}^{c(1)} + \mathbf{f}_d \hat{Q}^{(1)} \hat{H}_d^{(0)} \hat{D}^{c(1)} + \mathbf{f}_e \hat{L}^{(1)} \cdot \hat{H}_d^{(0)} \hat{E}^{c(1)}, \quad (5.11)$$

it is evident that the Higgs μ term will violate the continuous R-symmetry and must thus be excluded. The Yukawa coupling terms all have the correct R-charge. The $\Delta L = 1$ lepton number violating operators $\hat{Q} \hat{L} \hat{D}^c$, $\hat{L} \hat{L} \hat{E}^c$ and $\hat{H}_u \hat{L}$ are forbidden, as is the $\Delta B = 1$ baryon number violating operator $\hat{U}^c \hat{U}^c \hat{D}^c$. Furthermore, proton decay through the $B - L$ conserving operators $\hat{Q} \hat{Q} \hat{Q} \hat{L}$ and $\hat{U}^c \hat{U}^c \hat{D}^c \hat{E}^c$ are also forbidden by continuous R-symmetry.

If we consider now the $U(1)_R$ charges of the MSSM soft breaking terms given in (3.15),

$$\mathcal{L}_{\text{soft}}^{(0)} = \left[\tilde{Q}_i^{\dagger(-1)} \mathbf{m}_{Qij}^2 \tilde{Q}_j^{(1)} + \dots + m_{H_u}^2 |H_u|^{2(0)} + \dots \right] \quad (5.12)$$

$$- \frac{1}{2} \left[M_1 \tilde{\lambda}_0^{(-1)} \tilde{\lambda}_0^{(1)} + \dots \right] + \left[(\mathbf{a}_u)_{ij} \epsilon_{ab} \tilde{Q}_i^{a(1)} H_u^{b(0)} \tilde{u}_{Rj}^{\dagger(1)} + \dots \right] \quad (5.13)$$

$$+ \left[(\mathbf{c}_u)_{ij} \epsilon_{ab} \tilde{Q}_i^{a(1)} H_d^{b*(0)} \tilde{u}_{Rj}^{\dagger(1)} + \dots \right] + \left[b H_u^{(0)} H_d^{(0)} + \text{h.c.} \right], \quad (5.14)$$

we find that the gaugino masses and all scalar trilinear terms are forbidden. Only the scalar masses and the Higgs b -term survive. This leads to a greatly reduced parameter space. The absence of gaugino and Higgsino masses (the latter arises because of the forbidden μ -term), however, is of an immediate phenomenological concern that will be amended in the next section.

5.1.1 Superspace integration and spurions

The superspace coordinates θ_a ($a = 1, \dots, 4$) are Grassmann numbers and thereby obey the integration rule

$$\int d\theta_a \theta_a = 1. \quad (5.15)$$

By making the explicit identification

$$(\theta_1, \theta_2, \theta_3, \theta_4) \equiv (\theta_{L1}, \theta_{L2}, \theta_{L1}, \theta_{L2}) = (\theta_L, \theta_R), \quad (5.16)$$

the $U(1)_R$ charges of the superspace coordinate measures are

$$\begin{aligned} R_C[d\theta_{L1}] &= R_C[d\theta_{L2}] = -1 \\ \text{and } R_C[d\theta_{R1}] &= R_C[d\theta_{R2}] = +1. \end{aligned} \quad (5.17)$$

Superspace integration is useful for integrating out the D and F-term contributions of a superfield, namely the coefficients of the terms $-\frac{1}{2}(\bar{\theta}\gamma_5\theta)^2$ and $-\bar{\theta}\theta_L$ respectively. Defining

$$d^4\theta \equiv d\theta_{L1}d\theta_{L2}d\theta_{R1}d\theta_{R2} \quad (5.18)$$

$$d^2\theta_L \equiv d\theta_{L1}d\theta_{L2}, \quad (5.19)$$

and noting that

$$-\frac{1}{2}(\bar{\theta}\gamma_5\theta)^2 = -4\theta_{R2}\theta_{R1}\theta_{L2}\theta_{L1}, \quad (5.20)$$

$$-\bar{\theta}\theta_L = -2\theta_{L2}\theta_{L1}, \quad (5.21)$$

$$(-\bar{\theta}\theta_L)^\dagger(-\bar{\theta}\theta_L) = 4\theta_{R2}\theta_{R1}\theta_{L2}\theta_{L1}, \quad (5.22)$$

we have the following useful superspace integrations:

$$-\frac{1}{4} \int d^4\theta \left[-\frac{1}{2}(\bar{\theta}\gamma_5\theta)^2 \right] = 1, \quad (5.23)$$

$$-\frac{1}{2} \int d^2\theta_L [-\bar{\theta}\theta_L] = 1, \quad (5.24)$$

$$\frac{1}{4} \int d^4\theta [(-\bar{\theta}\theta_L)^\dagger(-\bar{\theta}\theta_L)] = 1. \quad (5.25)$$

Using the charges of the single measures defined above, we find

$$R_C[d^4\theta] = 0 \quad \text{and} \quad R_C[d^2\theta_L] = -2. \quad (5.26)$$

As all F-term contributions to the action can be written as a superspace integration over the superpotential

$$S_F = \int d^4x \mathcal{L}_F = -\frac{1}{2} \left[\int d^4x \int d^2\theta_L^{(-2)} \hat{f}^{(2)} + \text{h.c.} \right], \quad (5.27)$$

we verify that the superpotential charge is +2.

A possible mechanism for generating soft breaking terms is by introducing additional superfields known as *spurions* whose \mathcal{F} or \mathcal{D} -terms develop supersymmetry breaking vacuum expectation values (VEV). A \mathcal{F} -term spurion is a chiral scalar superfield \hat{X} that upon breaking gives

$$\hat{X} \rightarrow \dots - \bar{\theta}\theta_L \langle F \rangle + \dots, \quad (5.28)$$

where $\langle F \rangle$ is the VEV of the \mathcal{F} term. Because $\langle F \rangle$ will generate R-neutral terms such as masses, we require $R_C[\langle F \rangle] = 0$ and therefore that $R_C[\hat{X}] = 2$. Soft scalar masses are generated from the superspace integral

$$-\frac{1}{4} \int d^4\theta^{(0)} \frac{1}{M^2} \hat{X}^{\dagger(-2)} \hat{X}^{(2)} \hat{\mathcal{S}}^{\dagger(-1)} \hat{\mathcal{S}}^{(1)} = -\frac{|\langle F \rangle|^2}{M^2} \mathcal{S}^\dagger \mathcal{S} + \dots, \quad (5.29)$$

which is seen to conserve R symmetry. Soft gaugino mass terms and trilinear scalar terms are generated by the superspace integrals

$$\frac{1}{2} \int d^2\theta_L^{(-2)} \frac{1}{M} \hat{X}^{(2)} \overline{\hat{W}}_A^c{}^{(1)} \hat{W}_A^{(1)} = -\frac{\langle F \rangle}{M} \overline{\lambda}_R^{(-1)} \lambda_L^{(1)} + \dots \quad (5.30)$$

and

$$-\frac{1}{2} \int d^2\theta_L^{(-2)} \frac{1}{M} \hat{X}^{(2)} \hat{\mathcal{S}}_i^{(1)} \hat{\mathcal{S}}_j^{(1)} \hat{\mathcal{S}}_k^{(1)} = \frac{\langle F \rangle}{M} \mathcal{S}_i^{(1)} \mathcal{S}_j^{(1)} \mathcal{S}_k^{(1)}, \quad (5.31)$$

which both violate R symmetry, as expected from above. A \mathcal{D} -term spurion is a chiral spinor superfield \hat{Y} that upon breaking gives

$$\hat{Y} \rightarrow \dots - i\theta_L \langle D' \rangle + \dots \quad (5.32)$$

Likewise to $\langle F \rangle$, $\langle D' \rangle$ is required to have zero R-charge; thus $R_C[\hat{Y}] = 1$.

5.2 The MRSSM

In the previous section we saw that the Majorana masses of gauginos and higgsinos are forbidden by continuous R-symmetry, which is in serious conflict with experiment as we do not observe massless supersymmetric particles. A solution, known as the Minimal R-symmetric Supersymmetric Standard Model (MRSSM), is given by Kribs *et al.* [3][12]. To fix the missing gaugino masses, a chiral scalar superfield $\hat{\Phi}$ is added for each gauge group. The chiral spinor component field $\hat{\Phi}$ combines with the Majorana gaugino to give a Dirac spinor for the gaugino. By coupling the superfield $\hat{\Phi}$ to its partner gauge superfield and a \mathcal{D} -term spurion \hat{Y} as

$$-\frac{1}{\sqrt{2}M} \int d^2\theta_L \overline{\hat{Y}}_\alpha^c \hat{W}_A^\alpha \hat{\Phi}^A + \text{h.c} \in \mathcal{L}, \quad (5.33)$$

a Dirac spinor mass term is generated for the gaugino, which preserves $U(1)_R$ symmetry (more details will be given in section 5.4). To repair the missing Higgsino masses caused by the absent μ -term, the Higgs sector is enlarged with two extra multiplets \hat{R}_u and \hat{R}_d transforming identically to \hat{H}_d and \hat{H}_u , respectively, but with a R-charge of +2. These superfields can be combined with the Higgs superfields in the superpotential as

$$\hat{f} \ni \mu_u \hat{H}_u \hat{R}_u + \mu_d \hat{H}_d \hat{R}_d, \quad (5.34)$$

to give μ terms that generate Higgsino masses upon electroweak breaking. The full matter content of the MRSSM with all internal charges is given in table 5.2. All of the above additions preserve the continuous R-symmetry.

When cast into a chiral spinor field as in (5.7), the two complex degrees of freedom of a gaugino field carry an R charge of +1. This gives an anomalous coupling of the continuous R current to two gauge bosons via a gaugino loop. The addition, however, of the R neutral superfields $\hat{\Phi}^A$ gives adjoint chiral fermions that carry opposite R charge to the gauginos. Thus the anomalous couplings cancel and the continuous global R symmetry in the MRSSM is anomaly free.

Superfield	$SU(3)_C$	$SU(2)_L$	$U(1)_Y$	$U(1)_R$
\hat{Q}	3	2	$\frac{1}{3}$	1
\hat{U}^c	3*	1	$-\frac{4}{3}$	1
\hat{D}^c	3*	1	$\frac{2}{3}$	1
\hat{L}	1	2	-1	1
\hat{E}^c	1	1	2	1
$\hat{\phi}_G$	8	1	0	0
$\hat{\phi}_B$	1	1	0	0
$\hat{\phi}_W$	1	3	0	0
\hat{H}_u	1	2	1	0
\hat{H}_d	1	2	-1	0
\hat{R}_u	1	2	-1	2
\hat{R}_d	1	2	1	2

Table 5.2: Matter superfields of the MRSSM with all internal charges (including continuous R symmetry $U(1)_R$).

5.3 Squark flavour mixing

In the MSSM squark flavour mixing is heavily suppressed by $K-\bar{K}$ and $B-\bar{B}$ meson mixing experiments. This is because the measured mass differences between the mass eigenstates of these mesons, a manifestation of their mixing, are already explained very accurately by the Standard Model. Supersymmetry with squark flavour mixing will contribute to Kaon mixing through the box diagrams shown in figure 5.1. Define $\delta_{ij} \equiv m_{\tilde{q}_{ij}}/|m_{\tilde{q}}|$ as the ratio of the mixed squark mass over the average squark mass. Using the measured mass difference of the Kaon eigenstates K_S and K_L , Ciuchini *et al.* [13] have set the following limits on squark mixing:

$$\delta_{LL}, \delta_{RR} \leq 4.6 \times 10^{-2}, \quad (5.35)$$

in the case of only left or right handed mixing, or

$$\sqrt{\delta_{LL}\delta_{RR}} \leq 9.6 \times 10^{-4}, \quad (5.36)$$

in the case of both. Little or no squark mixing is thus a phenomenological constraint on the MSSM. One solution is to suppress the mixing by choosing squark masses of order 10 TeV. This will, however, re-introduce fine tuning of the scalar masses due to the residual logarithmic divergences that have squark mass terms as their coefficients. A more common solution is therefore to devise supersymmetry breaking mechanisms that align the squark and quark mass bases and thus eliminate the flavour mixing.

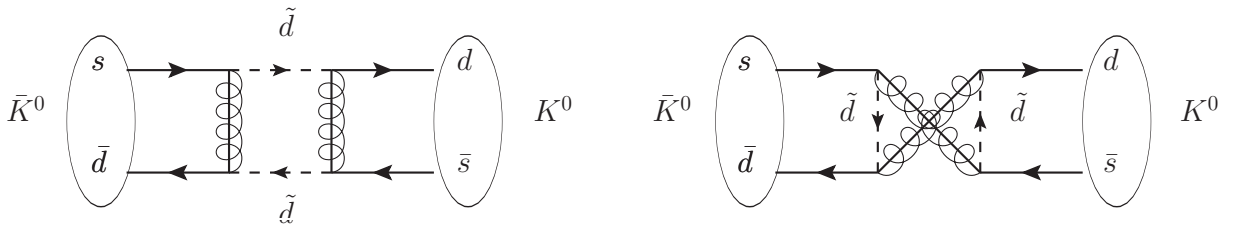


Figure 5.1: Box diagram contributions to K - \bar{K} meson mixing from squark flavour mixing.

In the MRSSM, the contributions of squark flavour mixing to the meson mass difference are suppressed, which means the mixing may in general be much larger than in the MSSM. To see this, consider again the two box diagram contributions to Kaon mixing given in figure 5.1. Due to the chiral nature of the $q - \tilde{q} - \tilde{g}$ coupling, the fermion chains appearing in the left and right diagrams will couple to either the kinetic term $\gamma^\mu \partial_\mu$ or the mass term $m_{\tilde{g}}$ in the gluino propagator respectively. In figure 5.2 we have illustrated this point by giving the relevant effective vertices of these fermion chains (obtained by integrating out the gluino). The diagram containing the vertices proportional to $1/m_{\tilde{g}}$ will dominate. This diagram, however, is seen to be dependent on the Majorana nature of the gluino. In the MRSSM the gluino is required to be a Dirac, as opposed to Majorana, fermion and thus the dominant diagram is forbidden. The remaining box diagram has an additional factor

$$\left(\frac{k_{\text{loop}}}{m_{\tilde{g}}} \right)^2, \quad (5.37)$$

where k_{loop} is the loop momentum of the box diagram. Assuming that the largest contribution to the box diagram comes from $k_{\text{loop}} \sim m_{\tilde{g}}$, we see that the effect of squark flavour mixing to the Kaon mass difference is suppressed when the gluino is set heavier than the squarks. Furthermore, in section 5.4 we use *supersoft* supersymmetry [14] breaking to give the gluino a Dirac mass. This means that the gluino corrections to the scalar masses in the theory will be finite rather than logarithmically divergent (as is the case for ordinary soft breaking). Thus we are free to

set the gluino mass an order of magnitude higher without there being a fine-tuning problem.

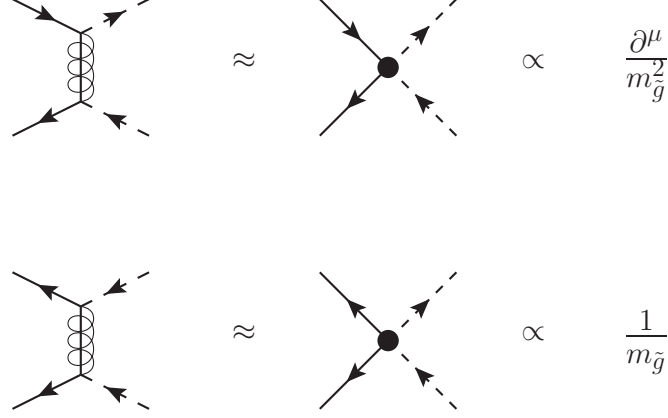


Figure 5.2: Effective vertices for the fermion chains that contribute to neutral Kaon mixing.

5.3.1 Squark masses

Contributions to the squark masses come from the superpotential, soft breaking scalar masses, soft breaking trilinear terms and D-term contributions. Mixing between L and R squarks in the MSSM arises from the μ term in the superpotential (upon electroweak breaking) and the soft trilinear terms. In the MRSSM these terms are forbidden, and therefore no L-R squark mixing takes place.

The superpotential contribution to the squark masses comes from the master Lagrangian term

$$-\sum_i \left| \frac{\partial \hat{f}}{\partial \hat{\mathcal{S}}_i} \right|_{\hat{\mathcal{S}}=\mathcal{S}}^2, \quad (5.38)$$

after electroweak breaking. The relevant superpotential terms are

$$(\mathbf{f}_u)_{ij} \hat{u}_i \hat{h}_u^0 \hat{U}_j^c + (\mathbf{f}_d)_{ij} \hat{d}_i \hat{h}_d^0 \hat{D}_j^c \in \hat{f}, \quad (5.39)$$

which for up-type quarks give

$$\frac{\partial \hat{f}}{\partial \hat{u}_k} = (\mathbf{f}_u)_{kj} \hat{h}_u^0 \hat{U}_j^c \xrightarrow{\text{EW}} (v_u \mathbf{f}_u)_{kj} \hat{U}_j^c = m_t \delta_{k3} \hat{T}^c, \quad (5.40)$$

$$\frac{\partial \hat{f}}{\partial \hat{U}_k^c} = (\mathbf{f}_u)_{ik} \hat{u}_i \hat{h}_u^0 \xrightarrow{\text{EW}} (v_u \mathbf{f}_u)_{ik} \hat{u}_i = m_t \delta_{k3} \hat{t}, \quad (5.41)$$

where only the third generation of quarks have been taken to be massive and the Yukawa matrices are assumed to be diagonal. The superpotential contribution is thus

$$\mathcal{L} \ni -m_t^2 \tilde{t}_L^* \tilde{t}_L - m_t^2 \tilde{t}_R^* \tilde{t}_R - m_b^2 \tilde{b}_L^* \tilde{b}_L - m_b^2 \tilde{b}_R^* \tilde{b}_R. \quad (5.42)$$

The soft SUSY breaking scalar mass terms are

$$\begin{aligned} \mathcal{L} \ni & -\tilde{Q}_i^* (\mathbf{m}_Q^2)_{ij} \tilde{Q}_j - \tilde{u}_{Ri}^* (\mathbf{m}_U^2)_{ij} \tilde{u}_{Rj} - \tilde{d}_{Ri}^* (\mathbf{m}_D^2)_{ij} \tilde{d}_{Rj} \\ & \ni -(\tilde{\mathbf{m}}_{uL}^2)_{ij} \tilde{u}_{Li}^* \tilde{u}_{Lj} - (\tilde{\mathbf{m}}_{dL}^2)_{ij} \tilde{d}_{Li}^* \tilde{d}_{Lj} - (\tilde{\mathbf{m}}_{uR}^2)_{ij} \tilde{u}_{Ri}^* \tilde{u}_{Rj} - (\tilde{\mathbf{m}}_{dR}^2)_{ij} \tilde{d}_{Ri}^* \tilde{d}_{Rj}, \end{aligned} \quad (5.43)$$

where

$$\tilde{\mathbf{m}}_{uL}^2 = \tilde{\mathbf{m}}_{dL}^2 = \mathbf{m}_Q^2, \quad \tilde{\mathbf{m}}_{uR}^2 = \mathbf{m}_U^2, \quad \tilde{\mathbf{m}}_{dR}^2 = \mathbf{m}_D^2. \quad (5.44)$$

Lastly, there are D-term contributions coming from the master Lagrangian term

$$-\frac{1}{2} \sum_A \left| \sum_i \mathcal{S}_i^\dagger g_\alpha t_{\alpha A} \mathcal{S}_i \right|^2. \quad (5.45)$$

These contribute to stop and sbottom masses (see Baer *et al.* [1] for further details) as

$$\mathcal{L} \ni M_z^2 \cos 2\beta (T_3 - Q \sin^2 \theta_W) (\tilde{t}_L^* \tilde{t}_L + \tilde{t}_R^* \tilde{t}_R + \tilde{b}_L^* \tilde{b}_L + \tilde{b}_R^* \tilde{b}_R), \quad (5.46)$$

where T_3 and Q are the third $SU(2)$ and the electric charge generator respectively. The total squark mass matrix in the Yukawa basis is thus

$$(\mathcal{M}_q^2)_{ij} = (\tilde{\mathbf{m}}_q^2)_{ij} + [m_q^2 + M_z^2 \cos 2\beta (T_3 - Q \sin^2 \theta_W)] \delta_{i3} \delta_{j3}, \quad (5.47)$$

with $q = \{u_L, d_L, u_R, d_R\}$, $m_{uL} = m_{iR} = m_t$ and $m_{dL} = m_{dR} = m_b$. Note that Kribs *et al.* [12] leave out the third term in their squark mass matrix.

Contrary to the MSSM, squark flavor mixing is not phenomenologically suppressed in the MRSSM. To find a mass eigenstate basis for squarks \tilde{q}_a we must therefore diagonalize the squark mass matrix:

$$-\tilde{q}_i^* (\mathcal{M}_q^2)_{ij} \tilde{q}_j = -\tilde{q}_a^* (\mathbf{D}_q)_{ab} \tilde{q}_b, \quad (5.48)$$

so that

$$\tilde{q}_a = \sum_i \left(U_q^\dagger \right)_{ai} \tilde{q}_i, \quad (5.49)$$

with $q = \{u_L, d_L, u_R, d_R\}$, i is the generation index of the Yukawa basis and U_q is a unitary transformation matrix.

5.4 Scalar gluons and Dirac gluinos

The presence of the new chiral scalar superfield $\hat{\Phi}_G$ promises interesting new phenomenology as its component fields will couple strongly to both matter and gauge fields. Of particular interest is that it contains a colour octet complex scalar field:

$$\hat{\Phi}_G^A = \phi_G^A + i\sqrt{2}\bar{\theta}\psi_{GL}^A + i\bar{\theta}\theta_L^{(2)}\mathcal{F}_G^A, \quad (5.50)$$

where A is the adjoint colour index. We proceed to derive the relevant Lagrangian terms and mass spectrum for the component fields of $\hat{\Phi}_G$.

The Kähler potential (introduced in section 2.3.2) for the superfield $\hat{\Phi}_G$ as a superspace integral is

$$S \ni -\frac{1}{4} \int d^4x d^4\theta \left[\hat{\Phi}_G^\dagger e^{-2gt_A \hat{V}_A} \hat{\Phi}_G \right]. \quad (5.51)$$

This gives the Lagrangian terms

$$\begin{aligned} \mathcal{L} \ni & \frac{i}{2} \bar{\psi}_{GA} \not{D}_{AB} \psi_{GB} + (D_\mu \phi_G)^\dagger_A (D^\mu \phi_G)_A + \mathcal{F}_{GA}^\dagger \mathcal{F}_{GA} \\ & - g \phi_{GA}^* (t \cdot \mathcal{D})_{AB} \phi_{GB} + \left(-\sqrt{2} g_S \phi_{GA}^* (t_C)_{AB} \bar{\lambda}_C P_L \psi_{GB} + \text{h.c} \right) \end{aligned} \quad (5.52)$$

where the Einstein summation convention over the adjoint colour indices A, B and C is assumed and the covariant derivative is given by

$$D_{\mu AB} = \delta_{AB} \partial_\mu + i g_S \left(t_C^{\text{adj}} G_{C\mu} \right)_{AB}. \quad (5.53)$$

We define the Dirac gluino \tilde{g} as the combination

$$\tilde{g} \equiv \psi_L + \lambda_R, \quad (5.54)$$

with properties such as

$$\tilde{g}^c = \psi_R + \lambda_L, \quad P_L \psi_G = P_L \tilde{g}, \quad P_R \psi_G = P_R \tilde{g}^c \quad \text{etc.} \quad (5.55)$$

The last term of expression (5.52) can be rewritten in terms of Dirac gluinos:

$$\begin{aligned} & -\sqrt{2} g_S \phi_{GA}^* (t_C)_{AB} \bar{\lambda}_C P_L \psi_{GB} + \text{h.c} \\ = & -\sqrt{2} i g_S \phi_{GA}^* f_{ACB} \bar{\lambda}_C P_L \psi_{GB} + \sqrt{2} i g_S \phi_{GA} f_{ACB} (\bar{\lambda}_C P_L \psi_{GB})^\dagger \end{aligned} \quad (5.56)$$

$$= -\sqrt{2} i g_S \phi_{GA}^* f_{ACB} \bar{\tilde{g}}_C P_L \tilde{g}_B + \sqrt{2} i g_S \phi_{GA} f_{ACB} \tilde{g}_B P_R \tilde{g}_C \quad (5.57)$$

$$= -\sqrt{2} i g_S f_{ABC} \bar{\tilde{g}}_B (\phi_{GA}^* P_L + \phi_{GA} P_R) \tilde{g}_C. \quad (5.58)$$

By adding the kinetic term for the Majorana gaugino we arrive at a complete kinetic term for the Dirac gluino

$$\frac{i}{2} \bar{\psi}_G \not{D} \psi_G + \frac{i}{2} \bar{\lambda} \not{D} \lambda = i \bar{\tilde{g}} \not{D} \tilde{g}. \quad (5.59)$$

Putting it all together, the Kähler potential contribution to the $\hat{\Phi}_G$ Lagrangian is

$$\begin{aligned} \mathcal{L}_{\text{Kähler}} = & i \bar{\tilde{g}}_A \not{D}_{AB} \tilde{g}_B + (D_\mu \phi_{GA})^\dagger (D^\mu \phi_{GA}) + \mathcal{F}_{GA}^\dagger \mathcal{F}_{GA} \\ & - g_S \phi_{GA}^* (t \cdot \mathcal{D})_{AB} \phi_{GB} - \sqrt{2} i g_S f_{ABC} \bar{\tilde{g}}_B (\phi_{GA}^* P_L + \phi_{GA} P_R) \tilde{g}_C, \end{aligned} \quad (5.60)$$

with the covariant derivative as above.

The motivation for adding the $\hat{\Phi}_G$ superfields is to generate a Dirac mass for the gluino. This is achieved by the superspace integral [14][3]

$$-\frac{1}{2} \int d^2\theta_L \frac{\sqrt{2}}{M} \overline{\hat{Y}}_\alpha^c \hat{W}_{3A}^\alpha \hat{\Phi}_{GA} + \text{h.c} \in \mathcal{L}, \quad (5.61)$$

where \hat{Y} is a spurion whose D-term acquires the VEV $\langle D' \rangle$ and α is a spinor index. The spurion takes the form

$$\overline{\hat{Y}}^c = \overline{(-i\theta_L \langle D' \rangle)^c} = -i\bar{\theta}_R \langle D' \rangle, \quad (5.62)$$

in order to preserve gauge and Lorentz invariance, R-symmetry and to remain a chiral spinor superfield¹. By expanding the superspace integration explicitly

$$\begin{aligned} & \frac{1}{2} \int d^2\theta_L \frac{\sqrt{2}}{M} \overline{\hat{Y}}_\alpha^c \hat{W}_{3A}^\alpha \hat{\Phi}_{GA} + \text{h.c} \\ &= \frac{1}{2} \int d^2\theta_L \frac{\sqrt{2}}{M} \left\{ (-i\bar{\theta}_{R\alpha} \langle D' \rangle) \right. \\ & \quad \times \left(\lambda_{AL}^\alpha + \frac{1}{2} \gamma^\mu \gamma^\nu F_{\mu\nu A} \theta_L^\alpha - i\bar{\theta}_L (\not{D} \lambda_{AR\alpha}) - i\mathcal{D}_A \theta_L^\alpha \right) \\ & \quad \times \left(\phi_{GA} + i\sqrt{2}\bar{\theta}\psi_{GLA} + i\bar{\theta}\theta_L^{(2)} \mathcal{F}_{GA} \right) \left. \right\} + \text{h.c} \\ &= \frac{1}{2} \frac{\langle D' \rangle}{M} \int d^2\theta_L \left\{ \bar{\theta} \lambda_{LA} \bar{\theta} \psi_{LA} - \frac{i}{\sqrt{2}} \gamma^\mu \gamma^\nu F_{\mu\nu A} \bar{\theta}_L \phi_{GA} - \sqrt{2} \mathcal{D}_A \phi_{GA} \bar{\theta} \theta_L \right\} + \text{h.c}, \quad (5.63) \end{aligned}$$

and rewriting the term

$$\begin{aligned} \bar{\theta}_\alpha \lambda_{LA}^\alpha \bar{\theta}_\beta \psi_{LA}^\beta &= -\bar{\theta}_\beta \theta_L^\alpha \bar{\lambda}_{A\alpha} \psi_{LA}^\beta \\ &= -\bar{\theta}_L \delta_\beta^\alpha \bar{\lambda}_{A\alpha} \psi_{LA}^\beta \\ &= (-\bar{\theta}_L) \bar{\lambda}_A \psi_{LA}, \end{aligned} \quad (5.64)$$

we can use the superspace integration rule from (5.24) to give

$$\begin{aligned} & -\frac{\langle D' \rangle}{M} \bar{\lambda}_A P_L \psi_A - \sqrt{2} \frac{\langle D' \rangle}{M} \mathcal{D}_A \phi_{GA} - \frac{i}{\sqrt{2}} \frac{\langle D' \rangle}{M} \gamma^\mu \gamma^\nu F_{\mu\nu A} \phi_{GA} + \text{h.c} \\ &= -\frac{\langle D' \rangle}{M} \bar{\lambda}_A (P_L + P_R) \psi_A - \sqrt{2} \frac{\langle D' \rangle}{M} (\phi_{GA} + \phi_{GA}^*) \mathcal{D}_A - \dots \end{aligned} \quad (5.65)$$

¹This is needed for the $d^2\theta_L$ measure to return a valid supersymmetric Lagrangian term (the F-term). If the integral contained a mixture of chiral and anti-chiral superfields, then only the $d^4\theta$ measure would return such a term (the D-term).

Using in addition the Dirac gluino definitions from (5.54), we thus find a Dirac spinor mass for the gluino and a \mathcal{D} -term for the scalar particle

$$-m_{\tilde{g}}\tilde{g}\tilde{g} - \sqrt{2}m_{\tilde{g}}(\phi_{G_A} + \phi_{G_A}^*)\mathcal{D}_A \in \mathcal{L}, \quad (5.66)$$

where the gluino mass has been defined as $m_{\tilde{g}} \equiv \frac{\langle D \rangle}{M}$ with D-term VEV assumed to be real.

We have derived a coupling between the scalar particle ϕ_G and the $SU(3)_C$ \mathcal{D} field. We proceed to collect the other $SU(3)_C$ \mathcal{D} fields so that we can put this auxiliary field on shell. The Kähler potentials for the quark superfields (analogous to what was done for $\hat{\Phi}_G$) give the $SU(3)_C$ \mathcal{D} field terms:

$$\mathcal{L}_{\text{D-terms}} \ni -g_S \sum_{\tilde{q}_{L,i}} \tilde{q}_{Lim}^* (t_A)_{mn} \mathcal{D}_A \tilde{q}_{Lin} - g_S \sum_{\tilde{q}_{R,i}} \tilde{q}_{Rim}^* (-t_A^*)_{mn} \mathcal{D}_A \tilde{q}_{Rin}, \quad (5.67)$$

where m, n are colour indices in the fundamental representation, $\tilde{q}_{L/R} \in \{\tilde{u}_{L/R}, \tilde{d}_{L/R}\}$ and i a generational index in the Yukawa basis (as opposed to the mass eigenstate basis). The $SU(3)_C$ gauge kinetic terms are generated by the superspace integral

$$-\frac{1}{2} \int d^2\theta_L \overline{\hat{W}}_A^c \hat{W}_A = \frac{i}{2} \bar{\lambda} \not{\partial} \lambda - \frac{1}{4} F_{\mu\nu A} F_A^{\mu\nu} + \frac{1}{2} \mathcal{D}_A \mathcal{D}_A, \quad (5.68)$$

and contribute a \mathcal{D}^2 term. All the \mathcal{D} -terms together are then

$$\begin{aligned} \mathcal{L}_{\text{D-terms}} &= \frac{1}{2} \mathcal{D}_A \mathcal{D}_A - g_S \mathcal{D}_A \sum_{\tilde{q}_{L,i}} \tilde{q}_{Li}^* t_A \tilde{q}_{Li} + g_S \mathcal{D}_A \sum_{\tilde{q}_{R,i}} \tilde{q}_{Ri}^* t_A \tilde{q}_{Ri} \\ &\quad - \sqrt{2} m_{\tilde{g}} \mathcal{D}_A (\phi_{G_A} + \phi_{G_A}^*) - g_S \mathcal{D}_A \phi_G^* t_A \phi_G. \end{aligned} \quad (5.69)$$

Putting them on shell gives

$$\mathcal{D}_A = \sqrt{2} m_{\tilde{g}} (\phi_{G_A} + \phi_{G_A}^*) + g_S \phi_G^* t_A \phi_G + g_S \sum_{\sigma=\{L,R\}} \sum_{\tilde{q}_{\sigma,i}} (-1)^\sigma \tilde{q}_{\sigma i}^* t_A \tilde{q}_{\sigma i}, \quad (5.70)$$

with

$$(-1)^\sigma \equiv \begin{cases} 1 & : \sigma = L \\ -1 & : \sigma = R \end{cases}, \quad (5.71)$$

and thus

$$\begin{aligned} \mathcal{L}_{\text{D-terms}} \Big|_{\text{on-shell}} &= -\frac{1}{2} \mathcal{D}_A^2 \\ &= -m_{\tilde{g}}^2 (\phi_{G_A} + \phi_{G_A}^*)^2 - \sqrt{2} g_S m_{\tilde{g}} (\phi_{G_A} + \phi_{G_A}^*) \sum_{\sigma=\{L,R\}} \sum_{\tilde{q}_{\sigma,i}} (-1)^\sigma \tilde{q}_{\sigma i}^* t_A \tilde{q}_{\sigma i} \\ &\quad - g_S^2 \phi_G^* t_A \phi_G \sum_{\sigma=\{L,R\}} \sum_{\tilde{q}_{\sigma,i}} (-1)^\sigma \tilde{q}_{\sigma i}^* t_A \tilde{q}_{\sigma i} - \frac{1}{2} g_S^2 (\phi_G^* t_A \phi_G)^2 \\ &\quad - \frac{1}{\sqrt{2}} g_S m_{\tilde{g}} (\phi_{G_A} + \phi_{G_A}^*) (\phi_G^* t_A \phi_G) - \frac{1}{2} g_S^2 \left[\sum_{\sigma=\{L,R\}} \sum_{\tilde{q}_{\sigma,i}} (-1)^\sigma \tilde{q}_{\sigma i}^* t_A \tilde{q}_{\sigma i} \right]^2. \end{aligned} \quad (5.72)$$

The first term gives a mass contribution to the scalar field, the second and third give scalar couplings to squarks, the fourth and fifth are self-interactions of the scalar field and the last term is the usual SUSY four squark interaction.

Other mass contributions to the complex scalar field come from soft breaking terms. Letting \hat{X} and \hat{Y} be \mathcal{F} -term and \mathcal{D} -term spurions respectively, the valid soft breaking terms are given by the superspace integrals:

$$\begin{aligned} \mathcal{L}_{\text{soft}} \ni & \frac{1}{4} \int d^4\theta \frac{1}{M_1^2} \hat{X}^\dagger \hat{X} \hat{\Phi}_G^\dagger \hat{\Phi}_G \\ & + \left\{ \frac{1}{4} \int d^4\theta \frac{1}{M_2^2} \hat{X}^\dagger \hat{X} \text{Tr} \left(\hat{\Phi}_G^2 \right) - \frac{1}{2} \int d^2\theta_L \frac{1}{M_3^2} \overline{\hat{Y}}^c \hat{Y} \text{Tr} \left(\hat{\Phi}_G^2 \right) + \text{h.c} \right\} \end{aligned} \quad (5.73)$$

$$\ni -\frac{|\langle F \rangle|^2}{M_1^2} |\phi_G|^2 - \frac{|\langle F \rangle|^2}{M_2^2} (\phi_G \phi_G + \phi_G^* \phi_G^*) + \frac{\langle D' \rangle^2}{M_3^2} \phi_G \phi_G + \frac{\langle D' \rangle^{*2}}{M_3^2} \phi_G^* \phi_G^*, \quad (5.74)$$

where the adjoint nature of the $\hat{\Phi}_G$ gauge transformation ensures the trace is gauge invariant. We now redefine the complex scalar field in terms of two real scalar fields ϕ_2 and ϕ_1 by

$$\phi_{GA} \equiv \frac{\phi_{2A} + i\phi_{1A}}{\sqrt{2}}. \quad (5.75)$$

These real scalar fields will be called scalar gluons or *sgluons*. Combining the soft breaking mass terms for ϕ_G with the \mathcal{D} -term contribution gives

$$\begin{aligned} \mathcal{L}_{\text{mass}} &= -m_{\tilde{g}}^2 (\phi_{GA} + \phi_{GA}^*)^2 + \mathcal{L}_{\text{soft}} \\ &= -2m_{\tilde{g}}^2 \phi_2^2 - \frac{|\langle F \rangle|^2}{2M_1^2} (\phi_2^2 + \phi_1^2) - \frac{|\langle F \rangle|^2}{M_2^2} (\phi_2^2 - \phi_1^2) \\ &\quad + \frac{1}{M_3^2} \left\{ [\Re(\langle D' \rangle)^2 - \Im(\langle D' \rangle)^2] (\phi_2^2 - \phi_1^2) - 4\Re(\langle D' \rangle) \Im(\langle D' \rangle) \phi_2 \phi_1 \right\}. \end{aligned} \quad (5.76)$$

We see that the sgluons become physical mass eigenstates if the VEV $\langle D' \rangle$ is purely real or imaginary. This could be achieved by equating this D-term spurion to the spurion that generates the real gluino mass, which would simultaneously limit the number of necessary spurions in the model. Either way, we take the D-term VEV to be real from here onwards. The sgluons are therefore physical particles and have the real mass terms

$$\mathcal{L}_{\text{mass}} = -\frac{1}{2} M_{\phi_2}^2 \phi_2^2 - \frac{1}{2} M_{\phi_1}^2 \phi_1^2, \quad (5.77)$$

where

$$M_{\phi_1}^2 = m_a^2 - m_b^2, \quad M_{\phi_2}^2 = m_a^2 + m_b^2, \quad (5.78)$$

with

$$m_a^2 = \frac{|\langle F \rangle|^2}{M_1^2} + 2m_{\tilde{g}}^2, \quad (5.79)$$

$$m_b^2 = \frac{2|\langle F \rangle|^2}{M_2^2} - \frac{2|\langle D' \rangle|^2}{M_3^2} + 2m_{\tilde{g}}^2. \quad (5.80)$$

It is important to note that the signs of the spurion scales M_i or M_i^2 can equally well be reversed. Degenerate sgluon masses can be achieved by setting $D'/M_3 = m_{\tilde{g}}$ and $\langle F \rangle = 0$ or $m_b^2 \rightarrow 0$ by some other means, giving $M_{\phi_1}^2 = M_{\phi_2}^2 \geq 2m_{\tilde{g}}^2$. If $|\langle F \rangle|^2 / M_1^2 < 0$ no restrictions can be placed on the sgluons mass values.

To complete this section, we give the already familiar quark-squark-gluino couplings in terms of the Dirac gluino \tilde{g} and in the squark mass eigenstate basis. The couplings originate from the master Lagrangian term

$$-\sqrt{2} \sum_k \mathcal{S}_k^\dagger g t_A \bar{\lambda}_A P_L \psi_k + \text{h.c.} \in \mathcal{L}, \quad (5.81)$$

giving

$$\begin{aligned} & -\sqrt{2} g_S \sum_{q,i} \left(\tilde{q}_{Li}^* t_A \bar{\lambda}_A P_L \psi_{qi} + \tilde{q}_{Ri}^* (-t_A)^* \bar{\lambda}_A P_L \psi_{Q^c i} \right) + \text{h.c.} \\ & = -\sqrt{2} g_S \sum_{q,i} \left(\tilde{q}_{Li}^* t_A \bar{\lambda}_A P_L \psi_{qi} - \tilde{q}_{Ri}^* t_A \bar{\lambda}_A^c P_R \psi_{Q_i^c} + \tilde{q}_{Li} t_A \bar{\lambda}_A^c P_R \psi_{qi}^c - \tilde{q}_{Ri} t_A \bar{\lambda}_A P_L \psi_{Q^c i} \right), \end{aligned} \quad (5.82)$$

where $q = P_L \psi_{qi} + P_R \psi_{Q^c i}$. Using the Dirac gluino definitions from (5.54) and the translations between the Yukawa and mass eigenstate basis'

$$\tilde{q}_{\sigma i} = \sum_a (U_{q\sigma})_{ia} \tilde{q}_{\sigma a}, \quad \tilde{q}_{\sigma i}^* = \sum_a \tilde{q}_{\sigma a}^* (U_{q\sigma}^\dagger)_{ai}, \quad (5.83)$$

the quark-squark-gluino couplings becomes

$$\begin{aligned} \mathcal{L} \ni & -\sqrt{2} g_S \sum_{i,a,A} \left\{ \left[\tilde{u}_{La}^* (U_{uL}^\dagger)_{ai} t_A \bar{g}_A P_L - \tilde{u}_{Ra}^* (U_{uR}^\dagger)_{ai} t_A \bar{g}_A P_R \right] u_i \right. \\ & + \left[(U_{uL})_{ia} \tilde{u}_{La} t_A \bar{g}_A^c P_R - (U_{uR})_{ia} \tilde{u}_{Ra} t_A \bar{g}_A^c P_L \right] u_i^c \\ & \left. + (u \leftrightarrow d) \right\}. \end{aligned} \quad (5.84)$$

5.5 Feynman Rules for $SU(3)_C \times U(1)_R$

The Feynman rules for supersymmetric QCD in the MRSSM are presented here. The term sgluon is used to refer to the real scalar components of the complex scalar field ϕ_G . We present here only the Feynman rules relevant for our analysis of single top processes in the MRSSM, omitting for example couplings with two or more sgluons. These rules extend (and override) those given in section 4.1 for supersymmetric QCD in the MSSM. Rules involving squarks that are not re-listed here are independent of the new mass eigenstate basis for squarks. These include, for example, the gluon-squark and four-squark vertices, where

$$\sum_i \tilde{q}_{\sigma im}^* \tilde{q}_{\sigma in} = \sum_{i,a,b} \tilde{q}_{\sigma am}^* (U_{q\sigma}^\dagger)_{ai} (U_{q\sigma})_{ib} \tilde{q}_{\sigma bn} = \sum_{a,b} \delta_{ab} \tilde{q}_{\sigma am}^* \tilde{q}_{\sigma bn} = \sum_a \tilde{q}_{\sigma am}^* \tilde{q}_{\sigma an}. \quad (5.85)$$

5.5.1 Tree-level

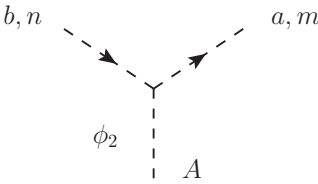
Sgluon-squark-squark

The sgluon-squark-squark coupling comes from the on-shell D-term Lagrangian terms (5.72)

$$-\sqrt{2}g_S m_{\tilde{g}} (\phi_{GA} + \phi_{GA}^*) \sum_{\sigma=\{L,R\}} \sum_{\tilde{q},i} (-1)^\sigma \tilde{q}_{\sigma im}^* (t_A)_{mn} \tilde{q}_{\sigma in}, \quad (5.86)$$

where because $\phi_G + \phi_G^* = \sqrt{2}\phi_2$, only one of the sgluons couples singularly to a squark pair. The squark terms appearing in this coupling can be expressed in either basis, as outlined in (5.85).

Sgluon-squark-squark:



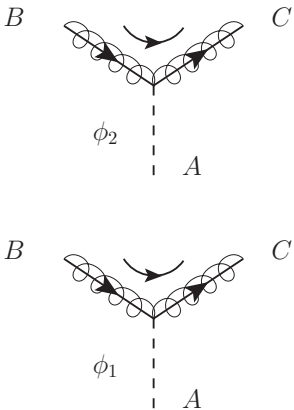
$$= -2ig_S m_{\tilde{g}} (-1)^\sigma \delta_{ab} (t_A)_{mn}$$

Sgluon-gluino-gluino

The sgluon-gluino-gluino coupling comes from the Kähler potential Lagrangian terms given in (5.60), where

$$\phi_G^* P_L + \phi_G P_R = \frac{1}{\sqrt{2}} (\phi_2 + i\gamma_5 \phi_1). \quad (5.87)$$

Sgluon-gluino-gluino:



$$= g_S f_{ABC}$$

$$= g_S (i\gamma_5) f_{ABC}$$

Gluino-quark-squark

The gluino-quark-squark coupling is given by the Lagrangian term in (5.84). Only the Majorana gaugino component λ_A (from the $SU(3)_C$ gauge superfield \hat{W}_{3A}) of the

Dirac gluino is present in this vertex, so we treat it as a Majorana fermion and use our Majorana fermion rules to avoid cumbersome C matrices just as in section 4.1.

Gluino-quark-squark:

$$= -(-1)^\sigma i\sqrt{2}g_S \left(U_{\tilde{q}\sigma}^\dagger \right)_{ai} (t_A)_{mn} P_\sigma$$

$$= -(-1)^\sigma i\sqrt{2}g_S (U_{\tilde{q}\sigma})_{ai} (t_A)_{mn} P_{\bar{\sigma}}$$

Gluon-gluino-gluino

The gluino now couples as a Dirac fermion to the strong force gauge bosons, as seen in (5.59). This causes a subtle change in the related Feynman rule from that given in section 4.1.

Gluon-gluino-gluino:

$$= \frac{g_S}{2} \gamma^\mu f_{ABC}$$

5.5.2 Effective one-loop

Sgluon-gluon-gluon

Figure 5.3 gives the four possible diagrams for the ϕ_2 sgluon coupling to gluons via a squark loop. It is also possible for ϕ_2 to couple to gluons via a gluino loop in the same way as it does via squarks in the first two diagrams. However, this amplitude vanishes due to the colour symmetry of the gluinos,

$$\mathcal{M}_{\tilde{g}\text{-loop}}^{\mu\nu} = -g_S^3 [f_{CEF}f_{ADF}f_{BED} + f_{CFE}f_{BDE}f_{AFD}] \gamma^\mu \gamma^\nu C_0(k_1, k_2; m_{\tilde{g}}, m_{\tilde{g}}, m_{\tilde{g}}) = 0, \quad (5.88)$$

and therefore gluinos do not contribute in this effective one-loop vertex. The amplitude for the first two squark loop diagrams is

$$\mathcal{M}_{1+2}^{\mu\nu} = \sum_{\sigma=\{L,R\}} \sum_{\tilde{q},a} 2m_{\tilde{g}}g_S^3 \text{Tr}[\{t_A, t_B\}t_C] (-1)^\sigma \int \frac{d^4l}{(2\pi)^4} \frac{(2l-k_1)^\nu (2l+k_2)^\mu}{D_1 D_2 D_3}, \quad (5.89)$$

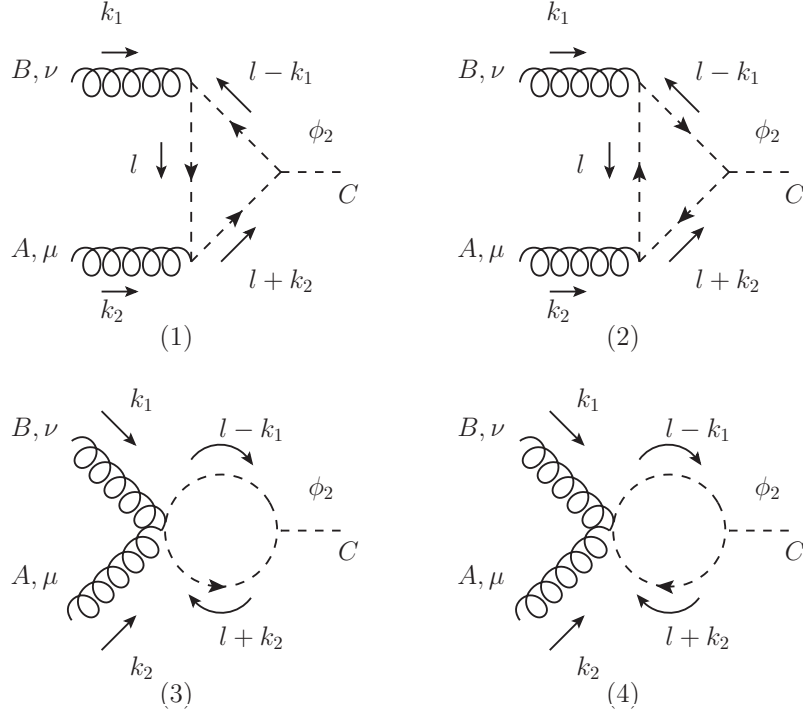


Figure 5.3: Feynman diagrams for the ϕ_2 sgluon coupling to gluons via a squark loop.

where

$$D_1 = l^2 - m_{\tilde{q}\sigma}^2, \quad (5.90)$$

$$D_2 = (l - k_1)^2 - m_{\tilde{q}\sigma}^2, \quad (5.91)$$

$$D_3 = (l + k_2)^2 - m_{\tilde{q}\sigma}^2. \quad (5.92)$$

As this is an effective vertex calculation, we take the gluons to be on shell so that

$$\epsilon(\lambda_i, k_i) \cdot k_i = 0 \quad (5.93)$$

for $i = 1, 2$, thereby killing the k_1^ν and k_2^μ terms. This leaves

$$\mathcal{M}_{1+2}^{\mu\nu} = \sum_{\sigma=\{L,R\}} \sum_{\tilde{q},a} 8m_{\tilde{q}}g_S^3 \text{Tr} [\{t_A, t_B\}t_C] (-1)^\sigma C^{\mu\nu}, \quad (5.94)$$

with

$$C^{\mu\nu} = \int \frac{d^4l}{(2\pi)^4} \frac{l^\mu l^\nu}{D_1 D_2 D_3}. \quad (5.95)$$

For the third and fourth diagrams:

$$\mathcal{M}_{3+4}^{\mu\nu} = - \sum_{\sigma=\{L,R\}} \sum_{\tilde{q},a} 2m_{\tilde{q}}g_S^3 \text{Tr} [\{t_A, t_B\}t_C] (-1)^\sigma g_{\mu\nu} B_0, \quad (5.96)$$

with the scalar two point function

$$B_0 \equiv B_0(k_1 + k_2; m_{\tilde{q}\sigma}, m_{\tilde{q}\sigma}) = \int \frac{d^4 l}{(2\pi)^4} \frac{1}{D_2 D_3}. \quad (5.97)$$

Using that

$$\{t_A, t_B\} = \frac{\delta_{AB}}{N} + \sum_D d_{ABD} t_D, \quad (5.98)$$

with d_{ABD} symmetric in all its indices, the trace simplifies to

$$\text{Tr} [\{t_A, t_B\} t_C] = \text{Tr}[t_C] \frac{\delta_{AB}}{N} + \sum_D d_{ABD} t_D \text{Tr}[t_D t_C] = \frac{1}{2} d_{ABC}. \quad (5.99)$$

Combining the two invariant amplitudes now gives

$$\mathcal{M}^{\mu\nu} = \mathcal{M}_{1+2}^{\mu\nu} + \mathcal{M}_{3+4}^{\mu\nu} = m_{\tilde{q}} g_S^3 d_{ABC} \sum_{\sigma=\{L,R\}} \sum_{\tilde{q},a} (-1)^\sigma [4C^{\mu\nu} - B_0 g^{\mu\nu}]. \quad (5.100)$$

We proceed to reduce the tensor integral $C_{\mu\nu}$ to a set of scalar integrals by expanding it in a basis of the momentum vectors k_i [15][16]. Such a basis, containing only terms that survive contraction with the gluon polarization vectors, is

$$C_{\mu\nu} = k_1^\mu k_2^\nu C_{12} + g^{\mu\nu} C_{00}. \quad (5.101)$$

The reduction functions C_{00} and C_{12} , with $k_1^2 = k_2^2 = 0$ and all internal masses equal, are given by

$$C_{00} = \frac{1}{d-2} \left(\frac{1}{2} B_0 + m_{\tilde{q}\sigma}^2 C_0(k_1, k_2; m_{\tilde{q}\sigma}, m_{\tilde{q}\sigma}, m_{\tilde{q}\sigma}) \right), \quad (5.102)$$

$$C_{12} = \frac{2}{(k_1 + k_2)^2} \left(\frac{1}{4} B_0 - \frac{1}{d-2} \left[\frac{1}{2} B_0 + m_{\tilde{q}\sigma}^2 C_0(k_1, k_2; m_{\tilde{q}\sigma}, m_{\tilde{q}\sigma}, m_{\tilde{q}\sigma}) \right] \right), \quad (5.103)$$

with d the spacetime dimension. Employing dimensional regularization, i.e. setting $d = 4 - 2\epsilon$, allows us to write

$$\frac{1}{d-2} = \frac{1}{2} (1 + \epsilon + \epsilon^2 + \dots). \quad (5.104)$$

Thus

$$4C^{\mu\nu} - B_0 g^{\mu\nu} = g^{\mu\nu} \{ (1 + \epsilon + \epsilon^2 + \dots) (B_0 + 2m_{\tilde{q}\sigma}^2 C_0) - B_0 \} \quad (5.105)$$

$$+ k_1^\mu k_2^\nu \frac{2}{(k_1 + k_2)^2} \{ B_0 - (1 + \epsilon + \epsilon^2 + \dots) (B_0 + 2m_{\tilde{q}\sigma}^2 C_0) \} \quad (5.106)$$

$$= \left[g^{\mu\nu} - \frac{2k_1^\mu k_2^\nu}{(k_1 + k_2)^2} \right] \{ B_0 (\epsilon + \epsilon^2 + \dots) + 2m_{\tilde{q}\sigma}^2 C_0 (1 + \epsilon + \epsilon^2 + \dots) \}. \quad (5.107)$$

The two and three point scalar functions are calculated in sections 5.7.1 and 5.7.2, where the latter is shown to be finite and the former has a divergence of the form

$$B_0 = \frac{i\mu^{2\epsilon}}{(4\pi)^2} \frac{1}{\epsilon} + O(1). \quad (5.108)$$

The divergence conveniently cancels with the linear ϵ term in its prefactor, and we obtain the finite result

$$4C^{\mu\nu} - B_0 g^{\mu\nu} = \left[g^{\mu\nu} - \frac{2k_1^\mu k_2^\nu}{(k_1 + k_2)^2} \right] \left(\frac{i}{(4\pi)^2} + 2m_{\tilde{q}\sigma}^2 C_0 \right). \quad (5.109)$$

The amplitude is then

$$\mathcal{M}_{ABC}^{\mu\nu} = 2m_{\tilde{q}} g_S^3 d_{ABC} \left[g^{\mu\nu} - \frac{2k_1^\mu k_2^\nu}{(k_1 + k_2)^2} \right] \sum_{\sigma=\{L,R\}} \sum_{\tilde{q}} (-1)^\sigma m_{\tilde{q}\sigma}^2 C_0(k_1, k_2; m_{\tilde{q}\sigma}, m_{\tilde{q}\sigma}, m_{\tilde{q}\sigma}). \quad (5.110)$$

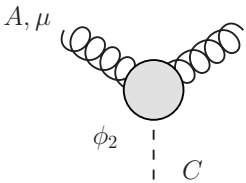
Using the result for $C_0(k_1, k_2; m_{\tilde{q}\sigma}, m_{\tilde{q}\sigma}, m_{\tilde{q}\sigma})$ calculated in section 5.7.2, we can further simplify the amplitude to

$$\mathcal{M}_{ABC}^{\mu\nu} = \frac{i}{(4\pi)^2} m_{\tilde{q}} g_S^3 d_{ABC} \left[g^{\mu\nu} - \frac{2k_1^\mu k_2^\nu}{(k_1 + k_2)^2} \right] \sum_{\tilde{q}} [\tau_L f(\tau_L) - \tau_R f(\tau_R)], \quad (5.111)$$

with

$$\tau_\sigma = \frac{4m_{\tilde{q}\sigma}^2}{(k_1 + k_2)^2}, \quad f(\tau_\sigma) = \frac{1}{4} \left[\ln \left(\frac{1 + \sqrt{1 - \tau_\sigma}}{1 - \sqrt{1 - \tau_\sigma}} \right) - i\pi \right]^2, \quad (5.112)$$

for $\tau_\sigma \leq 1$. The effective Feynman rule is thus:

Sgluon-gluon-gluon:  = $\mathcal{M}_{ABC}^{\mu\nu}$

Sgluon-quark-anti-quark

At the one-loop level the sgluons can couple to inter-generational up or down type quark-anti-quark pairs. This is possible due to the amplified flavour mixing in the MRSSM. The diagrams contributing to this process are shown in figure 5.4. In this figure $q = \{u, d\}$, i, j are generation indices in the Yukawa basis and m, n are colour indices in the fundamental representation. The pseudo-scalar field ϕ_1 only couples via the first diagram. Let

$$\Gamma_\phi \equiv \begin{cases} \mathbf{1} & : \phi_2 \\ i\gamma_5 & : \phi_1 \end{cases}, \quad (5.113)$$

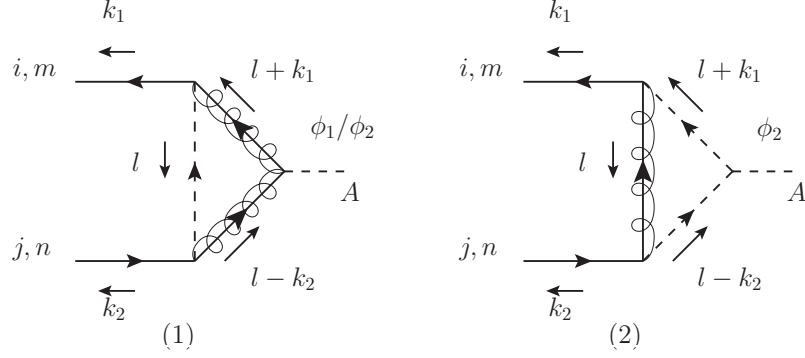


Figure 5.4: Feynman diagrams for a single sgluon coupling to a pair of inter-generational up or down type quarks

then the general amplitude for the first diagram is

$$\begin{aligned}
\mathcal{M}_1 &= 2ig_S^3 f_{ABC} (t_B t_C)_{mn} \sum_{\sigma=\{L,R\}} \sum_{\bar{q}a} (U_{\bar{q}\sigma})_{ia} (U_{\bar{q}\sigma}^\dagger)_{aj} \\
&\quad \times \int \frac{d^4 l}{(2\pi)^4} \frac{1}{D_1 D_2 D_3} \bar{u}_{im}(k_1) P_{\bar{\sigma}}(l + \mathcal{K}_1 + m_{\bar{g}}) \Gamma_\phi(l - \mathcal{K}_2 + m_{\bar{g}}) P_\sigma v_{jn}(k_2) \\
&= -3g_S^3 (t_A)_{mn} \sum_{\sigma=\{L,R\}} \sum_{\bar{q}a} (U_{\bar{q}\sigma})_{ia} (U_{\bar{q}\sigma}^\dagger)_{aj} \\
&\quad \times \int \frac{d^4 l}{(2\pi)^4} \frac{1}{D_1 D_2 D_3} \bar{u}_{im}(k_1) P_{\bar{\sigma}}(l + \mathcal{K}_1 + m_{\bar{g}}) \Gamma_\phi(l - \mathcal{K}_2 + m_{\bar{g}}) P_\sigma v_{jn}(k_2) \quad (5.114)
\end{aligned}$$

where P_σ are the chiral projection operators, $\bar{\sigma}$ is defined in (A.7), and

$$\begin{aligned}
D_1 &= l^2 - m_{\bar{q}\sigma}^2, \\
D_2 &= (l + k_1)^2 - m_{\bar{g}}^2, \\
D_3 &= (l - k_2)^2 - m_{\bar{g}}^2. \quad (5.115)
\end{aligned}$$

To simplify the colour structure we made use of the relation

$$f_{ABC} t_B t_C = \frac{1}{2} i C_2(G) t_A = i \frac{3}{2} t_A. \quad (5.116)$$

We now evaluate the spinor expression in the integral for $\Gamma_\phi = 1$ and $\Gamma_\phi = i\gamma_5$, corresponding to the coupling of the scalar field ϕ_2 and pseudo-scalar field ϕ_1 respectively. For $\Gamma_\phi = 1$:

$$\begin{aligned}
&\bar{u}_{im}(k_1) P_{\bar{\sigma}}(l + \mathcal{K}_1 + m_{\bar{g}}) (l - \mathcal{K}_2 + m_{\bar{g}}) P_\sigma v_{jn}(k_2) \\
&= m_{\bar{g}} \bar{u}_{im}(k_1) [(l + \mathcal{K}_1) P_\sigma + (l - \mathcal{K}_2) P_\sigma] v_{jn}(k_2) \\
&= m_{\bar{g}} \bar{u}_{im}(k_1) [2l + \mathcal{K}_1 - \mathcal{K}_2] P_\sigma v_{jn}(k_2). \quad (5.117)
\end{aligned}$$

For $\Gamma_\phi = i\gamma_5$:

$$\begin{aligned} & \bar{u}_{im}(k_1)P_{\bar{\sigma}}(l + \mathcal{K}_1 + m_{\bar{g}})i\gamma_5(l - \mathcal{K}_2 + m_{\bar{g}})P_{\sigma}v_{jn}(k_2) \\ &= m_{\bar{g}}\bar{u}_{im}(k_1)i\gamma_5[-\mathcal{K}_1 - \mathcal{K}_2]P_{\sigma}v_{jn}(k_2) \\ &= -im_{\bar{g}}(-1)^{\sigma}\bar{u}_{im}(k_1)[m_1P_{\sigma} - m_2P_{\bar{\sigma}}]v_{jn}(k_2), \end{aligned} \quad (5.118)$$

where we have assumed the external quarks to be on mass-shell i.e. satisfying the Dirac equation

$$(\mathcal{K}_1 - m_1)u_{im}(k_1) = 0, \quad (\mathcal{K}_2 + m_2)v_{jn}(k_2) = 0, \quad (5.119)$$

for outgoing quark masses m_1 and m_2 . The total effective one loop amplitude for the gluon field ϕ_1 is thus

$$\begin{aligned} \mathcal{M}^{\phi_1} &= 3im_{\bar{g}}g_S^3(t_A)_{mn} \sum_{\sigma=\{L,R\}} (-1)^{\sigma} \sum_{\bar{q}a} (U_{\bar{q}\sigma})_{ia} \left(U_{\bar{q}\sigma}^{\dagger} \right)_{aj} \\ &\quad \times \bar{u}_{im}(k_1) [m_1P_{\sigma} - m_2P_{\bar{\sigma}}] v_{jn}(k_2) C_0(k_1, k_2; m_{\bar{g}}, m_{\bar{q}\sigma}, m_{\bar{g}}). \end{aligned} \quad (5.120)$$

For the general form of the scalar integral C_0 see section 5.7.2. The contribution of the first diagram to the total amplitude of ϕ_2 is

$$\begin{aligned} \mathcal{M}_1^{\phi_2} &= -3m_{\bar{g}}g_S^3(t_A)_{mn} \sum_{\sigma=\{L,R\}} \sum_{\bar{q}a} (U_{\bar{q}\sigma})_{ia} \left(U_{\bar{q}\sigma}^{\dagger} \right)_{aj} \\ &\quad \times \int \frac{d^4l}{(2\pi)^4} \frac{1}{D_1 D_2 D_3} \bar{u}_{im}(k_1) [2l + \mathcal{K}_1 - \mathcal{K}_2] P_{\sigma} v_{jn}(k_2). \end{aligned} \quad (5.121)$$

The second diagram gives the amplitude

$$\begin{aligned} \mathcal{M}_2^{\phi_2} &= 4m_{\bar{g}}g_S^3(t_B t_A t_B)_{mn} \sum_{\sigma=\{L,R\}} (-1)^{\sigma} \sum_{\bar{q}a} (U_{\bar{q}\sigma})_{ia} \left(U_{\bar{q}\sigma}^{\dagger} \right)_{aj} \\ &\quad \times \int \frac{d^4l}{(2\pi)^4} \frac{1}{D'_1 D'_2 D'_3} \bar{u}_{im}(k_1) P_{\bar{\sigma}}(-l + m_{\bar{g}}) P_{\sigma} v_{jn}(k_2) \\ &= \frac{2}{3} m_{\bar{g}} g_S^3 (t_A)_{mn} \sum_{\sigma=\{L,R\}} (-1)^{\sigma} \sum_{\bar{q}a} (U_{\bar{q}\sigma})_{ia} \left(U_{\bar{q}\sigma}^{\dagger} \right)_{aj} \int \frac{d^4l}{(2\pi)^4} \frac{1}{D'_1 D'_2 D'_3} \bar{u}_{im}(k_1) \not{l} P_{\sigma} v_{jn}(k_2), \end{aligned} \quad (5.122)$$

where

$$\begin{aligned} D'_1 &= l^2 - m_{\bar{g}}^2, \\ D'_2 &= (l + k_1)^2 - m_{\bar{q}\sigma}^2, \\ D'_3 &= (l - k_2)^2 - m_{\bar{q}\sigma}^2, \end{aligned} \quad (5.123)$$

and in the second line we have used that

$$t_B t_A t_B = \left(C_2(N) - \frac{1}{2} C_2(G) \right) t_A = -\frac{1}{6} t_A. \quad (5.124)$$

Adding the amplitudes of the two contributing one-loop diagrams together gives

$$\begin{aligned} \mathcal{M}_{1+2}^{\phi_2} &= 2m_{\tilde{g}}g_S^3(t_A)_{mn} \sum_{\sigma=\{L,R\}} \sum_{\tilde{q}a} (U_{\tilde{q}\sigma})_{ia} \left(U_{\tilde{q}\sigma}^\dagger \right)_{aj} \\ &\times \bar{u}_{im}(k_1) \left[\frac{(-1)^\sigma}{3} \gamma^\mu C'_\mu - 3\gamma^\mu C_\mu + \frac{1}{2}(K_1 - K_2)C_0(k_1, k_2; m_{\tilde{g}}, m_{\tilde{q}\sigma}, m_{\tilde{g}}) \right] P_\sigma v_{jn}(k_2), \end{aligned} \quad (5.125)$$

with

$$C_\mu \equiv \int \frac{d^4l}{(2\pi)^4} \frac{l_\mu}{D_1 D_2 D_3}, \quad (5.126)$$

and C'_μ similar but with $D \rightarrow D'$. The vector integral C_μ can be decomposed into a momentum basis with scalar integral coefficients[15]

$$C_\mu = k_{1\mu} C_1 + k_{2\mu} C_2. \quad (5.127)$$

By again putting the outgoing quarks on mass-shell we arrive at a general expression for the ϕ_2 amplitude:

$$\begin{aligned} \mathcal{M}^{\phi_2} &= 2m_{\tilde{g}}g_S^3(t_A)_{mn} \sum_{\sigma=\{L,R\}} \sum_{\tilde{q}a} (U_{\tilde{q}\sigma})_{ia} \left(U_{\tilde{q}\sigma}^\dagger \right)_{aj} \\ &\times \left\{ m_1 \bar{u}_{im}(k_1) P_\sigma v_{jn}(k_2) \left[\frac{(-1)^\sigma}{3} C'_1 - 3 \left(C_1 + \frac{1}{2} C_0(k_1, k_2; m_{\tilde{g}}, m_{\tilde{q}\sigma}, m_{\tilde{g}}) \right) \right], \right. \\ &\quad \left. - m_2 \bar{u}_{im}(k_1) P_{\bar{\sigma}} v_{jn}(k_2) \left[\frac{(-1)^\sigma}{3} C'_2 - 3 \left(C_2 - \frac{1}{2} C_0(k_1, k_2; m_{\tilde{g}}, m_{\tilde{q}\sigma}, m_{\tilde{g}}) \right) \right] \right\}. \end{aligned} \quad (5.128)$$

The scalar integral functions C_1 and C_2 can be found by contracting C_μ with the momenta k_i and solving the corresponding equations,

$$k_1^2 C_1 + k_1 \cdot k_2 C_2 = \frac{1}{2} \int \frac{d^4l}{(2\pi)^4} \frac{D_2 - D_1 - k_1^2 + m_{\tilde{g}}^2 - m_{\tilde{q}\sigma}^2}{D_1 D_2 D_3}, \quad (5.129)$$

$$k_2^2 C_2 + k_1 \cdot k_2 C_1 = -\frac{1}{2} \int \frac{d^4l}{(2\pi)^4} \frac{D_3 - D_1 - k_2^2 + m_{\tilde{g}}^2 - m_{\tilde{q}\sigma}^2}{D_1 D_2 D_3}. \quad (5.130)$$

$$(5.131)$$

C'_1 and C'_2 can be found equivalently by interchanging $m_{\tilde{q}\sigma} \leftrightarrow m_{\tilde{g}}$. Because the top quark mass is much heavier than the other quark masses, we can simplify the solution by taking three special cases:

1. Single top production: $m_1 = m_t \gg m_2$.
2. Single anti-top production: $m_2 = m_t \gg m_1$.

3. Top pair (ttbar) production: $m_1 = m_2 = m_t$.

For the first two cases we have $m_i \gg m_j$ for $i \neq j = \{1, 2\}$ and thus take the limit $m_j \rightarrow 0$. The terms C_j and C'_j become irrelevant, and we find that

$$\begin{aligned} C_t(s; m_{\bar{q}\sigma}) &= C_1 = -C_2 \\ &\equiv \frac{1}{s - m_t^2} \left[B_0(s; m_{\bar{g}}, m_{\bar{g}}) - B_0(m_t^2; m_{\bar{q}\sigma}, m_{\bar{g}}) + C_0(k_1, k_2; m_{\bar{g}}, m_{\bar{q}\sigma}, m_{\bar{g}})(m_{\bar{q}\sigma}^2 - m_{\bar{g}}^2) \right], \end{aligned} \quad (5.132)$$

$$\begin{aligned} C'_t(s; m_{\bar{q}\sigma}) &= C'_1 = -C'_2 \\ &\equiv \frac{1}{s - m_t^2} \left[B_0(s; m_{\bar{q}\sigma}, m_{\bar{q}\sigma}) - B_0(m_t^2; m_{\bar{q}\sigma}, m_{\bar{g}}) + C_0(k_1, k_2; m_{\bar{q}\sigma}, m_{\bar{g}}, m_{\bar{q}\sigma})(m_{\bar{g}}^2 - m_{\bar{q}\sigma}^2) \right], \end{aligned} \quad (5.133)$$

where $s \equiv (k_1 + k_2)^2$. For the third case, where $m_1 = m_2 = m_t$, we find

$$\begin{aligned} C_{t\bar{t}}(s; m_{\bar{q}\sigma}) &= C_1 = -C_2 \\ &\equiv \frac{1}{s - 4m_t^2} \left[B_0(s; m_{\bar{g}}, m_{\bar{g}}) - B_0(m_t^2; m_{\bar{q}\sigma}, m_{\bar{g}}) \right. \\ &\quad \left. + C_0(k_1, k_2; m_{\bar{g}}, m_{\bar{q}\sigma}, m_{\bar{g}})(m_{\bar{q}\sigma}^2 - m_{\bar{g}}^2 + m_t^2) \right], \end{aligned} \quad (5.134)$$

$$\begin{aligned} C'_{t\bar{t}}(s; m_{\bar{q}\sigma}) &= C'_1 = -C'_2 \\ &\equiv \frac{1}{s - 4m_t^2} \left[B_0(s; m_{\bar{q}\sigma}, m_{\bar{q}\sigma}) - B_0(m_t^2; m_{\bar{q}\sigma}, m_{\bar{g}}) \right. \\ &\quad \left. + C_0(k_1, k_2; m_{\bar{q}\sigma}, m_{\bar{g}}, m_{\bar{q}\sigma})(m_{\bar{g}}^2 - m_{\bar{q}\sigma}^2 + m_t^2) \right]. \end{aligned} \quad (5.135)$$

We define for convenience the dimensionless functions

$$f_t(s; m_{\bar{q}\sigma}) = -i(4\pi)^2(s - m_t^2) \left[\frac{(-1)^\sigma}{3} C'_t(s; m_{\bar{q}\sigma}) - 3C_t(s; m_{\bar{q}\sigma}) - \frac{3}{2} C_0(k_1, k_2; m_{\bar{g}}, m_{\bar{q}\sigma}, m_{\bar{g}}) \right], \quad (5.136)$$

$$f_{t\bar{t}}(s; m_{\bar{q}\sigma}) = -i(4\pi)^2(s - 4m_t^2) \left[\frac{(-1)^\sigma}{3} C'_{t\bar{t}}(s; m_{\bar{q}\sigma}) - 3C_{t\bar{t}}(s; m_{\bar{q}\sigma}) - \frac{3}{2} C_0(k_1, k_2; m_{\bar{g}}, m_{\bar{q}\sigma}, m_{\bar{g}}) \right]. \quad (5.137)$$

Note that the factor $-i(4\pi)^2$ may be absorbed into the scalar integral functions B_0 and C_0 to match the normalization used by the LoopTools package [17]. The amplitudes, in terms of scalar one-loop integral functions, for the sgluon ϕ_2 are thus:

1. Single top $\phi_2 t \bar{q}_j$:

$$\mathcal{M}_t^{\phi_2} = \frac{ig_S^3 m_{\bar{g}} m_t}{8\pi^2 s - m_t^2} (t_A)_{mn} \left\{ \begin{aligned} & \bar{u}_{3m}(k_1) P_L v_{jn}(k_2) \left(\sum_{\bar{q}a} (U_{\bar{q}L})_{3a} (U_{\bar{q}L}^\dagger)_{aj} f_t(s; m_{\bar{q}aL}) \right) \\ & + \bar{u}_{3m}(k_1) P_R v_{jn}(k_2) \left(\sum_{\bar{q}a} (U_{\bar{q}R})_{3a} (U_{\bar{q}R}^\dagger)_{aj} f_t(s; m_{\bar{q}aR}) \right) \end{aligned} \right\} \quad (5.138)$$

2. Single anti-top $\phi_2 q_i \bar{t}$:

$$\mathcal{M}_{\bar{t}}^{\phi_2} = \frac{ig_S^3 m_{\bar{g}} m_t}{8\pi^2 s - m_t^2} (t_A)_{mn} \left\{ \begin{aligned} & \bar{u}_{im}(k_1) P_R v_{3n}(k_2) \left(\sum_{\bar{q}a} (U_{\bar{q}L})_{ia} (U_{\bar{q}L}^\dagger)_{a3} f_t(s; m_{\bar{q}aL}) \right) \\ & + \bar{u}_{im}(k_1) P_L v_{3n}(k_2) \left(\sum_{\bar{q}a} (U_{\bar{q}R})_{ia} (U_{\bar{q}R}^\dagger)_{a3} f_t(s; m_{\bar{q}aR}) \right) \end{aligned} \right\} \quad (5.139)$$

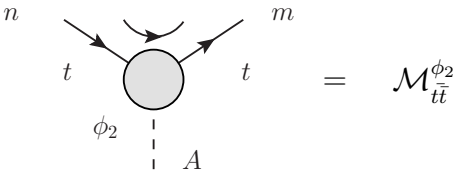
3. Top pair (ttbar) $\phi_2 t\bar{t}$:

$$\mathcal{M}_{t\bar{t}}^{\phi_2} = \frac{ig_S^3 m_{\bar{g}} m_t}{8\pi^2 s - 4m_t^2} (t_A)_{mn} \bar{u}_{3m}(k_1) v_{3n}(k_2) \times \left(\sum_{\bar{q}a} (U_{\bar{q}L})_{3a} (U_{\bar{q}L}^\dagger)_{a3} f_{t\bar{t}}(s; m_{\bar{q}aL}) + \sum_{\bar{q}a} (U_{\bar{q}R})_{3a} (U_{\bar{q}R}^\dagger)_{a3} f_{t\bar{t}}(s; m_{\bar{q}aR}) \right) \quad (5.140)$$

The effective one-loop Feynman rules for the sgluon field ϕ_2 are thus:

Sgluon-top-
[up/charm]:

$$\begin{aligned} & \begin{array}{c} j, n \\ \swarrow \quad \searrow \\ \text{---} \quad \text{---} \\ \text{---} \quad \text{---} \\ \downarrow \\ \phi_2 \quad A \end{array} = \mathcal{M}_t^{\phi_2} \\ & \begin{array}{c} n \\ \swarrow \quad \searrow \\ \text{---} \quad \text{---} \\ \text{---} \quad \text{---} \\ \downarrow \\ \phi_2 \quad A \end{array} = \mathcal{M}_{\bar{t}}^{\phi_2} \end{aligned}$$

Sgluon-top-pair:  = $\mathcal{M}_{tt}^{\phi_2}$

Because the sgluon field ϕ_1 does not couple to gluons its single production relative to ϕ_2 is greatly suppressed and we thus ignore its contribution to single top processes. We also do not write its effective one-loop Feynman rules, although these may be deduced in exactly the same way as for ϕ_2 from equation (5.120).

5.6 Sgluon decays

We are interested in MRSSM processes that mimic the signals of single top production. Single sgluon production offers such an avenue. Only the real component field ϕ_2 of the complex scalar field ϕ_G , however, couples singularly to a pair of gluons. As production by a pair of quarks will be suppressed, we will ignore the pseudo scalar field ϕ_1 (stating only some results for completeness). In order to calculate the total decay width of the field ϕ_2 , all partial decay rates are presented.

The generic formula for a $1 \rightarrow 2$ decay in the centre of momentum frame is

$$\Gamma(A \rightarrow BC) = \frac{1}{2m_A} \frac{1}{8\pi} \overline{\sum} |\mathcal{M}|^2 \lambda^{1/2} \left(1, \frac{m_B^2}{m_A^2}, \frac{m_C^2}{m_A^2} \right), \quad (5.141)$$

with λ defined in (A.22). When averaging over the squared amplitudes, one must remember that the sgluon fields are colour octets.

The sgluon tree-level decays are:

$$\Gamma(\phi_2 \rightarrow \tilde{q}_{a\sigma}^* \tilde{q}_{a\sigma}) = \frac{\alpha_S m_{\tilde{g}}^2}{2M_{\phi_2}} \sqrt{1 - \frac{4m_{\tilde{q}\sigma}^2}{M_{\phi_2}^2}}, \quad (5.142)$$

$$\Gamma(\phi_2 \rightarrow \tilde{g}\tilde{g}) = \frac{3\alpha_S M_{\phi_2}}{2} \left(1 - \frac{4m_{\tilde{g}}^2}{M_{\phi_2}^2} \right)^{\frac{3}{2}}, \quad (5.143)$$

$$\Gamma(\phi_1 \rightarrow \tilde{g}\tilde{g}) = \frac{3\alpha_S M_{\phi_1}}{2} \sqrt{1 - \frac{4m_{\tilde{g}}^2}{M_{\phi_1}^2}}. \quad (5.144)$$

The sgluon one-loop decay to two gluons is

$$\Gamma(\phi_2 \rightarrow gg) = \frac{5\alpha_S^3}{192\pi^2} \frac{m_{\tilde{g}}^2}{M_{\phi_2}} \left| \sum_{\tilde{q}} [\tau_L f(\tau_L) - \tau_R f(\tau_R)] \right|^2, \quad (5.145)$$

with τ_σ and $f(\tau_\sigma)$ defined in (5.112). Note that a factor of $1/2!$ was included for the identical outgoing particles.

Sgluon decays involving single top quarks are given by

$$\Gamma(\phi_2 \rightarrow \bar{t}_3 q_j) = \Gamma(\phi_2 \rightarrow \bar{q}_i t_3) = \frac{\alpha_S^3 m_{\bar{g}}^2 m_t^2}{32\pi^2 M_{\phi_2}^3} \left\{ \left| \sum_{\bar{q}a} (U_{\bar{q}L})_{ia} (U_{\bar{q}L}^\dagger)_{aj} f_t(s; m_{\bar{q}aL}) \right|^2 + \left| \sum_{\bar{q}a} (U_{\bar{q}R})_{ia} (U_{\bar{q}R}^\dagger)_{aj} f_t(s; m_{\bar{q}aR}) \right|^2 \right\}, \quad (5.146)$$

and to a top pair by

$$\Gamma(\phi_2 \rightarrow t\bar{t}) = \frac{\alpha_S^3 m_{\bar{g}}^2 m_t^2}{16\pi^2 M_{\phi_2}^3} \left(1 - \frac{4m_t^2}{M_{\phi_2}^2} \right)^{-1/2} \times \left| \sum_{\bar{q}a} (U_{\bar{q}L})_{3a} (U_{\bar{q}L}^\dagger)_{a3} f_{t\bar{t}}(s; m_{\bar{q}aL}) + \sum_{\bar{q}a} (U_{\bar{q}R})_{3a} (U_{\bar{q}R}^\dagger)_{a3} f_{t\bar{t}}(s; m_{\bar{q}aR}) \right|^2, \quad (5.147)$$

with $f_t(s; m_{\bar{q}\sigma})$ and $f_{t\bar{t}}(s; m_{\bar{q}\sigma})$ defined by equations (5.136) and (5.137) respectively.

The results presented in this chapter differ with the original analysis of sgluons in the MRSSM by Plehn *et al.* [18], specifically in the derivation of the sgluon-quark effective Feynman rules and the coupling asymmetry of the two sgluon components. In this paper the authors conclude that the two scalar sgluon states behave similarly at colliders up to a difference in their mass, which is not the case for the sgluon states ϕ_2 and ϕ_1 derived here. The results compare well with those of Choi *et al.* [19], who consider color-octet scalars of an $N = 2$ supersymmetry model. The results differ in the presence of squark flavour mixing, as their model has none. Also, the decays and cross sections are stated in terms of the complex scalar field ϕ_G rather than the scalar components fields, and are therefore off by a factor of a half for processes where only ϕ_2 couples.

5.7 Technical aside: scalar one-loop integrals

Here we derive expressions for the most general two and three point scalar one-loop functions $B_0(p; m_1, m_2)$ and $C_0(p_1, p_2; m_1, m_2, m_3)$. These functions appear in the effective one-loop vertices calculated in this chapter.

5.7.1 Two point function: $B_0(p; m_1, m_2)$

The general two point function is defined as the the scalar one-loop integral

$$B_0(p; m_1, m_2) = \int \frac{d^4 l}{(2\pi)^4} \frac{1}{(l^2 - m_1^2)((l+p)^2 - m_2^2)}, \quad (5.148)$$

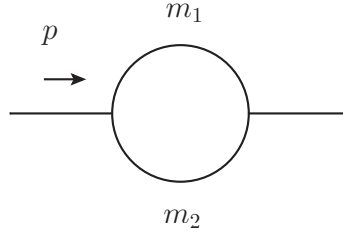


Figure 5.5: Bubble diagram corresponding to the general two point function $B_0(p; m_1, m_2)$

shown in figure 5.5. We use dimensional regularization with $d = 4 - 2\epsilon$ and introduce μ as an arbitrary mass scale, so that

$$B_0 = \mu^{2\epsilon} \int \frac{d^d l}{(2\pi)^d} \frac{1}{(l^2 - m_1^2)((l+p)^2 - m_2^2)}. \quad (5.149)$$

Applying the standard Feynman trick

$$\frac{1}{AB} = \int_0^1 dx \frac{1}{[xA + (1-x)B]^2}, \quad (5.150)$$

gives

$$B_0 = \mu^{2\epsilon} \int \frac{d^d l}{(2\pi)^d} \int_0^1 dx [l^2 + 2l \cdot px + x(p^2 - m_2^2 + m_1^2) - m_1^2]^{-2}, \quad (5.151)$$

which may be simplified by completing the square and performing a shift in the momentum coordinate $l = l' - xp$:

$$B_0 = \mu^{2\epsilon} \int \frac{d^d l'}{(2\pi)^d} \int_0^1 dx [l'^2 + x(p^2 - m_2^2 + m_1^2) - x^2 p^2 - m_1^2]^{-2}. \quad (5.152)$$

Using now the non-trivial result for d -dimensional integrals in Minkowski space (refer for example to Peskin and Schroeder [20])

$$\int \frac{d^d l}{(2\pi)^d} [l^2 - M^2 + i\epsilon]^{-t} = (-1)^t i (4\pi)^{\epsilon-2} \frac{\Gamma(t - d/2)}{\Gamma(t)} [M^2 - i\epsilon]^{d/2-t}, \quad (5.153)$$

we find that

$$B_0 = \mu^{2\epsilon} i (4\pi)^{\epsilon-2} \Gamma(\epsilon) \int_0^1 dx [x^2 p^2 - x(p^2 - m_2^2 + m_1^2) + m_1^2]^{-\epsilon}. \quad (5.154)$$

The gamma function obeys the relation

$$\Gamma(\epsilon) = \frac{1}{\epsilon} \Gamma(1 + \epsilon) \approx \frac{1}{\epsilon} e^{-\epsilon\gamma_E}, \quad (5.155)$$

with γ_E the Euler constant. Using also that

$$a^{-\epsilon} = 1 - \epsilon \ln a + O(\epsilon^2), \quad (5.156)$$

and

$$(4\pi)^\epsilon = \exp(\epsilon \ln 4\pi) = 1 + \epsilon \ln(4\pi) + O(\epsilon^2), \quad (5.157)$$

we may express B_0 as an expansion in powers of ϵ :

$$\begin{aligned} B_0 &= \frac{i\mu^{2\epsilon}}{(4\pi)^2} (1 + \epsilon \ln(4\pi) + O(\epsilon^2)) \\ &\quad \times \frac{1}{\epsilon} (1 - \epsilon\gamma_E + O(\epsilon^2)) \\ &\quad \times \left(1 - \epsilon \int_0^1 dx \ln [x^2 p^2 - x(p^2 - m_2^2 + m_1^2) + m_1^2] + O(\epsilon^2) \right) \end{aligned} \quad (5.158)$$

$$= \frac{i\mu^{2\epsilon}}{(4\pi)^2} \left(\ln(4\pi) - \gamma_E - \int_0^1 dx \ln [x^2 p^2 - x(p^2 - m_2^2 + m_1^2) + m_1^2] + \frac{1}{\epsilon} + O(\epsilon) \right). \quad (5.159)$$

The log argument is quadratic in x and can be factorized as

$$x_\pm = \frac{1}{2} \left(1 + \frac{m_1^2 - m_2^2}{p^2} \pm \lambda^{1/2} \right), \quad (5.160)$$

where

$$\lambda^{1/2} \equiv \sqrt{\lambda \left(1, \frac{m_1^2}{p^2}, \frac{m_2^2}{p^2} \right)}. \quad (5.161)$$

The x integral may then be computed as

$$\begin{aligned} &\int_0^1 dx \ln (p^2(x - x_+)(x - x_-)) \\ &= \ln(p^2) + \int_0^1 dx (\ln(x - x_+) + \ln(x - x_-)) \\ &= \ln(p^2) + [(x - x_+) \ln(x - x_+) + (x - x_-) \ln(x - x_-) - 2x]_0^1 \\ &= \ln(p^2) - 2 + \ln(1 - x_+)(1 - x_-) - x_+ \ln \left(1 - \frac{1}{x_+} \right) - x_- \ln \left(1 - \frac{1}{x_-} \right) \\ &= \ln(p^2) - 2 + \frac{m_1^2 - m_2^2}{p^2} \ln \left(\frac{m_1}{m_2} \right) + \ln \left(\frac{m_1 m_2}{p^2} \right) + \frac{\lambda^{1/2}}{2} \ln \left(\frac{(1 + \lambda^{1/2})^2 - (m_1^2 - m_2^2)/p^2}{(1 - \lambda^{1/2})^2 - (m_1^2 - m_2^2)/p^2} \right) \end{aligned} \quad (5.162)$$

The final solution for the scalar two point function is

$$B_0(p; m_1, m_2) = \Delta(\epsilon) - \frac{i}{(4\pi)^2} \left\{ \ln(p^2) - 2 + \frac{m_1^2 - m_2^2}{p^2} \ln\left(\frac{m_1}{m_2}\right) + \ln\left(\frac{m_1 m_2}{p^2}\right) + \frac{\lambda^{1/2}}{2} \ln\left(\frac{(1 + \lambda^{1/2})^2 - (m_1^2 - m_2^2)/p^2}{(1 - \lambda^{1/2})^2 - (m_1^2 - m_2^2)/p^2}\right) \right\} \quad (5.163)$$

where the divergences have been contained in

$$\Delta(\epsilon) = \frac{i\mu^{2\epsilon}}{(4\pi)^2} \left(\ln(4\pi) - \gamma_E + \frac{1}{\epsilon} + O(\epsilon) \right). \quad (5.164)$$

5.7.2 Three point function: $C_0(p_1, p_2; m_1, m_2, m_3)$

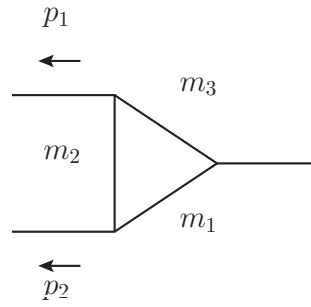


Figure 5.6: Triangle diagram corresponding to the general three point function $C_0(p_1, p_2; m_1, m_2, m_3)$

The general three point function is defined as the scalar one-loop integral

$$C_0(p_1, p_2; m_1, m_2, m_3) = \int \frac{d^4 l}{(2\pi)^4} \frac{1}{(l^2 - m_3^2)((l + p_1)^2 - m_2^2)((l + p_1 + p_2)^2 - m_1^2)}, \quad (5.165)$$

shown in figure 5.6. This integral is not divergent, so there is no need to use dimensional regularization. Using the Feynman trick

$$\begin{aligned} \frac{1}{ABC} &= \int_0^1 dx \int_0^1 dy \int_0^1 dz \delta(x + y + z - 1) \frac{(3-1)!}{[xA + yB + zC]^3} \\ &= 2 \int_0^1 dx \int_0^{1-x} dy \frac{1}{[xA + yB + (1-x-y)C]^3} \\ &= 2 \int_0^1 dx \int_0^x dy \frac{1}{[(1-x)A + yB + (x-y)C]^3}, \end{aligned} \quad (5.166)$$

gives

$$C_0 = 2 \int_0^1 dx \int_0^x dy \int \frac{d^4 l}{(2\pi)^4} \left[l^2 + 2l \cdot (p_1(1-y) + p_2(1-x)) - m_1^2 + y(m_2^2 - m_3^2 - p_1^2) + x(p_1^2 + m_2^2 + m_1^2 - (p_1 + p_2)^2) + (p_1 + p_2)^2 \right]^{-3}. \quad (5.167)$$

Completing the square and performing the shift in momentum $l = l' - p_1(1-y) + p_2(1-x)$ gives the simpler expression

$$C_0 = 2 \int_0^1 dx \int_0^x dy \int \frac{d^4 l'}{(2\pi)^4} \left[l'^2 - y^2 p_1^2 - x^2 p_2^2 - xy 2p_1 \cdot p_2 - m_1^2 + y(m_2^2 - m_3^2 + p_1^2 + 2p_1 \cdot p_2) + x(m_1^2 - m_2^2 + p_2^2) \right]^{-3}. \quad (5.168)$$

Using again the identity for d -dimensional integrals given in (5.153) with $\epsilon \rightarrow 0$ we can write the three point function as

$$C_0 = \frac{-i}{(4\pi)^2} \int_0^1 dx \int_0^x dy [ax^2 + by^2 + cxy + dx + ey + f]^{-1}, \quad (5.169)$$

with

$$a = p_2^2, \quad b = p_1^2, \quad (5.170)$$

$$c = 2p_1 \cdot p_2, \quad d = m_2^2 - m_1^2 - p_2^2, \quad (5.171)$$

$$e = m_3^2 - m_2^2 - p_1^2 - 2p_1 \cdot p_2, \quad f = m_1^2 - i\epsilon. \quad (5.172)$$

To remove the x^2 dependence in the integral we perform a shift $y = y' + \alpha x$ and make an appropriate choice for α . The denominator after this shift becomes

$$(b\alpha^2 + c\alpha + a)x^2 + by^2 + (c + 2\alpha b)xy + (d + e\alpha)x + ey + f, \quad (5.173)$$

and we thus choose

$$\begin{aligned} \alpha &= \frac{-c + \theta\sqrt{c^2 - 4ab}}{2b} \\ &= \frac{1}{2p_1^2} \left(-2p_1 \cdot p_2 + \theta\sqrt{\lambda((p_1 + p_2)^2, p_1^2, p_2^2)} \right), \end{aligned} \quad (5.174)$$

with $\theta = \pm 1$. This gives

$$\begin{aligned} i(4\pi)^2 C_0 &= \int_0^1 dx \int_{-\alpha x}^{(1-\alpha)x} dy [by^2 + (c + 2\alpha b)xy + (d + e\alpha)x + ey + f]^{-1} \\ &= \int_0^1 dx \int_0^{(1-\alpha)x} dy [\dots]^{-1} - \int_0^1 dx \int_0^{-\alpha x} dy [\dots]^{-1} \\ &= \int_0^{1-\alpha} dy \int_{y/(1-\alpha)}^1 dx [\dots]^{-1} - \int_0^{-\alpha} dy \int_{-y/\alpha}^1 dx [\dots]^{-1}. \end{aligned} \quad (5.175)$$

We now define the co-efficient of the remaining linear x term as $N \equiv y(c+2\alpha b)+e\alpha+d$, and proceed to integrate it out

$$\begin{aligned} i(4\pi)^2 C_0 &= \int_0^{1-\alpha} dy \frac{1}{N} \left[\ln \left(x + \frac{by^2 + ey + f}{N} \right) \right]_{x=y/(1-\alpha)}^{x=1} \\ &\quad - \int_0^{-\alpha} dy \frac{1}{N} \left[\ln \left(x + \frac{by^2 + ey + f}{N} \right) \right]_{x=-y/\alpha}^{x=1} \end{aligned} \quad (5.176)$$

$$\begin{aligned} &= \int_{-\alpha}^{1-\alpha} dy \frac{1}{N} \ln (N + by^2 + ey + f) \\ &\quad - \int_0^{1-\alpha} dy \frac{1}{N} \ln \left(\frac{Ny}{1-\alpha} + by^2 + ey + f \right) \\ &\quad + \int_0^{-\alpha} dy \frac{1}{N} \ln \left(\frac{-Ny}{\alpha} + by^2 + ey + f \right). \end{aligned} \quad (5.177)$$

Noting that

$$y_0 = -\frac{d + e\alpha}{c + 2\alpha b} \quad (5.178)$$

is the solution to $N = 0$, we add the following trivial term to C_0 to make it well defined at its poles

$$\frac{1}{i(4\pi)^2} \left(- \int_{-\alpha}^{1-\alpha} dy + \int_0^{1-\alpha} dy - \int_0^{-\alpha} dy \right) \frac{1}{N} \ln (by_0^2 + ey_0 + f) = 0. \quad (5.179)$$

We now shift each of the three integrals in (5.177) by $y = y' - \alpha$, $y = (1 - \alpha)y'$ and $y = -\alpha y'$ respectively:

$$\begin{aligned} i(4\pi)^2 C_0 &= \int_0^1 dy \frac{1}{(c + 2\alpha b)y + d + \alpha(c + e) + 2a} \left\{ \ln [by^2 + y(c + e) + a + d + f] - (y \rightarrow y_1) \right\} \\ &\quad - \int_0^1 dy \frac{1}{(c + 2\alpha b)y + (d + e\alpha)/(1 - \alpha)} \left\{ \ln [(a + b + c)y^2 + (e + d)y + f] - (y \rightarrow y_2) \right\} \\ &\quad + \int_0^1 dy \frac{1}{(c + 2\alpha b)y - d/\alpha - e} \left\{ \ln [ay^2 + dy + f] - (y \rightarrow y_3) \right\}, \end{aligned} \quad (5.180)$$

where $y_1 \equiv y_0 + \alpha$, $y_2 \equiv y_0/(1 - \alpha)$ and $y_3 \equiv -y_0/\alpha$. Substituting for N , α and a, \dots, f we have

$$\begin{aligned} i(4\pi)^2 \theta \lambda^{1/2} C_0 &= \int_0^1 dy \frac{1}{y - y_1} \left\{ \ln [p_1^2 y^2 + y(m_3^2 - m_2^2 - p_1^2) + m_2^2] - (y \rightarrow y_1) \right\} \\ &\quad - \int_0^1 dy \frac{1}{y - y_2} \left\{ \ln [(p_1 + p_2)^2 y^2 + y(m_3^2 - m_1^2 - (p_1 + p_2)^2) + m_1^2] - (y \rightarrow y_2) \right\} \\ &\quad + \int_0^1 dy \frac{1}{y - y_3} \left\{ \ln [p_2^2 y^2 + y(m_2^2 - m_1^2 - p_2^2) + m_1^2] - (y \rightarrow y_3) \right\}, \end{aligned} \quad (5.181)$$

with

$$y_1 = \frac{1}{2p_1^2 \theta \lambda^{1/2}} \left\{ p_1^2 (p_1^2 - p_2^2 - (p_1 + p_2)^2 + 2m_1^2 - m_3^2 - m_2^2) \right. \\ \left. + ((p_1 + p_2)^2 - p_2^2)(m_3^2 - m_2^2) + \theta \lambda^{1/2} (p_1^2 - m_3^2 + m_2^2) \right\}, \quad (5.182)$$

$$y_2 = \frac{-1}{2(p_1 + p_2)^2 \theta \lambda^{1/2}} \left\{ (p_1 + p_2)^2 ((p_1 + p_2)^2 - p_2^2 - p_1^2 + 2m_2^2 - m_3^2 - m_1^2) \right. \\ \left. + (p_1^2 - p_2^2)(m_3^2 - m_1^2) - \theta \lambda^{1/2} ((p_1 + p_2)^2 - m_3^2 + m_1^2) \right\}, \quad (5.183)$$

$$y_3 = \frac{1}{2p_2^2 \theta \lambda^{1/2}} \left\{ p_2^2 (p_2^2 - p_1^2 - (p_1 + p_2)^2 + 2m_3^2 - m_2^2 - m_1^2) \right. \\ \left. + (p_1^2 - (p_1 + p_2)^2)(m_2^2 - m_1^2) + \theta \lambda^{1/2} (p_2^2 - m_2^2 + m_1^2) \right\}, \quad (5.184)$$

where

$$\lambda^{1/2} \equiv \sqrt{\lambda ((p_1 + p_2)^2, p_1^2, p_2^2)}. \quad (5.185)$$

Factorizing the arguments of the logarithms gives

$$C_0 = \frac{1}{i(4\pi)^2 \theta \lambda^{1/2}} \sum_{i=1}^3 (-1)^{i-1} \int_0^1 dy \frac{1}{y - y_i} \{ \ln [(y - x_{i+})(y - x_{i-})] - \ln [(y_i - x_{i+})(y_i - x_{i-})] \} \\ = \frac{1}{i(4\pi)^2 \theta \lambda^{1/2}} \sum_{i=1}^3 \sum_{\sigma=\pm} (-1)^{i-1} \int_0^1 dy \frac{1}{y - y_i} \{ \ln [y - x_{i\sigma}] - \ln [y_i - x_{i\sigma}] \}, \quad (5.186)$$

with

$$x_{1\pm} = \frac{1}{2p_1^2} \left[p_1^2 - m_3^2 + m_2^2 \pm \sqrt{\lambda (p_1^2, m_3^2, m_2^2)} \right], \quad (5.187)$$

$$x_{2\pm} = \frac{1}{2(p_1 + p_2)^2} \left[(p_1 + p_2)^2 - m_3^2 + m_1^2 \pm \sqrt{\lambda ((p_1 + p_2)^2, m_3^2, m_1^2)} \right], \quad (5.188)$$

$$x_{3\pm} = \frac{1}{2p_2^2} \left[p_2^2 - m_2^2 + m_1^2 \pm \sqrt{\lambda (p_2^2, m_2^2, m_1^2)} \right]. \quad (5.189)$$

$$(5.190)$$

Note that we assume no imaginary logarithmic arguments, which is valid for on shell external momenta. For a discussion, including imaginary logarithmic arguments via η functions see 't Hooft *et al.* [21].

We now turn our attention to the integral

$$I = \int_0^1 dy \frac{1}{y - y_i} \{ \ln(y - x_{i\sigma}) - \ln(y_i - x_{i\sigma}) \}. \quad (5.191)$$

Performing the shift $y = y' + x_{i\sigma}$ gives

$$\begin{aligned} I &= \int_{-x_{i\sigma}}^{1-x_{i\sigma}} dy \frac{1}{y - y_i + x_{i\sigma}} \{ \ln(y) - \ln(y_i - x_{i\sigma}) \} \\ I &= \left(\int_0^{1-x_{i\sigma}} dy - \int_0^{-x_{i\sigma}} dy \right) \frac{1}{y - y_i + x_{i\sigma}} \{ \ln(y) - \ln(y_i - x_{i\sigma}) \}, \end{aligned} \quad (5.192)$$

and rescaling the two integrals by $y = (1 - x_{i\sigma})y'$ and $y = -x_{i\sigma}y'$ respectively:

$$\begin{aligned} I &= \int_0^1 dy \frac{1}{y - (y_i - x_{i\sigma})/(1 - x_{i\sigma})} \{ \ln(y(1 - x_{i\sigma})) - \ln(y_i - x_{i\sigma}) \} \\ &\quad - \int_0^1 dy \frac{1}{y - (x_{i\sigma} - y_i)/x_{i\sigma}} \{ \ln(-x_{i\sigma}y) - \ln(y_i - x_{i\sigma}) \} \end{aligned} \quad (5.193)$$

$$\begin{aligned} &= \int_0^1 dy \left[\frac{d}{dy} \ln \left(1 - y \left(\frac{1 - x_{i\sigma}}{y_i - x_{i\sigma}} \right) \right) \right] \{ \ln(y(1 - x_{i\sigma})) - \ln(y_i - x_{i\sigma}) \} \\ &\quad - \int_0^1 dy \left[\frac{d}{dy} \ln \left(1 - y \left(\frac{x_{i\sigma}}{x_{i\sigma} - y_i} \right) \right) \right] \{ \ln(-x_{i\sigma}y) - \ln(y_i - x_{i\sigma}) \}. \end{aligned} \quad (5.194)$$

Partially integrating penultimately gives

$$\begin{aligned} I &= \text{Li}_2 \left(\frac{x_{i\sigma} - 1}{x_{i\sigma} - y_i} \right) + \ln \left(\frac{1 - y_i}{x_{i\sigma} - y_i} \right) \{ \ln(1 - x_{i\sigma}) - \ln(y_i - x_{i\sigma}) \} \\ &\quad - \text{Li}_2 \left(\frac{x_{i\sigma}}{x_{i\sigma} - y_i} \right) - \ln \left(\frac{-y_i}{x_{i\sigma} - y_i} \right) \{ \ln(-x_{i\sigma}) - \ln(y_i - x_{i\sigma}) \}, \end{aligned} \quad (5.195)$$

where

$$\text{Li}_2(x) = - \int_0^x dy \frac{\ln(1 - y)}{y} \quad (5.196)$$

is the dilogarithm function. Using the dilogarithm property that

$$\text{Li}_2(x) = -\text{Li}_2(1 - x) + \frac{\pi^2}{6} - \ln(x) \ln(1 - x), \quad (5.197)$$

we can cast the integral into its final form

$$I = \text{Li}_2 \left(\frac{y_i}{y_i - x_{i\sigma}} \right) - \text{Li}_2 \left(\frac{y_i - 1}{y_i - x_{i\sigma}} \right), \quad (5.198)$$

where again all possible η functions have been suppressed.

To cast the final solution into a symmetric form, let

$$\Pi_i = \begin{cases} p_1 & i = 1 \\ p_1 + p_2 & i = 2 \\ p_2 & i = 3 \end{cases} \quad (5.199)$$

and set $\theta = 1$ for $i = 1, 3$ and $\theta = -1$ for $i = 2$. The three point scalar function is then

$$C_0(p_1, p_2; m_3^2, m_2^2, m_1^2) = \frac{i}{(4\pi)^2} \frac{1}{\sqrt{\lambda((p_1 + p_2)^2, p_1^2, p_2^2)}} \times \sum_{i=1}^3 \sum_{\sigma=\pm} \left\{ \text{Li}_2 \left(\frac{Y_i - 2\Pi_i^2}{Y_i - X_{i\sigma}} \right) - \text{Li}_2 \left(\frac{Y_i}{Y_i - X_{i\sigma}} \right) \right\}, \quad (5.200)$$

with

$$Y_i = \frac{1}{\sqrt{\lambda((p_1 + p_2)^2, p_1^2, p_2^2)}} \left\{ \Pi_i^2 (\Pi_i^2 - \Pi_j^2 - \Pi_k^2 + 2m_i^2 - m_j^2 - m_k^2) + (\Pi_j^2 - \Pi_k^2)(m_k^2 - m_j^2) + \sqrt{\lambda((p_1 + p_2)^2, p_1^2, p_2^2)} (\Pi_i^2 - m_k^2 + m_j^2) \right\}, \quad (5.201)$$

$$X_{i\pm} = \Pi_i^2 + (-1)^i (m_k^2 - m_j^2) \pm \sqrt{\lambda(\Pi_i^2, m_j^2, m_k^2)}, \quad (5.202)$$

and i, j, k are cyclic. For $\Pi_i^2 = 0$ the i th contribution vanishes. This solution differs to Denner [16] by the factor $(-1)^i$ appearing in the $X_{i\pm}$ term.

Special case: $m_1 = m_2 = m_3$ and $p_1^2 = p_2^2 = 0$

Consider the special case where $m_j = m$ for $j = 1, \dots, 3$ and $p_1^2 = p_2^2 = 0$. Only $\Pi_2 \equiv s = 2p_1 \cdot p_2$ is non-zero, and subsequently $i = 2$ gives the only contribution to the sum. We thus find

$$Y_2 = 2s \quad \text{and} \quad X_{2\pm} = s(1 \pm \beta), \quad (5.203)$$

with

$$\beta \equiv \sqrt{1 - \frac{4m^2}{s}}. \quad (5.204)$$

The scalar integral therefore becomes

$$C_0 = \frac{i}{(4\pi)^2} \frac{1}{s} \left\{ -\text{Li}_2 \left(\frac{2}{1 + \beta} \right) - \text{Li}_2 \left(\frac{2}{1 - \beta} \right) \right\} = \frac{i}{(4\pi)^2} \frac{-1}{s} \left\{ \text{Li}_2(1 - x) - \text{Li}_2(1 - x^{-1}) \right\}, \quad (5.205)$$

where

$$x = -\frac{1 + \beta}{1 - \beta}. \quad (5.206)$$

Using now the dilogarithm identity

$$\mathrm{Li}_2(1-x) - \mathrm{Li}_2(1-x^{-1}) = -\frac{1}{2}(\ln x)^2, \quad (5.207)$$

and that for a negative logarithm argument $\ln(-x) = \ln(x) + i\pi$, we arrive at the solution

$$C_0(s = 2p_1 \cdot p_2; m, m, m) = \frac{i}{(4\pi)^2} \frac{1}{2s} \left[\ln \left(\frac{1+\beta}{1-\beta} \right) - i\pi \right]^2, \quad (5.208)$$

for $s \geq 4m^2$.

Chapter 6

Numerical Methods

6.1 Phase space integration

The measure for integration over the phase space of N outgoing particles is

$$d\text{PS}(N) = \prod_{j=1}^N \frac{d^3 \mathbf{p}_j}{(2\pi)^3 2E_j} (2\pi)^4 \delta^{(4)}(q - \sum_{j=1}^N p_j). \quad (6.1)$$

The presence of the delta function ensures conservation of energy and momentum and makes this a $3N - 4$ dimensional integral (when $N \geq 2$). Although not explicit in this expression, every outgoing momentum is on mass-shell. To compute this integral in a numerical setting it is convenient to make a change of coordinates from the components of the four momenta p_j to unit normalized coordinates $x_i \in [0, 1]$ where $i = 1, \dots, 3N - 4$. To achieve this, we first build up the physical phase space by performing successive two particle decays in the centre of momentum frame. At each decay step one external particle is created on-shell and the remaining mass and momentum is carried away by an off-shell particle that gives the subsequent decay. The degrees of freedom that arise at each decay step are parameterized by the new coordinates x_i . The remaining last two momenta in this decay chain are both on-shell.

We begin by defining the quantities:

$$\sigma_i \equiv \sum_{j=i}^N m_j, \quad \tilde{m}_i^2 \equiv \left(\sum_{j=i}^N p_j \right)^2, \quad \tilde{E}_i^2 \equiv \sum_{j=i}^N E_j. \quad (6.2)$$

The decay chain process is shown in figure 6.1. The term \tilde{m}_i is the mass carried away by the off-shell decay partner, and therefore the available mass of the next decay. The incoming energy of the entire process is given by $\tilde{m}_1 = \tilde{E}_1 = \sqrt{s}$. The energy and three momenta of the decay process that generates the outgoing on-shell momentum p_i , from an incoming energy \tilde{m}_i in the centre of momentum frame, are

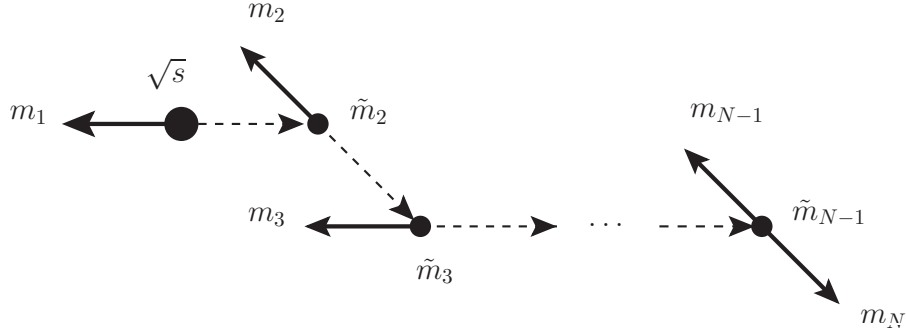


Figure 6.1: The successive chain of decays used to build up the phase space.

given by

$$E_i = \frac{\tilde{m}_i^2 - \tilde{m}_{i+1}^2 + m_i^2}{2\tilde{m}_i}, \quad \mathbf{p}_i = (|\mathbf{p}_i| \sin \phi \sin \theta, |\mathbf{p}_i| \cos \phi \sin \theta, |\mathbf{p}_i| \cos \theta), \quad (6.3)$$

$$\tilde{E}_{i+1} = \frac{\tilde{m}_i^2 + \tilde{m}_{i+1}^2 - m_i^2}{2\tilde{m}_i}, \quad \tilde{\mathbf{p}}_{i+1} = -\mathbf{p}_i, \quad (6.4)$$

where

$$|\mathbf{p}_i| = \frac{\lambda^{1/2}(\tilde{m}_i^2, m_i^2, \tilde{m}_{i+1}^2)}{2\tilde{m}_i}. \quad (6.5)$$

The free variables in this decay are the off-shell mass \tilde{m}_{i+1} , and the spherical polar angles θ and ϕ specifying the direction of the outgoing three momenta. The maximum value \tilde{m}_{i+1} can take is all of the incoming energy \tilde{m}_i minus the on-shell mass of the i th particle. The minimum value is the sum of all the remaining particle masses. We may therefore make the parameterizations

$$\phi = 2\pi x_1^i, \quad (6.6)$$

$$\cos \theta = 1 - 2x_2^i, \quad (6.7)$$

$$\tilde{m}_{i+1} = \sigma_{i+1} + (\tilde{m}_i - \sigma_i)x_3^i, \quad (6.8)$$

where $x_k^i \in [0, 1]$ for $k = 1, 2, 3$. The phase space measure for the momentum p_i can be written in terms of the spherical polar angles and the off-shell mass as

$$\begin{aligned} \frac{d^3 \mathbf{p}_i}{(2\pi)^3 2E_i} &= \frac{|\mathbf{p}_i|^2}{(2\pi)^3 2E_i} d|\mathbf{p}_i| d\cos \theta d\phi \\ &= \frac{|\mathbf{p}_i|}{2(2\pi)^3} \frac{\tilde{m}_{i+1}}{\tilde{m}_i} d\tilde{m}_{i+1} d\cos \theta d\phi. \end{aligned} \quad (6.9)$$

Rewritten in terms of the unit normalized coordinates $x_k^i \in [0, 1]$ it is thus

$$\frac{d^3 \mathbf{p}_i}{(2\pi)^3 2E_i} = \frac{1}{4\pi^2} \frac{\tilde{m}_{i+1}}{\tilde{m}_i} |\mathbf{p}_i| (\tilde{m}_i - \sigma_i) dx_1^i dx_2^i dx_3^i. \quad (6.10)$$

For the evaluation of the final two phase space measures in this procedure we make use of the delta function that is still present to eliminate one of them:

$$\frac{d^3 \mathbf{p}_{N-1}}{(2\pi)^3 2E_{N-1}} \frac{d^3 \mathbf{p}_N}{(2\pi)^3 2E_N} (2\pi)^4 \delta^{(4)}(q - \sum_{j=1}^N p_j) = \frac{d^3 \mathbf{p}_{N-1}}{(2\pi)^2 4E_{N-1} E_N} \delta(\sqrt{s} - \tilde{m}_1). \quad (6.11)$$

This means that there are two rather than six degrees of freedom remaining and (equivalently) that both of the outgoing momenta from this last decay are produced on-shell. Proceeding similar to above, with

$$E_{N-1} = \sqrt{|\mathbf{p}_{N-1}|^2 + m_{N-1}^2}, \quad E_N = \sqrt{|\mathbf{p}_N|^2 + m_N^2}, \quad (6.12)$$

and

$$|\mathbf{p}_{N-1}| = |\mathbf{p}_N| = \frac{\lambda^{1/2}(\tilde{m}_{N-1}^2, m_N^2, m_{N-1}^2)}{2\tilde{m}_{N-1}}, \quad (6.13)$$

we have

$$\begin{aligned} \frac{d^3 \mathbf{p}_{N-1}}{(2\pi)^2 4E_{N-1} E_N} \delta(\sqrt{s} - \tilde{m}_1) &= \frac{|\mathbf{p}_{N-1}|^2}{4\pi E_{N-1} E_N} dx_1^{N-1} dx_2^{N-1} d|\mathbf{p}_{N-1}| \delta(\sqrt{s} - \tilde{m}_1) \\ &= \frac{|\mathbf{p}_{N-1}|^2}{4\pi E_{N-1} E_N} dx_1^{N-1} dx_2^{N-1} \left. \frac{\partial |\mathbf{p}_{N-1}|}{\partial \tilde{m}_1} \right|_{\tilde{m}_1 = \sqrt{s}}. \end{aligned} \quad (6.14)$$

The phase space measure for the final two momenta can therefore be expressed in unit normalized coordinates as

$$\frac{|\mathbf{p}_{N-1}|}{4\pi} \frac{1}{\tilde{m}_{N-1}} dx_1^{N-1} dx_2^{N-1}, \quad (6.15)$$

where \tilde{m}_{N-1} is the initial ingoing energy.

Finally, as each outgoing momentum is the product of a decay in its parent's centre of momentum frame, it must be successively boosted back to the original frame of the incoming particles. The N physical outgoing momenta generated in this way can then be combined with the incoming momenta to compute a squared scattering amplitude and ultimately, together with the phase space measure above, a differential cross section.

6.2 Resonant Particles

6.2.1 Review: particle stability

Physical particles, as opposed to virtual particles, are the excitations of a field that travel over asymptotically large time scales, thus allowing us to detect them. To see

how resonant internal particles fit into this context, we briefly review what makes an excitation stable¹. Consider the excitations of a field $\phi(x)$ due to a source $J(x)$,

$$\delta\phi(x) = \int d^4y i\Delta(x-y)J(y), \quad (6.16)$$

where in the case of a scalar field the propagator $\Delta(x-y)$ is the Green's function that solves the Klein Gordon equation. Assuming a scalar field, the propagator in momentum space is given by

$$\Delta(k) = \frac{1}{i(2\pi)^4} \frac{1}{k^2 + m^2}, \quad (6.17)$$

and the excitations may be written as

$$\delta\phi(x) = i(2\pi)^4 \int d^4k e^{-ik \cdot x} \Delta(k) J(k) \quad (6.18)$$

$$= \int d^3\mathbf{k} e^{i\mathbf{k} \cdot \mathbf{x}} \int dk_0 e^{-ik_0 t} \frac{J(k_0, \mathbf{k})}{k_0^2 - \omega(\mathbf{k})^2}, \quad (6.19)$$

where $\omega(\mathbf{k}) = \sqrt{m^2 + \mathbf{k}^2}$. The Riemann Lebesgue lemma states that if the integral

$$\int_{-\infty}^{\infty} dk_0 |f(k_0)| \quad (6.20)$$

is convergent (finite), then

$$\lim_{t \rightarrow \pm\infty} \int_{-\infty}^{\infty} dk_0 e^{-ik_0 t} f(k_0) = 0. \quad (6.21)$$

The contrary of this lemma implies that the field excitations (6.19) can only survive for asymptotic time scales, i.e. not go to zero in the limit $t \rightarrow \pm\infty$, if the k_0 integral over the integrand

$$\left| \frac{J(k_0, \mathbf{k})}{k_0^2 - \omega(\mathbf{k})^2} \right| \quad (6.22)$$

is divergent. This divergence occurs at the integrand's poles,

$$k_0 = \pm\omega(\mathbf{k}), \quad (6.23)$$

or (equivalently) $k^2 = m^2$, the familiar mass-shell condition for a physical particle.

In a quantum field theory however this is not the full story because (6.17) is not the full propagator. The propagator will pick up quantum corrections from its self energy diagrams, as shown in figure 6.2. Letting $\Sigma(k)$ represent all irreducible self

¹For further details see for example [22]

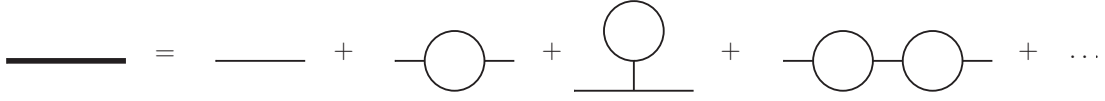


Figure 6.2: Example of self energy corrections to a full propagator.

energy diagrams (those that cannot be split in two by cutting one internal line), the full propagator can be written as

$$\begin{aligned}
 \Delta(k) &= \frac{1}{i(2\pi)^4} \frac{1}{k^2 + m^2} + \frac{1}{i(2\pi)^4} \frac{1}{k^2 + m^2} \Sigma(k) \frac{1}{i(2\pi)^4} \frac{1}{k^2 + m^2} + \dots \\
 &= \frac{1}{i(2\pi)^4} \frac{1}{k^2 + m^2} \sum_{j=0}^{\infty} \left(\Sigma(k) \frac{1}{i(2\pi)^4} \frac{1}{k^2 + m^2} \right)^j \\
 &= \frac{1}{i(2\pi)^4} \frac{1}{k^2 - m^2 - \Sigma(k)/i(2\pi)^4}, \tag{6.24}
 \end{aligned}$$

where in the last step we have performed the sum for the infinite geometric series. We define the Lorentz invariant quantity

$$\gamma = \text{Im} \left(\frac{1}{i(2\pi)^4} \Sigma(k) \right), \tag{6.25}$$

and absorb the real part into m^2 to give a new physical mass for the field. The poles giving rise to stable field excitations $\delta\phi$ are now given by

$$\begin{aligned}
 k_0 &= \pm \sqrt{\omega(\mathbf{k})^2 + i\gamma} \\
 &\approx \pm \left(\omega(\mathbf{k}) - \frac{i\gamma}{2\omega(\mathbf{k})} \right). \tag{6.26}
 \end{aligned}$$

Crucially, the presence of this imaginary term in k_0 will dampen the time propagation of the stable particle

$$e^{ik_0 t} = e^{-i\omega(\mathbf{k})t} e^{-t/2\tau(\mathbf{k})}, \tag{6.27}$$

where $\tau(\mathbf{k}) \equiv \omega(\mathbf{k})/\gamma$ is the mean lifetime. This gives rise to a decay rate for the particle $\Gamma(\mathbf{k}) = 1/\tau(\mathbf{k})$, a quantity often also referred to as the total decay width. Due to the Lorentz invariance of γ , the decay width in any frame can be related to that of its rest frame

$$\omega(\mathbf{k})\Gamma(\mathbf{k}) = m\Gamma. \tag{6.28}$$

The denominator of a massive propagator can thus be written as

$$\frac{1}{k^2 - m^2 - im\Gamma}. \tag{6.29}$$

By use of the optical theorem the decay rate

$$\Gamma(\mathbf{k}) = \frac{1}{\omega(\mathbf{k})} \text{Im} \left(\frac{1}{i(2\pi)^4} \Sigma(k) \right),$$

may be written as

$$\Gamma(\mathbf{k}) = \frac{(2\pi)^4}{2\omega(\mathbf{k})} \int \prod_j \frac{d^3\mathbf{p}_j}{(2\pi)^3 2\omega(\mathbf{k}_j)} \delta^{(4)}(k - \sum_j p_j) |\mathcal{M}(k; p_j)|^2, \quad (6.30)$$

where $\mathcal{M}(k; p_j)$ is the amplitude of the self energy diagrams, and can thereby be computed analogously to a cross section.

6.2.2 Breit-Wigner factorization

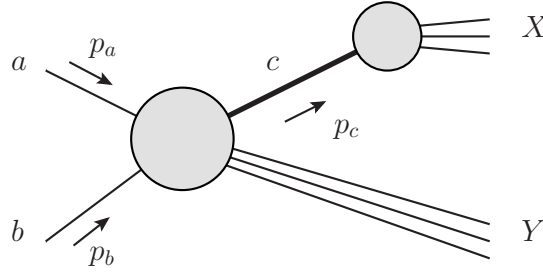


Figure 6.3: A generic process for which Breit-Wigner factorization is applicable. The particle c is assumed to be close to satisfying its mass shell condition $p_c^2 \approx m_c^2$.

Consider the process shown in figure 6.3. If we assume that the dominant contribution to the cross section is given when the four momentum p_c of the intermediate particle c is close to being on-shell $p_c^2 \approx m_c^2$, then we may approximate this process by factorizing the total amplitude into independent pieces. These pieces are the amplitudes of the production and decay processes and the c particle's propagator with the decay width included. The particle c here is treated as a massive scalar regardless of its true internal degrees of freedom. Possible spin correlations between the amplitude and propagator terms are thus neglected. The total amplitude is now written as

$$\mathcal{M}^{\text{tot}}(a + b \rightarrow X + Y) \approx \mathcal{M}^{\text{dec}}(c \rightarrow X) \frac{1}{p_c^2 - m_c^2 - im_c\Gamma} \mathcal{M}^{\text{prod}}(a + b \rightarrow c + Y), \quad (6.31)$$

where $\Gamma = \Gamma(c \rightarrow \text{all})$ is the total decay width of the particle c at rest. Because we have defined the amplitudes as being independent, we may square them independently to obtain

$$|\mathcal{M}^{\text{tot}}|^2 = |\mathcal{M}^{\text{dec}}|^2 \left| \frac{1}{p_c^2 - m_c^2 - im_c\Gamma} \right|^2 |\mathcal{M}^{\text{prod}}|^2. \quad (6.32)$$

The differential cross section of the total process is given by

$$d\sigma^{\text{tot}} = \frac{(2\pi)^4}{2\lambda^{1/2}(s, m_a^2, m_b^2)} \delta(p_a + p_b - \sum_i^{X+Y} k_i) |\mathcal{M}^{\text{tot}}|^2 \prod_j^{X+Y} \frac{d^3k_j}{(2\pi)^3 2\omega(\mathbf{k}_j)}, \quad (6.33)$$

where $s = (p_a + p_b)^2$. Introducing an identity integral over the four momentum p_c , and substituting in the factorization approximation (6.32) for the invariant amplitude the differential cross section becomes

$$d\sigma^{\text{tot}} = \frac{(2\pi)^4}{2\lambda^{1/2}(s, m_a^2, m_b^2)} \delta(p_a + p_b - \sum_i k_i - p_c) \prod_j^Y \frac{d^3 k_j}{(2\pi)^3 2\omega(\mathbf{k}_j)} |\mathcal{M}^{\text{prod}}|^2 \cdot d^4 p_c \delta(p_c - \sum_{i'} k_{i'}) \prod_{j'}^X \frac{d^3 k_{j'}}{(2\pi)^3 2\omega(\mathbf{k}_{j'})} |\mathcal{M}^{\text{dec}}|^2 \frac{1}{(s_c - m_c^2)^2 + m_c^2 \Gamma^2}, \quad (6.34)$$

where we have defined $s_c \equiv p_c^2$ to be the off-shell squared mass of particle c . The four momentum integral can be rewritten as

$$d^4 p_c = d^3 p_c dp_{c0} = d^3 p_c ds_c \left| \frac{\partial p_{c0}}{\partial s_c} \right| = \frac{d^3 p_c}{2\sqrt{s_c + \mathbf{p}_c^2}} ds_c. \quad (6.35)$$

The differential cross section then becomes

$$d\sigma^{\text{tot}} = \frac{(2\pi)^4}{2\lambda^{1/2}(s, m_a^2, m_b^2)} \delta(p_a + p_b - \sum_i k_i - p_c) \prod_j^Y \frac{d^3 k_j}{(2\pi)^3 2\omega(\mathbf{k}_j)} \frac{d^3 p_c}{(2\pi)^3 2\sqrt{s_c + \mathbf{p}_c^2}} |\mathcal{M}^{\text{prod}}|^2 \cdot \frac{(2\pi)^4}{2\sqrt{s_c + \mathbf{p}_c^2}} \delta(p_c - \sum_{i'} k_{i'}) \prod_{j'}^X \frac{d^3 k_{j'}}{(2\pi)^3 2\omega(\mathbf{k}_{j'})} |\mathcal{M}^{\text{dec}}|^2 \cdot \frac{(2\pi)^3}{(2\pi)^4} \sqrt{s_c + \mathbf{p}_c^2} \frac{1}{(s_c - m_c^2)^2 + m_c^2 \Gamma^2} ds_c, \quad (6.36)$$

which simplifies to the expression

$$d\sigma^{\text{tot}} = d\sigma^{\text{prod}} \cdot \frac{\sqrt{s_c + \mathbf{p}_c^2} d\Gamma(p_c)}{m_c \Gamma} \cdot \left\{ \frac{1}{\pi} \frac{m_c \Gamma}{(s_c - m_c^2)^2 + m_c^2 \Gamma^2} \right\} ds_c, \quad (6.37)$$

where $d\Gamma(p_c)$ is the differential decay rate for the process $c \rightarrow X$ in the p_c frame. The term in curly brackets is the relativistic *Breit-Wigner resonance formula*, indicating a peak in amplitude as the resonance particle c approaches its on-shell mass $s_c \rightarrow m_c^2$. Although not denoted, the condition $p^2 = s_c$ for $d\sigma$ and $d\Gamma$ still holds.

When integrating the factorised differential cross section, as given in equation (6.37), it is often desirable to choose a domain centred around the on-shell resonant mass. For example, integrating $\sqrt{s_c}$ over n total decay widths, $\sqrt{s_c} \in (m_c - n\Gamma, m_c + n\Gamma)$, where the relevant Jacobian term

$$ds_c \rightarrow 2\sqrt{s_c} d\sqrt{s_c}, \quad (6.38)$$

should be included. To implement this factorization method numerically, it is convenient to replace $\sqrt{s_c}$ by a unit normalized parameter $x \in [0, 1]$ such that

$$\sqrt{s_c} = m_c - n\Gamma(1 - 2x), \quad (6.39)$$

with the Jacobian factor

$$ds_c \rightarrow 4n\Gamma\sqrt{s_c} dx. \quad (6.40)$$

6.2.3 Narrow width approximation

The relativistic Breit-Wigner resonance formula obtained in equation (6.37),

$$f_{\text{BW}}(s_c) = \frac{1}{\pi} \frac{m_c \Gamma}{(s_c - m_c^2)^2 + m_c^2 \Gamma^2} \quad (6.41)$$

describes a peak centred around the on-shell mass m_c . If the total decay width Γ (effectively the full width at half maximum of the resonant peak) is very narrow, the Breit-Wigner formula may be approximated by taking the limit $m_c \Gamma \rightarrow 0$:

$$\lim_{m_c \Gamma \rightarrow 0} \left\{ \frac{1}{\pi} \frac{m_c \Gamma}{(s_c - m_c^2)^2 + m_c^2 \Gamma^2} \right\} = \delta(s_c - m_c^2). \quad (6.42)$$

In this *narrow width approximation* the total differential cross section becomes

$$\begin{aligned} \sigma^{\text{tot}} &\simeq \int d\sigma^{\text{prod}} \Big|_{(p^2 = s_c)} \cdot \frac{\sqrt{s_c + \mathbf{p}_c^2} d\Gamma(p_c)}{m_c \Gamma} \cdot \delta(s_c - m_c^2) ds_c \\ &= \frac{\omega(\mathbf{p}_c) \Gamma(c \rightarrow X)(\mathbf{p}_c)}{m_c \Gamma} \sigma^{\text{prod}} \\ &= \frac{m_c \Gamma(c \rightarrow X)}{m_c \Gamma} \sigma^{\text{prod}} \end{aligned} \quad (6.43)$$

where we have used the Lorentz invariant relation (6.28) to write the numerator term in its rest frame. The total cross section is therefore related to the production cross section by a constant,

$$\sigma^{\text{tot}} = \text{Br}(c \rightarrow X) \sigma^{\text{prod}}, \quad (6.44)$$

known as the branching ratio:

$$\text{Br}(c \rightarrow X) = \frac{\Gamma(c \rightarrow X)}{\Gamma}. \quad (6.45)$$

A branching ratio gives the likelihood of a specific partial decay taking place with respect to all possible decays. In summary, when the resonant particle of a process has a very narrow width it exists for a long enough time to be effectively treated as on-shell. We may therefore split the probability (cross section) of the process into the probability of creating this on-shell particle times the likelihood that it will decay into the observed final state. This is the narrow width approximation.

A special case of Breit-Wigner factorization is when only the unstable resonant particle is created in the production process. In this case the momentum of the internal particle is fixed and the resonance formula is not integrated over. Further, the production cross section for a $2 \rightarrow 1$ process can be expressed in terms of the inverse two body decay in the rest frame as

$$\sigma^{\text{prod}}(a + b \rightarrow c) = \frac{16\pi^2 m_c}{N \lambda(m_c^2, m_a^2, m_b^2)} \Gamma(\bar{c} \rightarrow \bar{a} + \bar{b}), \quad (6.46)$$

where the factor N accounts for differences in the averaging factors of the ingoing degrees of freedom and for multiplicity factors of possibly identical outgoing states. Making the above substitution into equation (6.37) with the integral over $\sqrt{s_c}$ removed gives the total cross section

$$\begin{aligned}\sigma^{\text{tot}} &= \frac{16\pi^2 m_c^3}{N\lambda(m_c^2, m_a^2, m_b^2)} \Gamma(\bar{c} \rightarrow \bar{a} + \bar{b}) \frac{\Gamma(c \rightarrow X)}{\Gamma} \left\{ \frac{1}{\pi} \frac{m_c \Gamma}{(s_c - m_c^2)^2 + m_c^2 \Gamma^2} \right\} \\ &= \frac{16\pi m_c^4}{N\lambda(m_c^2, m_a^2, m_b^2)} \frac{\Gamma(\bar{c} \rightarrow \bar{a} + \bar{b}) \Gamma(c \rightarrow X)}{(s_c - m_c^2)^2 + m_c^2 \Gamma^2}.\end{aligned}\quad (6.47)$$

For a narrow width the cross section will only take sizable values very close to its peak $s_c = m_c^2$, where it can be expressed purely in terms of the branching ratios for the particle c

$$\sigma^{\text{tot}} = \frac{16\pi m_c^2}{N\lambda(m_c^2, m_a^2, m_b^2)} \text{Br}(\bar{c} \rightarrow \bar{a} + \bar{b}) \text{Br}(c \rightarrow X).\quad (6.48)$$

6.3 Multi-dimensional integration

In section 4.2.1 we solved a two dimensional phase space integral for a $2 \rightarrow 2$ partonic cross section analytically. In general we will not be so lucky. As we saw in section 6.1, N outgoing particles come with $3N - 4$ degrees of freedom that must be integrated over. Furthermore, any ingoing hadronic states must be integrated over their parton momentum fraction (as discussed in section 4.3). It is then easy to see how a cross section integral can have many more than two integration variables, and such integrals can be very difficult or even impossible to solve analytically by known methods. The necessary alternative is to resort to numerical methods for the multi-dimensional integration. A good introduction to numerical multi-dimensional integration techniques in high energy physics is given by Weinzierl [23].

In one dimension, the two classical techniques for numerical integration are the Newton Cotes formulas and the Gaussian quadratures rules. Newton Cotes formulas work by evaluating and weighting an integrand at equally spaced sub-intervals. Gaussian quadratures rules operate in a similar way but with a potentially more optimal sub-interval spacing for reducing the error. The simplest Newton Cotes formula is the trapezium rule:

$$\int_{x_0}^{x_n} dx f(x) = \Delta x \sum_{i=0}^n w_i f(x_i) + O\left(\frac{1}{n^2}\right),\quad (6.49)$$

where $x_i = x_0 + i \cdot \Delta x$ with

$$\Delta x = \frac{x_n - x_0}{n}\quad (6.50)$$

the length of the n sub-interval spacings, $w_0 = w_n = 1/2$ and $w_i = 1$ otherwise. The number of integrand evaluations needed for this method is $N = n + 1$. The

computation time of an integration is effectively proportional to N , and for large N we see that the error scales as $1/n^2 \simeq 1/N^2$. This result is typical of numerical integration, where a compromise must be reached between computation time and numerical accuracy.

As we are concerned with multi-dimensional integrals, we consider applying such a one-dimensional method iteratively to an integral over the hypercube $[0, 1]^d$. For example, applying the trapezium rule iteratively gives

$$\int d^d u f(u_1, \dots, u_d) = \frac{1}{n^d} \sum_{i_1=0}^n \dots \sum_{i_d=0}^n w_{i_1} \dots w_{i_d} f((u_1)_{i_1}, \dots, (u_d)_{i_d}) + O\left(\frac{1}{n^2}\right). \quad (6.51)$$

The number of integrand evaluations needed is now $N = (n + 1)^d$, and so the error scales as $N^{-2/d}$. We thus see that this method becomes much less efficient as the number of dimensions is increased. The situation does not improve much for more advanced Newton Cotes formulas (or for the Gaussian quadrature rules) applied iteratively in multiple dimensions. The solution is to turn to a more efficient prescription for higher dimensional integrals, known as *Monte Carlo integration*, which we discuss in the following section. This method works by randomly sampling the integrand and gives an error that scales as $1/\sqrt{N}$ independent of the number of dimensions.

6.3.1 The Monte Carlo integration method

Consider the d -dimensional integral

$$I = \int d^d \mathbf{x} f(\mathbf{x}) = \int du_1 \dots du_d f(u_1, \dots, u_d) \quad (6.52)$$

over the unit hypercube $\mathbf{x} = (u_1, \dots, u_d) \in [0, 1]^d$. By the law of large numbers, the integral may be written as the average of an infinite number of integrand evaluations

$$I = \lim_{N \rightarrow \infty} \frac{1}{N} \sum_{n=1}^N f(\mathbf{x}_n). \quad (6.53)$$

By taking instead the number of evaluations N to be large but finite, we can construct an estimate for the integral

$$E = \frac{1}{N} \sum_{n=1}^N f(\mathbf{x}_n). \quad (6.54)$$

This is the basic premise of Monte Carlo integration, where the points \mathbf{x}_n are selected from a uniform random distribution. The detail remaining is what error of the estimate we expect for a given N . Consider the variance of the integrand

$$\sigma^2 = \int d^d \mathbf{x} (f(\mathbf{x}) - I)^2. \quad (6.55)$$

By noting that the integral

$$\int d^d \mathbf{x} (f(\mathbf{x}) - I) = 0, \quad (6.56)$$

the variance can be written as

$$\begin{aligned} \sigma^2 &= \frac{1}{N} \int d^d \mathbf{x}_1 \dots \int d^d \mathbf{x}_N \left(\sum_{n=1}^N (f(\mathbf{x}_n) - I) \right)^2 \\ &= N \int d^d \mathbf{x}_1 \dots \int d^d \mathbf{x}_N (E - I)^2, \end{aligned} \quad (6.57)$$

and thus the squared error of the estimate as

$$\int d^d \mathbf{x}_1 \dots \int d^d \mathbf{x}_N (E - I)^2 = \frac{\sigma^2}{N}. \quad (6.58)$$

The error in the Monte Carlo estimate $E - I$ therefore takes the average value σ/\sqrt{N} i.e. it scales as $1/\sqrt{N}$ independent of the number of dimensions. More precisely, by invoking the central limit theorem

$$\lim_{N \rightarrow \infty} \text{Prob} \left(-a \frac{\sigma}{\sqrt{N}} \leq E - I \leq b \frac{\sigma}{\sqrt{N}} \right) = \frac{1}{\sqrt{2\pi}} \int_{-a}^b dt e^{-t^2/2}, \quad (6.59)$$

the error is seen to approach a Gaussian distribution with standard deviation σ/\sqrt{N} . This is clearly an improvement over the iterative multi-dimensional methods discussed earlier for a high number of dimensions. Realistically we will not know the variance σ^2 and must use the unbiased sample variance as an estimate:

$$\begin{aligned} S^2 &= \frac{1}{N-1} \sum_{n=1}^N (f(\mathbf{x}_n) - E)^2 \\ &= \frac{1}{N-1} \sum_{n=1}^N (f(\mathbf{x}_n))^2 - \frac{N}{N-1} E^2 \\ &\approx \frac{1}{N} \sum_{n=1}^N (f(\mathbf{x}_n))^2 - E^2, \end{aligned} \quad (6.60)$$

where in the last line we have assumed large N . We see that for this error measurement to hold, the function $f(\mathbf{x})$ should be square integrable.

6.3.2 Improving convergence

The error in the Monte Carlo estimate of an integral is given by σ/\sqrt{N} , where σ is the standard deviation of the integrand. Although dimensional independence of the $1/\sqrt{N}$ rate of convergence is a strong improvement, it is still not particularly fast.

To speed up the convergence we can attempt to reduce the size of the integrand's variance σ^2 . Two common techniques used to do this are *stratified sampling* and *importance sampling*.

In stratified sampling the integration domain $X = [0, 1]^d$ is split into K independent subspaces X_k and a separate Monte Carlo integration is performed on each. The estimate of the integral is then

$$E = \sum_{k=1}^K \frac{\text{Volume}(X_k)}{N_k} \sum_{n=1}^{N_k} f(\mathbf{x}_{nk}), \quad (6.61)$$

and its squared error

$$(E - I)^2 = \sum_{k=1}^K \text{Volume}(X_k)^2 \frac{\sigma_k^2}{N_k}. \quad (6.62)$$

It is hence possible to significantly reduce the error by choosing N_k to be large in regions with large variance, and to boost performance by setting it lower in regions with smaller variance. The art to stratified sampling is finding the optimal subspaces.

In importance sampling the integrand evaluation points are chosen from a non-uniform probability distribution $P(\mathbf{x})$, with a normalized probability density function

$$p(\mathbf{x}) = \frac{dP(\mathbf{x})}{d\mathbf{x}} \geq 0. \quad (6.63)$$

By a change of variables to the new probability distribution the integral becomes

$$I = \int \frac{f(\mathbf{x})}{p(\mathbf{x})} p(\mathbf{x}) d^d \mathbf{x} = \int \frac{f(\mathbf{x})}{p(\mathbf{x})} d^d P(\mathbf{x}), \quad (6.64)$$

and its estimate is now

$$E = \frac{1}{N} \sum_{n=1}^N \frac{f(\mathbf{x}_n)}{p(\mathbf{x}_n)}. \quad (6.65)$$

The sample variance from (6.60) becomes

$$S^2 \approx \frac{1}{N} \sum_{n=1}^N \left(\frac{f(\mathbf{x}_n)}{p(\mathbf{x}_n)} \right)^2 - E^2, \quad (6.66)$$

which can be minimized by making an informed choice for the density $p(\mathbf{x}_n)$. The ideal choice of the probability density is $p(\mathbf{x}_n) = f(\mathbf{x}_n)/I$ at which the variance vanishes completely.

Both stratified and importance sampling require existing knowledge of the integral to be implemented effectively. To acquire this, an adaptive algorithm is often used that learns about the integrand as it proceeds. More precisely, such an algorithm analyzes its own integrated result after each iteration and subsequently

adjusts its sampling strategy to reduce the variation of the next iteration. Typically the number of integrand evaluations are increased per iteration to optimize convergence.

In both methods of variance reduction the integrand evaluation is assigned a weighting: $\text{Volume}(X_k)/N_k$ in the case of stratified sampling and the probability $p(\mathbf{x}_n)$ in importance sampling. The implementation of such methods is thus known as *weighted Monte Carlo*. In some applications, such as continuously running event generators, it is desirable to preserve the true value of the integrand and its likelihood of occurring i.e. to keep the integrand unweighted and improve convergence by other methods. This is known as *unweighted Monte Carlo* which we will not discuss here.

6.3.3 The VEGAS algorithm

The VEGAS algorithm [24][25] is an adaptive weighted Monte Carlo algorithm that is often used for calculating cross sections numerically. It combines both stratified and importance sampling for variation reduction. Similar to stratified sampling, it divides the integration region into a rectangular grid and performs a Monte Carlo integration in each subspace using a uniform probability distribution. Similar to importance sampling, it attempts to find the optimal probability density for the integrand by adaptively moving the grid boundaries after each iteration. An example illustrating how the grid of two dimensional integrand is placed and adjusted is given in figure 6.4. To save on memory and computation, the grid lines are not allowed to deviate locally in a subspace i.e. they are kept straight. The downside to this restriction is that it factorizes the probability density along its d coordinate axes,

$$p(u_1, \dots, u_d) = p_1(u_1) \cdot p_2(u_2) \cdot \dots \cdot p_d(u_d), \quad (6.67)$$

which may not be true for the ideal probability density. Said differently, the VEGAS algorithm is less effective when the regions of the integrand with high variance are not localized with respect to the coordinate axes. When refining the grid point positions after an iteration, the weight m_j affecting how a grid point x_j is shifted is often damped to avoid destabilization of the grid. That is, rather than defining (for example)

$$m_j = \frac{\bar{f}_j \Delta x_j}{\sum_j \bar{f}_j \Delta x_j}, \quad (6.68)$$

a damping function is used

$$m_j = \left[\left(\frac{\bar{f}_j \Delta x_j}{\sum_j \bar{f}_j \Delta x_j} - 1 \right)^{-1} \log \left(\frac{\bar{f}_j \Delta x_j}{\sum_j \bar{f}_j \Delta x_j} \right) \right]^{-\alpha}, \quad (6.69)$$

where α is the damping parameter, usually set between 0.2 and 2 for maximum or minimum damping respectively.

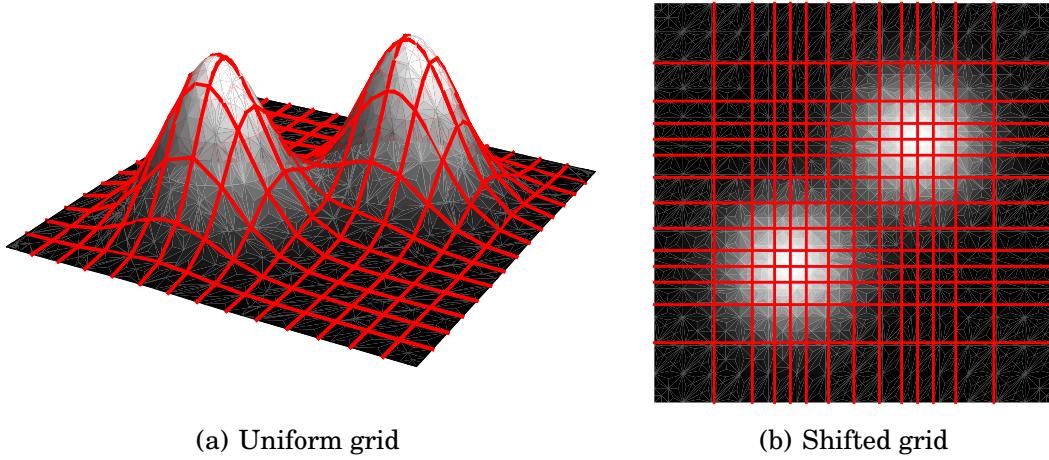


Figure 6.4: Example of VEGAS acting on a two dimensional integrand. VEGAS initially divides the integration domain into a uniform grid (a). After each iteration, the grid lines are shifted towards the regions with greater variance (b).

The estimate of the integral after one iteration j is

$$E_j = \frac{1}{N_j} \sum_{n=1}^{N_j} \frac{f(\mathbf{x}_n)}{p(\mathbf{x}_n)}, \quad (6.70)$$

and that of its variance

$$S_j^2 = \frac{1}{N_j} \sum_{n=1}^{N_j} \left(\frac{f(\mathbf{x}_n)}{p(\mathbf{x}_n)} \right)^2 - E_j^2. \quad (6.71)$$

Estimates from a number of iterations can be combined by weighting them by their number of evaluations and the sample variance:

$$E_{\text{tot}} = \left(\sum_{j=1}^M \frac{N_j}{S_j^2} \right)^{-1} \sum_{j=1}^M \frac{N_j E_j}{S_j^2}, \quad (6.72)$$

where M is the number of iterations being combined.

6.4 Custom implementation

To perform the cross section calculations in this Master's thesis a custom program was written to perform weighted Monte Carlo integrations. The program was written in C++ and based in part on the code of Erik Lascaris [26]. For its integrand sampler the program uses a custom VEGAS-like algorithm discussed in section

6.3.3. The phase space is built up as described in section 6.1. Both cross sections and decays for N outgoing states with arbitrary masses can be computed. Only the squared matrix elements must be entered manually. Standard PDF tables can be included for ingoing hadronic states, and the strong coupling constant is computed at one or two loop order. Hadronization of outgoing particles has not been implemented. Figure 6.5 gives a schematic of the most important C++ object classes and files present in the program and their interdependency. The *main* program runs the Monte Carlo simulation using the MonteCarlo object. A program named *historian* is also included that can re-plot the histograms using the saved weighted event data and apply cuts on the kinematic variables.

There is an option to build up a process using the Breit-Wigner factorization method outlined in section 6.2.2, where a production process can be connected to a decay chain of arbitrary length. For example, starting with the production process $p + p \rightarrow \text{top} + \text{jet}$, the outgoing top can decay into a W boson and b quark and subsequently the outgoing W into a positron and a neutrino. We thus have an approximation for this $2 \rightarrow 4$ process without having to compute the squared amplitude. Note that an extra integration variable is used to set the (possibly off-shell) mass for the decaying particle (see equation (6.37)), so that this is not simply the narrow width approximation.

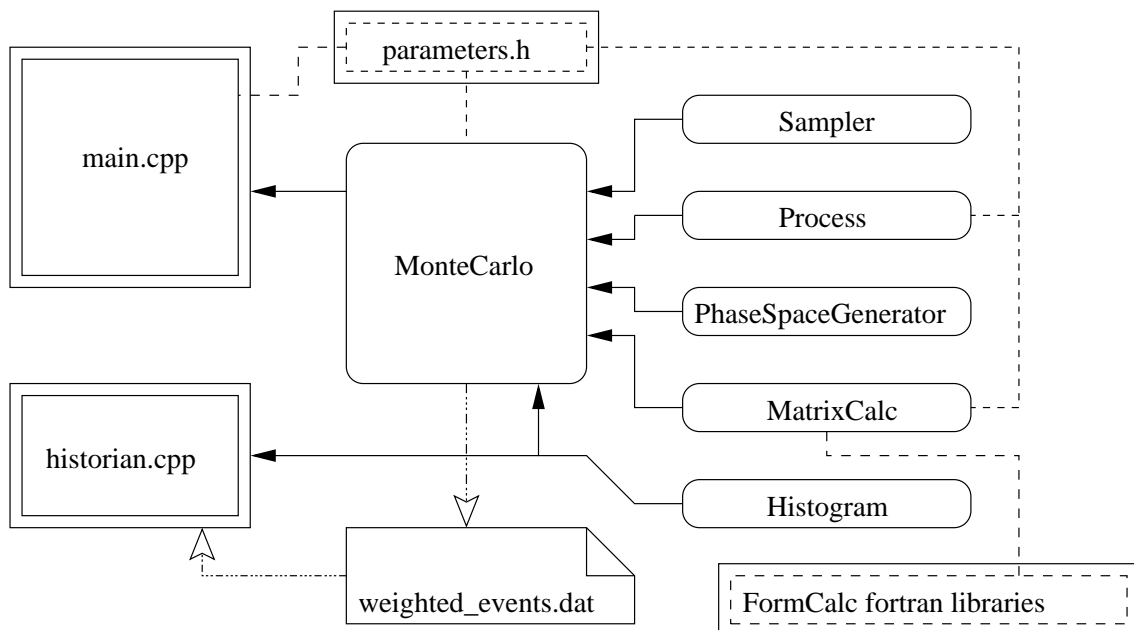


Figure 6.5: The structure of the most important custom Monte Carlo program. Rounded boxes denote C++ object classes. Only the important classes are shown.

To compute the scalar one loop functions appearing in the effective couplings from section 5.5.2, the LoopTools library [17] was used². An interface was also

²Expressions for the scalar two and three loop integrals are worked out in section 5.7.1, but are

written that can link to fortran libraries, generated by FormCalc [27], that contain the squared matrix elements of specific processes. The FormCalc package is an interface between the Mathematica package FeynArts [28], which automatically generates amplitudes from given topologies and Feynman rules, and the symbolic manipulation system FORM [29] that excels at squaring amplitudes. The majority of squared amplitudes in this Master's thesis were calculated and entered by hand, but the package tools just mentioned proved very useful for calculating the one-loop squared amplitudes discussed in section 7.2.3.

Unless otherwise stated, the simulations performed in this thesis use the CTEQ6M PDF table, calculate the running of the strong coupling constant to the two loop level (see appendix B) and have the renormalization and factorization scales set equal to the top mass $m_t = 173.4$ GeV.

6.4.1 Validity check

A clear test to check if our Monte Carlo program is working correctly is to compare its cross section results against the analytic cross section results calculated in section 4.2.1 for gluino production via quark-anti-quark annihilation. To add extra confidence to our result, we also compute the same process using the reliable event generator Madgraph/MadEvent [30][31]. We choose as model parameters the SUSY benchmark point SPS1a [32] but with the scalar quark masses all set equal at $m_{\tilde{q}_L} = m_{\tilde{q}_R} = 555$ GeV. In the absence of PDFs we use the two loop running coupling equation for α_s (see appendix B) in the modified minimal subtraction scheme (just as Madgraph does when no PDF's are specified). The number of light fermions is set to $n_f = 5$, so that the QCD mass scale is $\Lambda_{\text{QCD},2} = 226$ MeV or $\Lambda_{\text{QCD},1} = 146$ MeV for the two or one loop running respectively. The renormalization and factorization scales are both set equal to the gluino mass where relevant.

In table 6.1 we see that the cross section results of the parton level process all agree within their numerical uncertainties for the three methods considered. When the parton level process is integrated over the parton distribution functions (PDFs) the results agree less well (no longer within their numerical uncertainties), but still to within 5%. The Monte Carlo program and analytical solutions also matched very closely when comparing the partonic cross section distributions with respect to the transverse momentum and rapidity of an outgoing gluino, as shown in figure 6.6.

It is also worth testing our interface between the fortran libraries generated by FormCalc (containing the squared matrix elements for some of our one-loop processes) and the C++ Monte Carlo program³. In table 6.2 we have compared the result of this method to that of Madgraph/MadEvent for the hadronic process of gluon fusion proceeding via an s-channel gluon to top-anti-top production. They

not implemented in the program due to the already excellent functionality of the LoopTools package.

³Especially the memory mapping between external structs in C++ and common blocks in fortran can be quite fragile.

Method	$\hat{\sigma}$ [fb] (2 TeV)	σ [fb] (14 TeV, CTEQ5L)
Analytical	691.693	$5051.3 \pm 7.0^*$
Custom Monte Carlo	691.754 ± 0.069	5164.1 ± 9.4
Madgraph/MadEvent	693.610 ± 3.102	4876.9 ± 21.0

*The uncertainty arises from numerical integration over the PDFs.

Table 6.1: A comparison of the partonic and hadronic cross section results attained using the custom Monte Carlo program, Madgraph and by solving the integral analytically. The process in question is gluino production $q\bar{q} \rightarrow \tilde{g}\tilde{g}$.

agree sufficiently to conclude that the interface has been implemented correctly.

Method	$\hat{\sigma}$ [pb] (14 TeV, CTEQ6M)
Custom Monte Carlo*	260.2 ± 0.7
Madgraph/MadEvent	258.2 ± 0.4

*Linked with fortran libraries containing the squared matrix elements.

Table 6.2: A comparison of the hadronic cross section results attained using the custom Monte Carlo program linked with FormCalc fortran libraries (containing squared matrix elements) versus Madgraph. The process in question is gluon fusion to t-tbar (via an s-channel gluon) $gg \rightarrow t\bar{t}$ at leading order.

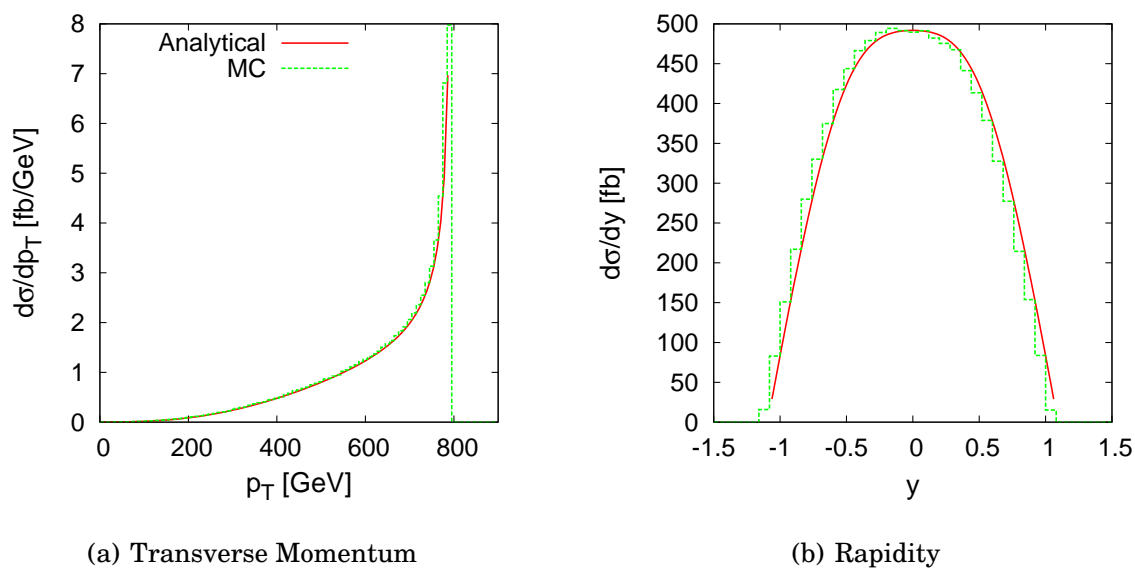


Figure 6.6: A comparison of the partonic cross section distribution attained using the custom Monte Carlo program versus the analytical solution. The process in question is gluino production $q\bar{q} \rightarrow \tilde{g}\tilde{g}$ at leading order.

Chapter 7

MRSSM Single Top Phenomenology

7.1 Single top in the Standard Model

Single top refers to the production of a single top quark from incoming partons in a hadron collider. The term production is fitting as the top itself is generally excluded as an initial parton state. This is because its probability of being encountered inside a given hadron is heavily suppressed by its large mass (~ 173 GeV) relative to the other quarks. The production of a single top must therefore proceed via a flavour changing interaction. In the Standard Model the only flavour changing interactions come from the top's coupling to the charged weak boson

$$\frac{g}{\sqrt{2}} V_{ti} \bar{t} \gamma^\mu P_L d_i W_\mu + \text{h.c.} \in \mathcal{L}_{\text{SM}}, \quad (7.1)$$

where $d_i = \{d, s, b\}$ are the down-type quarks and V_{ti} is an element of the CKM mixing matrix. From experiments it has been deduced that $V_{td} \sim 0 \sim V_{ts}$ and $V_{tb} \sim 1$ in the Standard Model, so to a good approximation we assume that single top production will involve a W boson and a b quark. Single top production may be divided into the s-channel, t-channel and Wt associated production channel processes shown in figure 7.1.

The large mass of the top quark gives it a large decay width $\Gamma = 1.5$ GeV and thus once produced the top decays very rapidly, before it has time to hadronize. The dominant decay channel of the top quark is to a W boson and b quark via the same flavour changing coupling given in (7.1), with a branching ratio $\text{Br}(t \rightarrow W^+ b) \sim 1$. Subsequently, the b quark will hadronize and form a jet in the detector and the massive W boson will itself decay into either a pair of quarks or leptons.

Although a b quark is assumed to hadronize and form a jet similar to those formed by the four lighter quarks and gluons, it is possible to distinguish it from the rest. Whereas the four lighter quarks and gluons will typically leave the detector without decaying, the larger mass of the b quark means that it will decay inside the detector at some distance from the collision point. By identifying a second vertex point in a detector from which a jet and b decay products originate it is thus possible

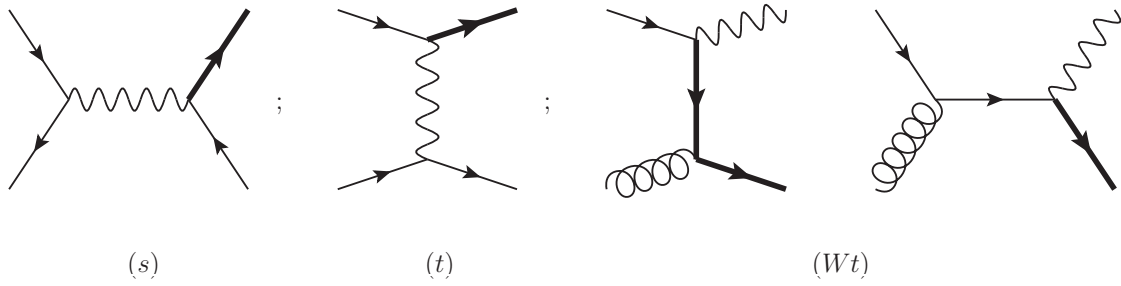


Figure 7.1: The s-channel, t-channel and Wt associated production channel processes for single top production in the Standard Model. The top quark is denoted by a bold propagator line.

to determine the b quark origin of the jet. This procedure is known as *b-tagging* and will have an efficiency of about 50% at the LHC's ATLAS and CMS detectors.

For our purposes of detecting single top (anti-top), the W^+ (W^-) boson decay to a charged lepton $l^+ = \{e^+, \mu^+\}$ (l^-) and a neutrino $\bar{\nu}_l$ (ν_l) is the most interesting. This is because the charged lepton is a distinct addition to the two jets already produced and the neutrino will escape undetected, leaving only characteristic missing transverse energy¹. The branching ratio of the W^+ boson to a pair of leptons is $\text{Br}(W^+ \rightarrow l^+ \bar{\nu}_l) = 0.108$

In figure 7.2 we draw the outgoing states of an s or t-channel single top process in the Standard Model, with the W boson decaying to two leptons. These are:

1. Two b-jets, a charged lepton and missing transverse energy:

$$2b\text{-jets} + l^+ + \cancel{E_T}. \quad (7.2)$$

2. One b-jet, a non-b-tagged jet and missing transverse energy:

$$b\text{-jet} + \text{jet} + l^+ + \cancel{E_T}. \quad (7.3)$$

The s-channel single top production process can only produce the first outgoing state, whereas the t-channel process can produce both. We ignore the Wt channel, because it will not serve as a background to the MRSSM single top processes discussed in this chapter. All outgoing light quarks or gluons produced are assumed to become well formed single jets. We thus ignore any parton shower and hadronization effects. To compute the cross sections of these $2 \rightarrow 4$ processes involving a double decay chain we used the Breit-Wigner factorization method (the theory and implementation of which are discussed in sections 6.2.2 and 6.4 respectively).

¹It is not possible to apply conservation of four momentum in all directions because particles can escape down the beam pipe undetected. Because the detector is built transverse to the beam pipe, missing momentum in the transverse plane is detectable.

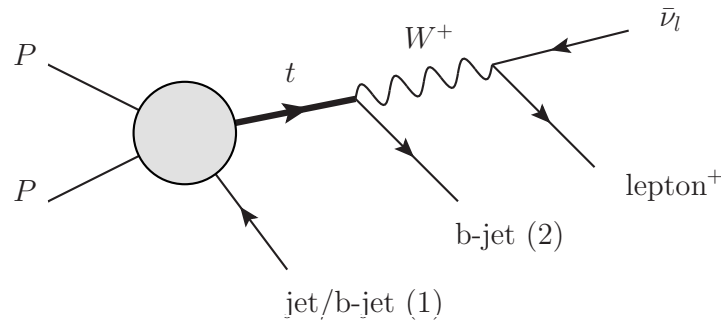


Figure 7.2: Possible outgoing states of s and t-channel single top production involving the W boson decaying to two leptons.

7.2 Single top in the MRSSM

Single top in the MRSSM can be produced either via a mediating sgluon at the two loop level or purely from squark mixing at the one loop level, both supersymmetric QCD processes. In this section we discuss both production processes as well as the independent production and decays of a single sgluon. We begin by choosing relevant points in the MRSSM QCD parameter space.

7.2.1 Setting points in parameter space

The parameter space of MRSSM QCD consists of the sgluon mass $M_{\phi 2}$, the gluino mass $m_{\tilde{g}}$, the squark masses $m_{\tilde{q}\sigma}$ and the squark mixing matrices $U_{\tilde{q}\sigma}$. The masses are assumed to be between 300 GeV and a couple of TeV; heavy enough to have avoided detection so far and light enough to not reintroduce fine tuning of the Higgs mass (from the logarithmic divergences). For simplicity, we mix only the first and third flavours of the up-type squarks, giving the unitary mixing matrices

$$U_{\tilde{u}L} = \begin{pmatrix} \cos \theta_L & 0 & \sin \theta_L \\ 0 & 1 & 0 \\ -\sin \theta_L & 0 & \cos \theta_L \end{pmatrix} \quad \text{and} \quad U_{\tilde{u}R} = \begin{pmatrix} \cos \theta_R & 0 & \sin \theta_R \\ 0 & 1 & 0 \\ -\sin \theta_R & 0 & \cos \theta_R \end{pmatrix}. \quad (7.4)$$

We are primarily interested in single top production processes in which down-type quarks do not appear as final states and hence the mixing of down-type states has no effect. An exception is the production of single top with a b quark in the MRSSM, discussed in section 7.2.3, where we assume no down-type squark mixing for simplicity. The mixing is taken to be maximal for all but one of the parameter points.

Sgluon production via gluon fusion is dependent on the effective vertex given in (5.111), which is seen to vanish if left and right handed squarks are degenerate. To keep the vertex from vanishing but to avoid artificially amplifying sgluon production, we take a moderate mass difference of 10%. Sgluon production is also

proportional to the gluino mass, which enters into the amplitude via the sgluon-squark vertex. Because the sgluon-quark vertex is dependent on the gluino mass as well, it will be informative to choose parameter points with different gluino masses. In section 5.3 we argued that squark flavour mixing is only phenomenologically possible if the gluino mass is large relative to the squark masses. We thus set default values for the gluino and squark masses of 1000 and ~ 500 GeV respectively, and dedicate two parameter points for gluino masses of 500 and 2000 GeV.

The amplitude for sgluon decay to single top vanishes if the squark masses are degenerate within their mass eigenstate basis, for example if the masses of \tilde{u}_{La} are degenerate for $a = 1, 2, 3$. This is clear from the effective vertex given in (5.138), where for degenerate masses we are left with a sum over orthogonal elements of the unitary mixing matrix. We therefore choose one parameter point to have a small squark mass splitting relative to the others, and also one to have substantially heavier squarks of ~ 1000 GeV. The six points in parameter space chosen are given in table 7.1. The sgluon mass is left as a free parameter.

Benchmark	$m_{\tilde{g}}$	$m_{\tilde{u}L} = m_{\tilde{d}L}$	$m_{\tilde{u}R} = m_{\tilde{d}R}$	$\theta_L = \theta_R$
Point A	1000	{400, 400, 1000}	{360, 360, 900}	$\pi/4$
Point B	1000	{900, 900, 1500}	{810, 810, 1350}	$\pi/4$
Point C	1000	{400, 400, 500}	{360, 360, 450}	$\pi/4$
Point D	2000	{400, 400, 1000}	{360, 360, 900}	$\pi/4$
Point E	500	{400, 400, 1000}	{360, 360, 900}	$\pi/4$
Point F	1000	{400, 400, 1000}	{360, 360, 900}	$\pi/3$

Table 7.1: Selected benchmarks points of the MRSSM QCD parameter space.

7.2.2 Sgluon mediated single top

Single sgluon production

The production cross section of a single sgluon from gluon fusion is proportional to the decay rate of the inverse process, as we outlined for general single particle production in equation (6.46). The cross section for sgluon production is thus given by

$$\begin{aligned} \sigma(gg \rightarrow \phi_2) &= \frac{\pi^2}{M_{\phi_2}^3} \Gamma(\phi_2 \rightarrow gg) \\ &= \frac{5\alpha_S^3 m_{\tilde{g}}^2}{192 M_{\phi_2}^4} \left| \sum_{\tilde{q}} [\tau_L f(\tau_L) - \tau_R f(\tau_R)] \right|^2, \end{aligned} \quad (7.5)$$

where in the second line we have inserted the sgluon decay rate to two gluons from (5.145). Single sgluon production via gluon fusion is only possible through squark loops, which makes it the leading order process and therefore non-divergent.

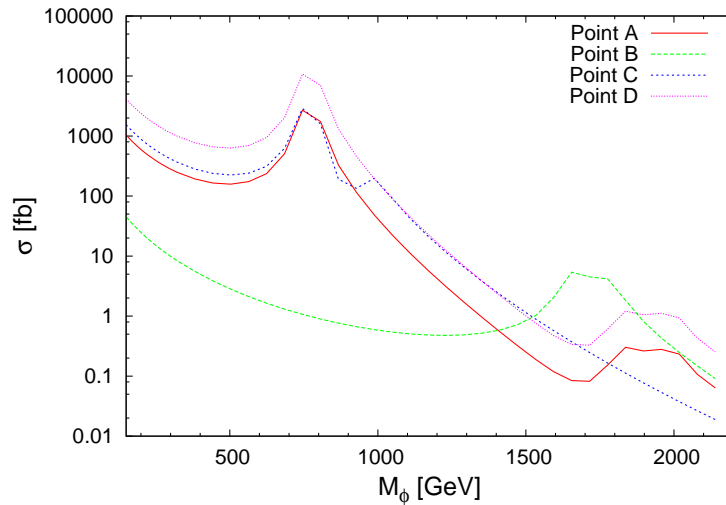


Figure 7.3: Single sgluon production at the LHC (14 TeV) as a function of the sgluon mass.

In figure 7.3 we give the cross section for on-shell sgluon production at the LHC for a range of sgluon masses at four of the parameter points specified in the previous section. The centre of mass energy of the LHC is taken to be 14 TeV and the renormalization and factorization scales are set equal to the top quark mass throughout this chapter. Clearly noticeable in this plot is that the sgluon production peaks precisely at the points where the sgluon mass is twice that of a squark mass. Due to the mass splitting introduced for the squarks, there are two peaks visible for each parameter point (except point B, whose second peak is off the sgluon mass scale). The close proximity of point C's peaks is explained by its small squark mass splitting. This phenomena of the cross section peaking at twice the mass of its internal loop particles is also seen in Standard Model single Higgs production via gluon fusion, where the production cross section peaks at twice the top quark mass[33].

The dependence of the production cross section on the gluino mass is clearly visible in the plot, with point D's production cross section being an order of magnitude larger than that of point A as a result of its gluino mass being twice as big. The significantly lower cross section plot of point B illustrates that single sgluon production disfavours heavy squarks. For all the parameter points sgluon production is seen to fall off rapidly with respect to the sgluon mass.

Sgluon branching ratios

Using the sgluon decay rates calculated in section 5.6 we can compute the total decay width of the sgluon and in turn the branching ratios of its various decay channels. The sgluon's total decay width and branching ratios for a range of sgluon masses are given in figures 7.4 and 7.5 respectively. The striking feature of these plots is the jump by several orders of magnitude of the total decay width when

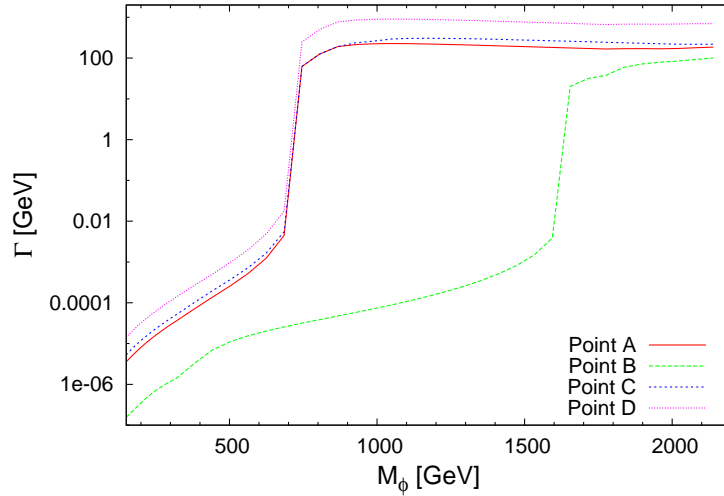


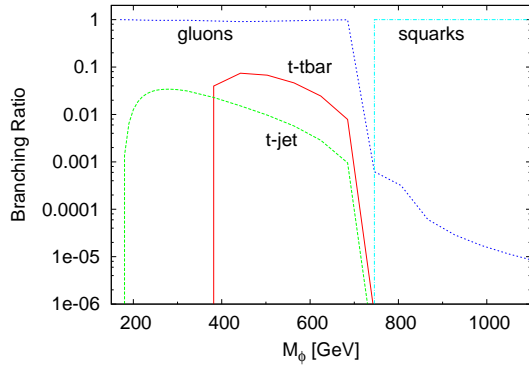
Figure 7.4: Total decay width of the sgluon with respect to the its mass.

sgluon decay to either a pair of squarks (or gluinos) is kinematically possible. The total decay width above this critical sgluon mass point flattens out to the order of 100 GeV for all of the parameter points.

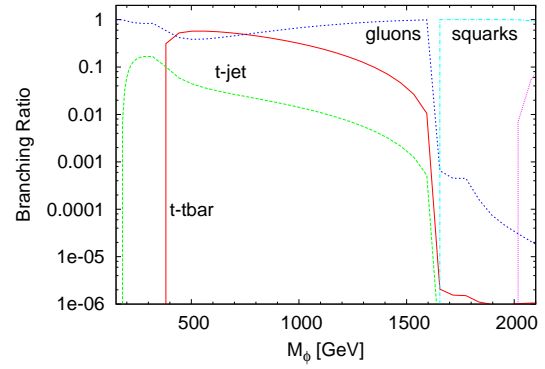
Sgluon decays to gluons and quarks only have significant branching ratios when decays to squarks and gluinos are not possible. In this mass range the decay widths to single top, t-tbar and a pair of gluons sum to give a very narrow total width. We observe from point D that decays to gluons dominate for large gluino mass. This was to be expected, as we saw in the previous section that the relevant squared amplitude is amplified by the gluino mass. On the contrary, we see that quark decays dominate in point B where the squark masses are large. At all six parameter points t-tbar has a more prominent branching ratio than single top (when kinematically accessible). This is not surprising, because the sgluon-t-tbar vertex (5.140), as opposed to the sgluon-single top vertex, does not vanish for degenerate squark masses. To reinforce this point, we see that the single top branching ratio performs the worst relative to t-tbar at point C, where the squark mass splitting is smallest. From point F we see that the change in squark mixing has a minor effect on the branching ratios.

Full cross section and the narrow width approximation

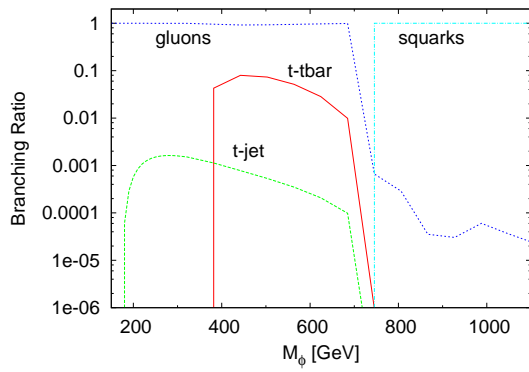
The cross section for gluon fusion giving a top and an up quark via a s-channel sgluon can be constructed by combining the effective one-loop vertices calculated in



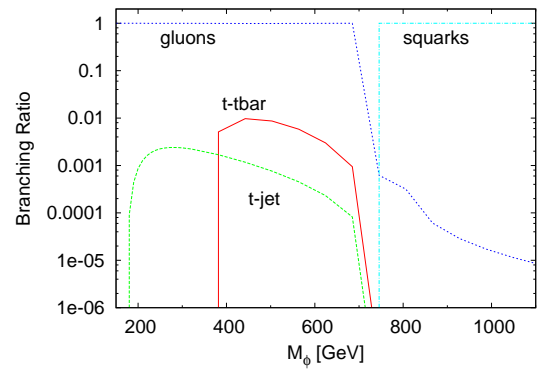
(a) Point A



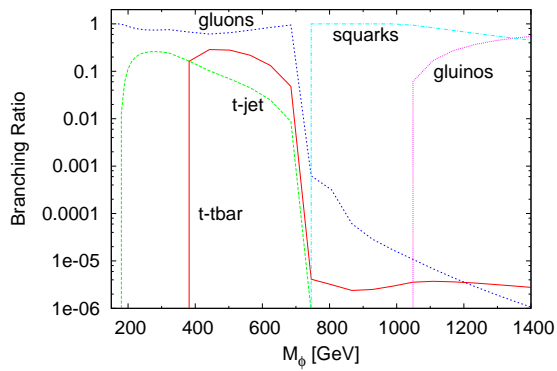
(b) Point B



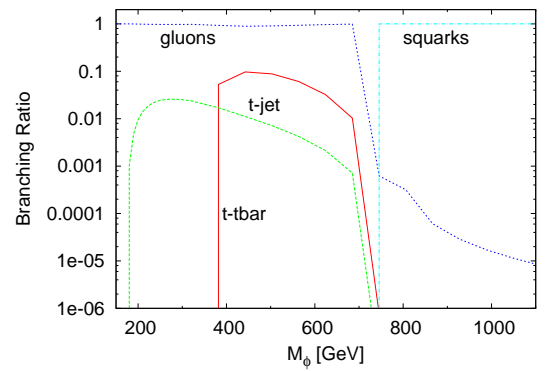
(c) Point C



(d) Point D



(e) Point E



(f) Point F

Figure 7.5: Branching ratios for sgluon decay into $t\bar{t}$, t-jet, gg , $\tilde{q}\tilde{q}$ and $\tilde{g}\tilde{g}$ at the chosen parameter space points.

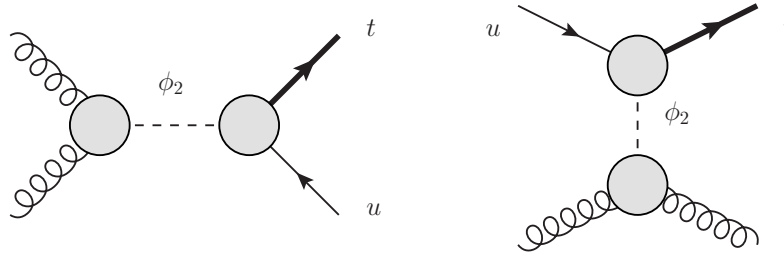


Figure 7.6: Feynman diagrams for MRSSM single top production via a s-channel (left) and t-channel (right) sgluon. The effective vertices contain scalar one loop integrals.

section 5.5.2. The non-averaged squared amplitude² is

$$\begin{aligned} \sum |\mathcal{M}|^2 &= \frac{40\alpha_S^6 m_{\tilde{g}}^4 m_t^2}{3\pi^2 \hat{s} - m_t^2} \frac{1}{(\hat{s} - M_\phi^2)^2 + M_\phi^2 \Gamma_\phi^2} \{ |A_L(\hat{s})|^2 + |A_R(\hat{s})|^2 \} \\ &\times \left| -i(4\pi)^2 \sum_{\tilde{q}, \sigma} (-1)^\sigma m_{\tilde{q}\sigma}^2 C_0(\hat{s}, 0, 0; m_{\tilde{q}\sigma}, m_{\tilde{q}\sigma}, m_{\tilde{q}\sigma}) \right|^2, \end{aligned} \quad (7.6)$$

with

$$A_\sigma(\hat{s}) = \sum_{\tilde{q}a} (U_{\tilde{q}\sigma})_{3a} (U_{\tilde{q}\sigma}^\dagger)_{aj} f_t(s; m_{\tilde{q}a\sigma}). \quad (7.7)$$

The cross channel of this process also produces a single top, with the top instead accompanied by a gluon that we will treat identically to the outgoing up-quark of the s-channel process in so far as classifying it as a (non-b-tagged) jet. The Feynman diagrams for the s and t-channel processes are given in figure 7.6.

We have seen that the total sgluon decay width is very narrow for sgluon masses that kinematically forbid decays to squarks or gluinos. For such narrow widths it is no longer practical to integrate the differential cross section of the s-channel process using our numerical methods as this will not produce a reliable result³. Instead we can make use of the narrow width approximation given in equation (6.44), using the on-shell sgluon production cross section discussed in section 7.2.2 and the branching ratios from section 7.2.2. In an ideal detector such a signal would appear as a single spiked bin in cross section distribution plots.

In figure 7.7 we have plotted the cross section for the s-channel sgluon process with respect to sgluon mass at the LHC (14 TeV). The cross section is seen to be many orders of magnitude smaller in the sgluon mass region where decays to squarks and gluinos are possible. With the most optimistic cross section in this region already one tenth of an atto barn, its prospects of providing a LHC signal are

²For a worked example of how a cross section is computed from a squared amplitude refer to section 4.2

³To see this, consider applying the numerical methods discussed in the previous chapter to a delta function.

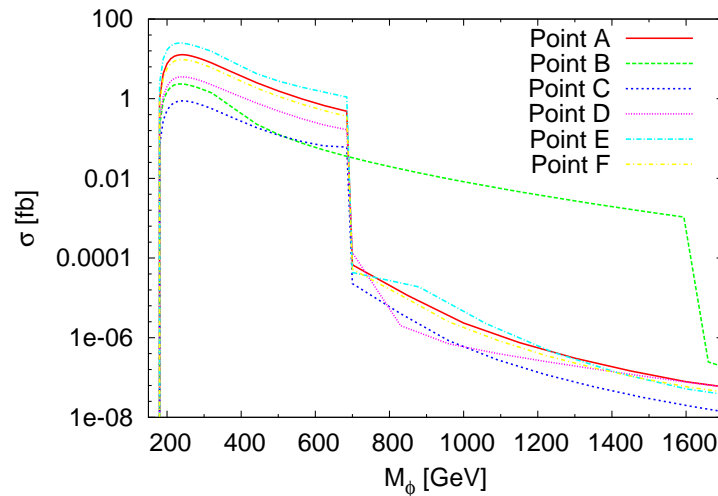


Figure 7.7: Cross section of single top (with non-b-tagged jet) production via s-channel sgluons at the LHC (14 TeV).

ruled out. In the narrow width region, however, the cross section ranges in the tens of femto barns, becoming larger for smaller sgluon masses. A signal in this region could thus be a single spiked bin in a histogram plotting the differential cross section with respect to the invariant mass measured with an ideal detector. This bin would be located at the sgluon mass and have as magnitude the total cross section divided by the bin width.

The cross sections for the t and u-channel sgluon processes behave similarly to the s-channel process in the region of large sgluon decay widths, approaching atto barns at best.

7.2.3 Non-sgluon mediated single top

Due to the large squark mixing present in the MRSSM, single top production is also possible at the one-loop level without a mediating sgluon. These processes serve as both a background to sgluon mediated single top but also as their own signal for MRSSM single top production. In figure 7.8 we have drawn some of these diagrams, which illustrate how the production proceeds through up-squark mixing. Unlike sgluon mediated production that consisted of just one diagram and its cross-channels, non-sgluon mediated production has altogether 60 diagrams when all possible incoming parton combinations are included and the four lightest quarks and the gluon are classified as jets. For an outgoing b-jet there are six possible diagrams if we assume no down squark mixing. To handle all these one-loop processes, we used the FeynArts package [28] to generate the amplitudes from our own custom written MRSSM model file. The amplitudes were then squared using the FormCalc package and linked to our Monte Carlo program, as discussed in section 6.4.

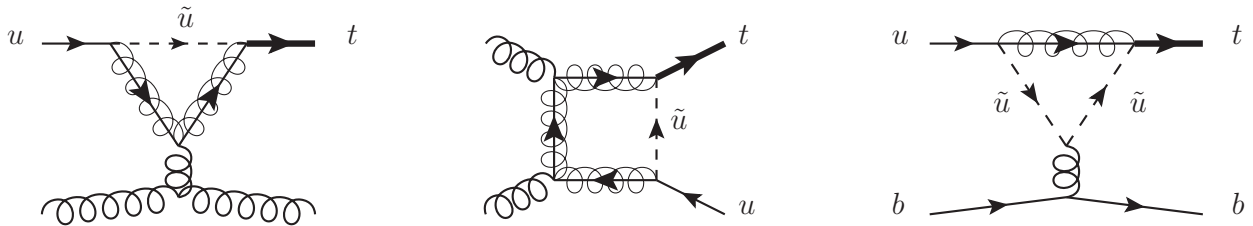


Figure 7.8: Some of the Feynman diagrams that give non-sgluon mediated single top production in the MRSSM.

7.3 Signals at the LHC

As was discussed in the last section, sgluon mediated single top production will only have a viable detection signal in the sgluon mass region where the sgluon has a very narrow width. This signal is a single spiked bin on cross section distribution plots. The question remaining is therefore what background this spiked bin will be relative to. From the Standard Model only the single top processes with accompanying non-b-jets will contribute (i.e. only the t-channel), because sgluon mediated production cannot produce b-jets. The rest of the background comes from non-sgluon mediated MRSSM single top production. This is itself, however, also a signal for beyond the Standard Model physics. In this section we thus proceed by treating non-sgluon mediated single top production as the signal and the Standard Model as the background. Once our analysis for this signal and background are complete, including distribution plots, we will shift our attention back to the sgluon mediated production signal.

	$\sigma_{\text{LO}}(t + \text{jet})$ [pb]	$\sigma_{\text{LO}}(t + \text{b-jet})$ [pb]
Point A	25.8 ± 0.1	0.715 ± 0.003
Point B	16.3 ± 0.07	0.452 ± 0.002
Point C	0.875 ± 0.004	0.0239 ± 0.0001
Point D	7.6 ± 0.03	0.211 ± 0.010
Point E	57.0 ± 0.3	1.582 ± 0.007
Point F	19.06 ± 0.09	0.537 ± 0.002
Standard Model	67.7 ± 0.1	3.215 ± 0.001

Table 7.2: Cross sections for non-sgluon mediated single top production at the LHC (14 TeV) in the MRSSM and Standard Model at leading order. Detector b-tagging efficiencies have not been included.

We consider first the direct production of a single top along with a jet or b-jet in the MRSSM by non-sgluon mediated means (see section 7.2.3). The leading order cross sections for these processes at the LHC (we assume 14 TeV throughout this

chapter) are given in table 7.4 for the four MRSSM parameter points and the Standard Model. We have applied kinematic detector acceptance cuts to the outgoing jet (b-jet) of $p_T(\text{jet}) \geq 20$ GeV and $\eta(\text{jet}) \leq 2.5$. It is seen that the process with no b-jet dominates. In figures 7.9 and 7.10 we have plotted the kinematic distribution plots of the top accompanied by a jet or b-jet respectively. The top is observed to be very forward (high rapidity) in both processes. This forwardness could be due to a t-channel internal gluon, which is present in the diagrams of both processes, as already illustrated in figure 7.8. The single top plus jet cross section is dominated by the one-loop parton process $ug \rightarrow tg$, which contributes 95%.

In section 7.1 we reviewed the decay of the top quark to a b quark and W boson, and the subsequent decay of the W to a pair of leptons or quarks in the Standard Model. The same will happen for MRSSM single top production, and in both cases we simulate this double decay chain using the already mentioned Breit-Wigner factorization method. The MRSSM single top production processes we are considering therefore have the possible outgoing states (7.2) and (7.3). We take for the background the *irreducible* Standard model processes i.e. processes that give exactly the same number of jets and leptons as the signal. The relevant irreducible background is given by Standard Model s and t-channel single top production. The Wt associated channel will contribute either one extra jet or lepton and therefore falls into the *reducible* background category which we do not consider. To simulate the detection thresholds of the LHC detectors (namely ATLAS and CMS), we place the following kinematic *acceptance cuts*:

- $p_T(\text{jet/b-jet}) \geq 20$ GeV and $p_T(\text{lepton}) \geq 10$ GeV.
- $\eta(\text{jet/b-jet/lepton}) \leq 2.5$.

We assume a detector b-tagging efficiency of 50%. This means that for an integrated luminosity L , the number of observed signal and background events for a process with two outgoing b-jets are given by

$$S = (0.5)^2 \times \sigma(2\text{b-jets}) \times L, \quad \text{and} \quad B = (0.5)^2 \times \sigma_{\text{SM}}(2\text{b-jets}) \times L.$$

For events involving one outgoing b-jet, processes that have two outgoing b-jets of which one failed to be tagged will also contribute, so that

$$\begin{aligned} S &= 0.5 \times \sigma(\text{b-jet}) \times L + 2 \times (0.5)^2 \times \sigma(2\text{b-jets}) \times L, \\ B &= 0.5 \times \sigma_{\text{SM}}(\text{b-jet}) \times L + 2 \times (0.5)^2 \times \sigma_{\text{SM}}(2\text{b-jets}) \times L. \end{aligned}$$

Because top and anti-top production can be distinguished by the outgoing positive or negative charged lepton respectively, we ignore the latter process in our analysis.

The kinematic cross section distribution plots of the outgoing states (7.2) and (7.3) are given in figures 7.11 and 7.12 respectively. The Standard Model is seen to be a significant background in both cases. To maximize signal over background we choose the following kinematic cuts:

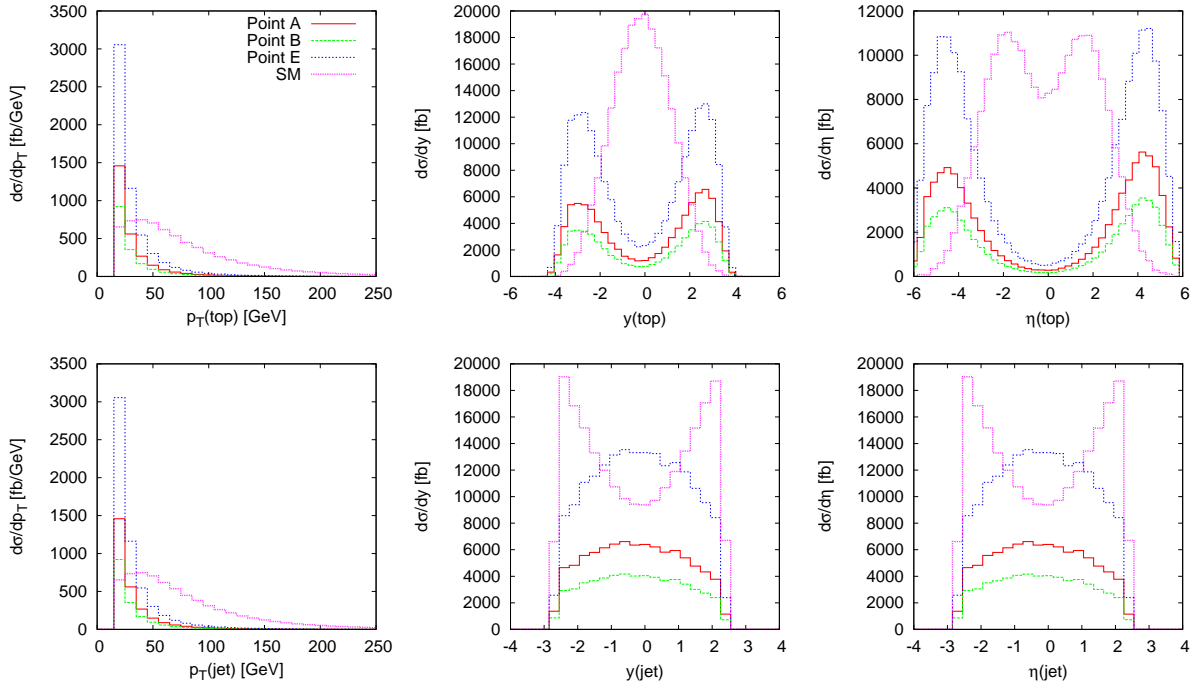


Figure 7.9: Non sgluon-mediated single top production giving $t + \text{jet}$ at the LHC (14 TeV): cross section distributions with respect to the transverse momentum (p_T), rapidity (y) and pseudo-rapidity (η) of the outgoing states for the MRSSM parameter points and in the Standard Model.

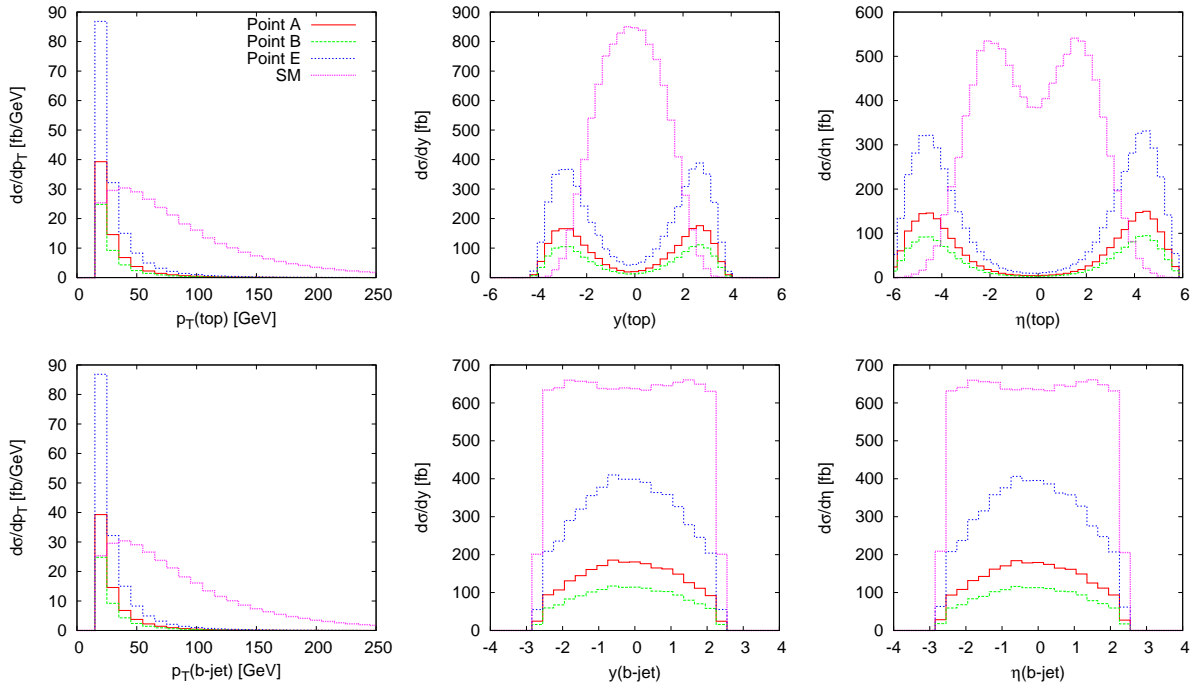


Figure 7.10: Non sgluon-mediated single top production giving $t + \text{b-jet}$ at the LHC (14 TeV): cross section distributions with respect to the transverse momentum (p_T), rapidity (y) and pseudo-rapidity (η) of the outgoing states for the MRSSM parameter points and in the Standard Model.

1. $p_T(\text{jet}/b\text{-jet } 1) \leq 75 \text{ GeV}$.
2. $|\eta(l^+)| \geq 0.5$ and $|\eta(b\text{-jet } 2)| \geq 0.5$.

The cross sections of the non-sgluon mediated single top production signals and background before and after cuts are given in tables 7.3 and 7.4 for the outgoing states (7.2) and (7.3) respectively. The integrated luminosity has been set to 10 fb^{-1} , which the LHC is expected to obtain after approximately a year of operation. For a signal to have a chance of being detected at the LHC it must have at least one tenth the strength of the background: $S/B \gtrsim 0.1$. To claim a discovery, it must be certain the signal is not a Gaussian fluctuation of the background and thus the statistical significance is required to be five or greater: $S/\sqrt{B} \geq 5$.

For the outgoing state with two b -jets, points A, B, E and F have the necessary signal over background ratio to be detectable. Point D requires a softer cut on the first b -jet's transverse momentum to meet this threshold. Only point E has enough statistical significance to be discovered after the kinematic cuts have been placed. All but points C and D could be discovered (with respect to the irreducible background) after an integrated luminosity of 40 fb^{-1} is collected.

The outgoing state with one b -jet gives more favourable results. Points A, B, D, E and F all meet the signal over background threshold. All of these points also have sufficient statistical significance to be discovered. Point C demonstrates that a low squark mass splitting gives a negligible signal. From the dominance of point E it is clear that the single top signal favours both light gluinos and squarks. Recall that this discovery potential is with respect to the irreducible background. In reality the background can be much larger. Realistic detectors can fail to detect a lepton or jet, or miss-associate jets from other scattering processes. It is thus necessary to also take into account the reducible backgrounds: processes that have the same signal plus or minus a number of jets or leptons. For the $2b\text{-jets} + l^+ + \cancel{E}_T$ signal considered here, sizable reducible backgrounds will come from Wt associated single top, $W + \text{jet}$ and $t\bar{t}$ production. This is the next step in the phenomenological analysis of MRSSM single top production at the LHC, which we have yet to carry out at the time of writing. In section 7.4 we check to see if the the data already collected by the Tevatron can be used to rule out points A, B, D, E or F.

The sgluon mediated signal

As we discussed in section 7.2.2, sgluon mediated single top production will only give a non-trivial result when its width is very narrow. In this case it would ideally give a single spiked bin with an amplitude equal to its cross section over the bin's width. In figure 7.13 we have plotted the invariant mass of the outgoing single b -jet signal given in (7.3) for both the MRSSM and SM that together give the effective background. Even under the aforementioned ideal circumstances, it is clear that the cross sections given in figure 7.7 for sgluon mediated single top production in the narrow width approximation will be overwhelmed by this background.

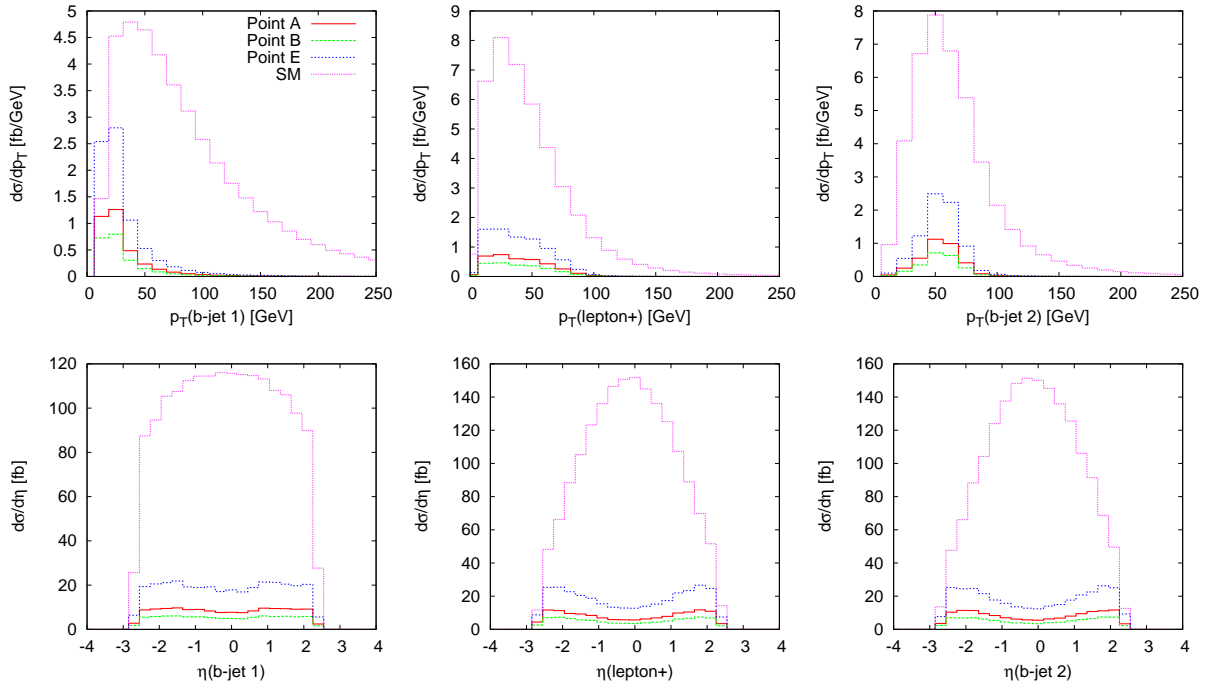


Figure 7.11: Non sgluon-mediated MRSSM single top production giving $2b\text{-jets} + l^+ + \cancel{E}_T$ at the LHC (14 TeV): cross section distributions with respect to the transverse momentum (p_T) and pseudo-rapidity (η) of the experimentally detectable outgoing states for MRSSM parameter points 1 and 2 and in the Standard Model.

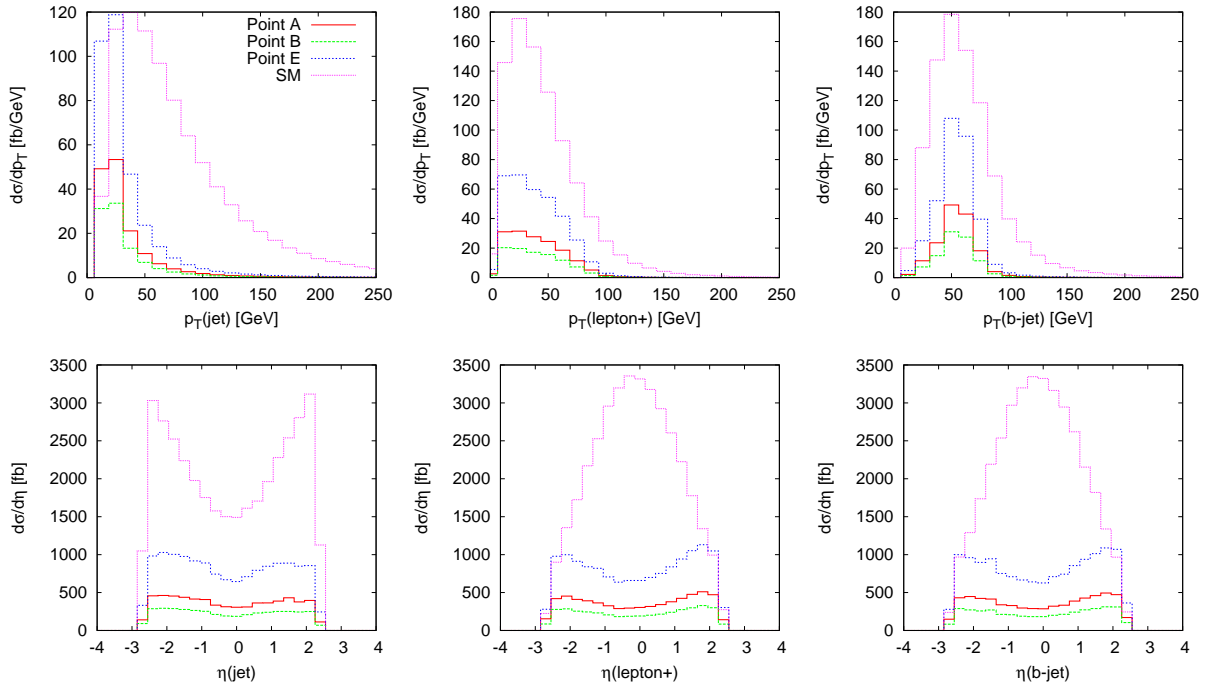


Figure 7.12: Non sgluon-mediated single top production giving $b\text{-jet} + \text{jet} + l^+ + \cancel{E}_T$ at the LHC (14 TeV): cross section distributions with respect to the transverse momentum (p_T) and pseudo-rapidity (η) of the experimentally detectable outgoing states for MRSSM parameter points 1 and 2 and in the Standard Model.

		No Cuts [†]	Cut 1	Cuts 1 & 2
Standard Model*	σ [fb]	529.8 ± 1.4	245.0	131.0
Point A	σ [fb]	44.0 ± 0.5	40.6	31.2
	S/B	0.08	0.17	0.24
	S/\sqrt{B}	3.0	4.1	4.3
Point B	σ [fb]	27.8 ± 0.3	25.8	19.8
	S/B	0.05	0.11	0.15
	S/\sqrt{B}	1.9	2.6	2.7
Point C	σ [fb]	1.47 ± 0.02	1.37	1.05
	S/B	0.00	0.01	0.01
	S/\sqrt{B}	0.1	0.1	0.2
Point D	σ [fb]	13.0 ± 0.2	12.0	9.2
	S/B	0.02	0.05	0.07
	S/\sqrt{B}	0.9	1.2	1.3
Point E	σ [fb]	97.7 ± 1.2	90.3	69.3
	S/B	0.18	0.27	0.53
	S/\sqrt{B}	6.7	9.1	9.6
Point F	σ [fb]	33.0 ± 0.4	30.5	23.4
	S/B	0.06	0.12	0.18
	S/\sqrt{B}	2.3	3.1	3.2

*The background. Only single top processes are included.

†Kinematic acceptance cuts for the detector have been included.

Table 7.3: Non sgluon-mediated MRSSM single top production giving $2b$ -jets+ l^+ + \cancel{E}_T at the LHC (14 TeV): the cross section, signal to background ratio (S/B) and statistical significance (S/\sqrt{B}) for the MRSSM parameter points for various cuts on the kinematic variables. The integrated luminosity is taken to be 10 fb^{-1} .

7.4 Signal exclusions from the Tevatron run

In the previous section we found several parameter points of the MRSSM to have strong signals over background for non-sgluon mediated single top production at the LHC. We thus proceed to check if these signals are strong enough to be detectable at the already operational Tevatron proton-anti-proton collider. Single top quark production has recently been discovered by both the D0 and CDF detectors with a statistical significance of 5.0σ . For the signal of $l + \cancel{E}_T + 2\text{jets}$ including all background channels, with single and double b -jet production combined, the CDF collaboration observed a total of 3315 events with an integrated luminosity of 3.2 fb^{-1} [34]. Similarly, the D0 collaboration observed a total of 2579 events with an integrated luminosity of 2.3 fb^{-1} [35]. The Standard Model predictions given by the CDF and D0 collaborations for these observations are 2615 ± 192 and 3377 ± 505 events respectively. We use these numbers as the background to the MRSSM Teva-

		No Cuts [†]	Cut 1	Cuts 1 & 2
Standard Model*	σ [fb]	11106 ± 29	5963	3085
Point A	σ [fb]	1922 ± 18	1760	1300
	S/B	0.17	0.29	0.41
	S/\sqrt{B}	41.1	51.1	52.4
Point B	σ [fb]	1221 ± 12	1110	820
	S/B	0.11	0.18	0.26
	S/\sqrt{B}	26.0	32.3	33.1
Point C	σ [fb]	64.6 ± 0.6	58.9	43.4
	S/B	0.01	0.01	0.01
	S/\sqrt{B}	1.4	1.7	1.8
Point D	σ [fb]	569 ± 6	520	384
	S/B	0.05	0.09	0.12
	S/\sqrt{B}	12.1	15.1	15.5
Point E	σ [fb]	4264 ± 42	3875	2855
	S/B	0.38	0.64	0.91
	S/\sqrt{B}	90.7	112.5	115.3
Point F	σ [fb]	1442 ± 14	1319	972
	S/B	0.13	0.22	0.31
	S/\sqrt{B}	30.8	38.3	39.3

*The background. Only single top processes are included.

†Kinematic acceptance cuts for the detector have been included.

Table 7.4: Non sgluon-mediated MRSSM single top production giving b -jet + jet + l^+ + E_T at the LHC (14 TeV): the cross section, signal to background ratio (S/B) and statistical significance (S/\sqrt{B}) for the MRSSM parameter points for various cuts on the kinematic variables. The integrated luminosity is taken to be 10 fb^{-1} .

tron signals. Our simulations for the Tevatron are run identically to those of the LHC, modifying only the PDFs to match proton-anti-proton collisions and the incoming centre of momentum energy to 2 TeV. No changes are made to the kinematic acceptance cuts. The expected number of events, signal to background ratio and statistical significance of MRSSM single top production at the parameter points of interest are given in table 7.5. We conclude that none of the MRSSM parameter points have a discovery potential at the Tevatron.

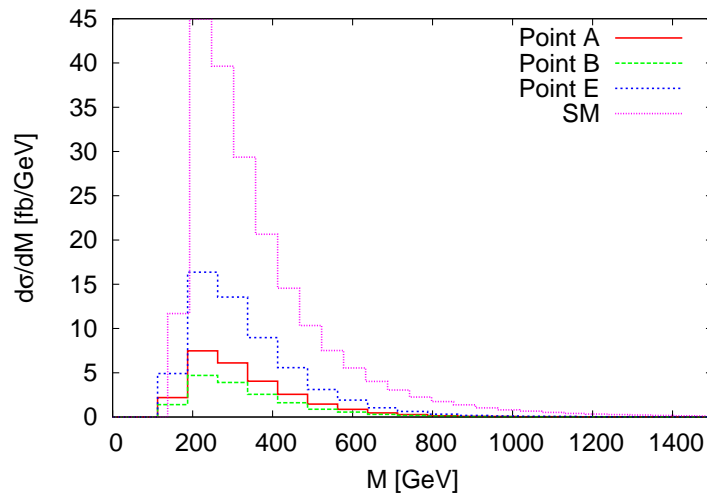


Figure 7.13: Cross section distribution with respect to the invariant mass for MRSSM and SM single top production giving b -jet + jet + l^+ + E_T at the LHC (14 TeV).

		CDF (3.2 fb ⁻¹)	D0 (2.3 fb ⁻¹)
Tevatron data		3315	2579
Standard Model [†]	B	3377 ± 505	2615 ± 192
Point A	S	58.1	41.8
	S/B	0.02	0.02
	S/√B	1.0	0.8
Point B	S	36.6	26.3
	S/B	0.01	0.01
	S/√B	0.6	0.5
Point D	S	17.1	12.3
	S/B	0.01	0.00
	S/√B	0.3	0.2
Point E	S	129.6	92.1
	S/B	0.04	0.04
	S/√B	2.2	1.8
Point F	S	43.5	31.3
	S/B	0.01	0.01
	S/√B	0.8	0.6

[†]Includes all background channels, not only single top.

Table 7.5: MRSSM non sgluon-mediated single top production giving the signal $l + E_T + 2$ jets at the Tevatron (2 TeV): the number of expected events, signal to background ratio (S/B) and statistical significance (S/√B) for the MRSSM parameter points with only acceptance cuts.

Chapter 8

Conclusion

The original aim of this thesis was to find and simulate supersymmetric processes that have a significant single top production background. We focused on single top production in particular, because it has been extensively studied at both the LHC and Tevatron and is thus well understood as both a signal and a background. In chapter 4 we considered strong supersymmetric processes in the MSSM and found that SUSY signals in this model typically have long cascade decay chains involving many jets and leptons and large missing transverse energy. Single top processes on the contrary have characteristically few jets and leptons and low missing energy. We thus concluded that the MSSM offers no satisfactory signals with a dominant single top background. With the MSSM ruled out, we shifted our focus to SUSY models that could give a single top signal. This brought to our attention the recently formulated MRSSM, a minimal SUSY model that employs a continuous R symmetry to avoid rapid proton decay. The MRSSM allows single top production both via a mediating sgluon at the two loop level and through squark flavour mixing at the one loop level. Both the existence of the sgluon, a colour scalar octet, and the presence of squark flavour mixing that is not phenomenologically suppressed are characteristic features of the MRSSM QCD sector.

The Feynman rules and sgluon decays for the MRSSM were derived in chapter 5. These rules were used in combination with the custom written Monte Carlo program described in chapter 6 to study the phenomenology of the MRSSM at the LHC. We set six benchmark points in the MRSSM parameter space. These were chosen specifically to reflect the dependence of single top production on the gluino mass, squark mass splitting and the squark flavour mixing.

Sgluons were found to have very narrow widths in the lower sgluon mass regions where decays to squarks or gluinos are not kinematically possible. In this mass region the narrow width approximation for sgluon mediated single top production gives cross section predictions of the order of tens of femto barns. Outside this mass range, where the sgluon picks up a sizable decay width, the production of single top is very suppressed and negligible as a detectable signal. Assuming an ideal detector, the narrow width signal could give a single peaked bin on invariant mass

distribution plots. Even under such ideal circumstances, however, the Standard Model and MRSSM backgrounds dwarf this signal. We thus conclude that sgluon detection via the process of single top production is unlikely.

Non-sgluon mediated single top production in the MRSSM proceeds via squark flavour mixing at the one loop level. The results for these processes giving the LHC signal of $l + \cancel{E}_T + 2\text{jets}$ at the six parameter points considered were promising with respect to the irreducible Standard Model background. For the outgoing state with one b-jet, five of the points have the necessary signal to background ratio and statistical significance for discovery after 10 fb^{-1} . For the LHC signal with two b-tagged jets, one parameter point is discoverable at this luminosity. It is important to note that the irreducible background consists of only the Standard Model single top processes. The significant reducible backgrounds, such as Wt , $W + \text{jet}$ and $t\bar{t}$, have not yet been included. In terms of the MRSSM parameter space, single top production favours lighter squarks and gluinos, a large squark mass splitting and maximal squark flavour mixing. A small squark mass splitting of 100 GeV as opposed to 600 GeV is enough to kill the signal completely. Also, raising the gluino mass up to 2000 GeV with all other parameters kept optimal will push the signal to background ratio below the detectable limit. Signals of non-sgluon mediated single top production were also considered at the already operational Tevatron using as background the data and predictions from the CDF and D0 collaborations for the full $l + \cancel{E}_T + 2\text{jets}$ signal. The MRSSM signals were found to be absent with respect to this background.

Although the parameter point with the lightest squarks and gluinos (both ~ 500 GeV) has the strongest LHC signal, it is possible that the gluino is not heavy enough to sufficiently suppress the supersymmetric contribution to meson mixing. A further study should include an analysis of which MRSSM points are compatible with this suppression, as well as including reducible backgrounds and hadronization effects for the $l + \cancel{E}_T + 2\text{jets}$ signal at the LHC.

Appendix A

Notation and Conventions

We use natural units, where

$$\hbar = 1 = c. \quad (\text{A.1})$$

The Minkowski metric is $\eta_{\mu\nu} = \text{diag}(1, -1, -1, -1)$, giving the four momentum relation

$$p^2 = E^2 - |\mathbf{p}|^2 = m^2. \quad (\text{A.2})$$

Spinors

Four component Dirac spinor notation is used. Gamma matrices are chosen in the chiral representation

$$\gamma^0 = \begin{pmatrix} 0 & 1 \\ 1 & 0 \end{pmatrix}, \quad \gamma^i = \begin{pmatrix} 0 & \sigma^i \\ -\sigma^i & 0 \end{pmatrix}, \quad \gamma^5 = \begin{pmatrix} -1 & 0 \\ 0 & 1 \end{pmatrix}, \quad (\text{A.3})$$

$$\{\gamma^\mu, \gamma^\nu\} = 2\eta^{\mu\nu} \quad , \quad \sigma^{\mu\nu} \equiv \frac{i}{2}[\gamma^\mu, \gamma^\nu], \quad (\text{A.4})$$

$$\{\gamma_5, \gamma^\mu\} = 0 \quad , \quad (\gamma^\mu)^\dagger = \gamma^0 \gamma^\mu \gamma^0. \quad (\text{A.5})$$

Left and right chiral projectors are defined as

$$P_\sigma \equiv \begin{cases} P_L = \frac{1-\gamma_5}{2} & : \quad \sigma = L, \\ P_R = \frac{1+\gamma_5}{2} & : \quad \sigma = R. \end{cases} \quad (\text{A.6})$$

To compactify the notation, we further define

$$\bar{\sigma} = \sigma(L \leftrightarrow R) \quad (\text{A.7})$$

and

$$(-1)^\sigma \equiv \begin{cases} 1 & : \quad \sigma = L, \\ -1 & : \quad \sigma = R. \end{cases} \quad (\text{A.8})$$

The generic lagrangian term for a massive fermion is written as

$$\mathcal{L} = \bar{\psi}(i\not{\partial} - m)\psi, \quad (\text{A.9})$$

where the conjugate spinor is defined as

$$\bar{\psi} = \psi^\dagger \gamma^0. \quad (\text{A.10})$$

Plane-wave solutions to the Dirac equation of motion are

$$\psi = u(p)e^{-ip \cdot x} \quad , \quad \bar{\psi} = v(p)e^{ip \cdot x}, \quad (\text{A.11})$$

for $p^0 > 0$, with the momentum space spinors satisfying

$$(\not{p} - m)u(p) = 0 \quad , \quad (\not{p} + m)v(p) = 0, \quad (\text{A.12})$$

$$\sum_s u(p)_s^a \bar{u}(p)_s^b = (\not{p} + m)^{ab} \quad , \quad \sum_s v(p)_s^a \bar{v}(p)_s^b = (\not{p} - m)^{ab}. \quad (\text{A.13})$$

Charge conjugation is defined as transforming annihilation operators to creation operators e.g. $a_{\mathbf{k}} \rightarrow a_{\mathbf{k}}^c = b_{\mathbf{k}}$ and $b_{\mathbf{k}} \rightarrow b_{\mathbf{k}}^c = a_{\mathbf{k}}$ for a canonically quantized spinor field

$$\psi(x) = \sum_s \int \frac{d^3k}{(2\pi)^3} \frac{1}{2E_{\mathbf{k}}} (a_{\mathbf{k},s} u(k)_s e^{-ik \cdot x} + b_{\mathbf{k},s}^\dagger v(k)_s e^{ik \cdot x}). \quad (\text{A.14})$$

Using the spinor relations $u(p) = -i\gamma^2 v(p)^*$ and $v(p) = -i\gamma^2 u(p)^*$, charge conjugation acts on a Dirac fermion as

$$\psi \rightarrow \psi^c = C\bar{\psi}^T \quad \text{for} \quad C = -i\gamma^2 \gamma^0, \quad (\text{A.15})$$

where we can also rewrite the spinor relations as

$$u = C\bar{v}^T \quad \text{and} \quad v = C\bar{u}^T. \quad (\text{A.16})$$

The charge conjugation matrix C satisfies

$$C^{-1} = C^\dagger \quad , \quad C^T = -C \quad , \quad C\gamma_\mu^T C^{-1} = -\gamma_\mu, \quad (\text{A.17})$$

and

$$[C, \gamma_5] = 0. \quad (\text{A.18})$$

In the chiral representation chosen above C is real, so that $C^{-1} = C^T = -C$.

A Majorana fermion is a Dirac fermion that satisfies $\psi = \psi^c$. In the chiral representation this implies that the right chiral component of the Majorana fermion is completely determined by the left chiral component

$$\psi_R = P_R \psi^c = \frac{1 + \gamma_5}{2} C\bar{\psi}^T = C\gamma^0 \psi_L^*. \quad (\text{A.19})$$

When fields are expanded in terms of superspace coordinates, an L or R subscript label can imply that it is Majorana (whether it is or not should be clear from the context).

Feynman rules

Where applicable, the progression of ingoing to outgoing states in Feynman diagrams is from left to right. Majorana Feynman rules are written with an additional arrow denoting *fermion flow*, as discussed in section 4.5. Arrows placed on particle lines denote charge flow. Gauge boson propagators are written in the Feynman gauge. The functions B_0 and C_0 are scalar one loop integrals with normalization $1/(2\pi)^4$ (see section 5.7).

Lie group generators

Generators t_A of non-abelian Lie groups are defined to be hermitian, so that they obey the Lie algebra relation

$$[t_A, t_B] = if_{ABC}t_C. \quad (\text{A.20})$$

For $SU(2)$, the generators in the fundamental representation are defined as $t_i^F = \sigma_i/2$, where σ_i are the Pauli matrices for $i = 1, 2, 3$. For $SU(3)$ the generators in the fundamental representation are defined as $t_A^F = \lambda_A/2$, where λ_A are the Gell-Mann matrices for $A = 1, \dots, 8$.

Cross sections

Partonic cross sections and mandelstam variables are denoted with a hat. A bar on a summed squared amplitude,

$$\overline{\sum |\mathcal{M}|^2}, \quad (\text{A.21})$$

denotes an average over the ingoing degrees of freedom e.g spin, polarization, colour etc. Two commonly appearing kinematic functions are:

$$\lambda(x, y, z) = x^2 + y^2 + z^2 - 2xy - 2xz - 2yz. \quad (\text{A.22})$$

and

$$\beta_X = \sqrt{1 - \frac{4m_X}{s}}, \quad (\text{A.23})$$

where m_X is the mass of particle X .

Supersymmetry

Fields carrying hats, e.g $\hat{\Phi}(x, \theta)$, denote superfields spanning superspace. The coordinate \hat{x} is a superspace coordinate defined by

$$\hat{x}_\mu \equiv x_\mu + \frac{i}{2}\bar{\theta}\gamma_5\gamma_\mu\theta. \quad (\text{A.24})$$

The superpotential is denoted by \hat{f} rather than \hat{W} . The latter is reserved for the chiral spinor gauge superfields.

Appendix B

Two Loop Calculation of α_S

We will employ dimensional regularization in the minimal subtraction scheme $\overline{\text{MS}}$, so that the number of dimensions is given by $d = 4 - 2\epsilon$. The bare strong interaction coupling $g_{S,0}$, as it appears in the QCD covariant derivative

$$D_\mu = \partial_\mu + ig_{S,0} t_A G_{A\mu}, \quad (\text{B.1})$$

is renormalized as

$$g_{S,0} = \mu^{-\epsilon/2} Z_g\left(\frac{1}{\epsilon}, g_{S,R}\right) g_{S,R}(\mu). \quad (\text{B.2})$$

Here μ is an arbitrary mass scale introduced to keep the renormalized coupling $g_{S,R}(\mu)$ dimensionless and all of the infinities are contained in the function

$$Z_g\left(\frac{1}{\epsilon}, g_{S,R}\right) = 1 + \frac{1}{\epsilon} g_{S,R}^2(\mu) \frac{\beta_0}{(4\pi)^2} + \dots \quad (\text{B.3})$$

with β_0 corresponding to corrections at the one loop level (see for example [36] for details). We rewrite the coupling $g_{S,R}$ as $\alpha_S = g_{S,R}^2/4\pi$ and define the beta function equation for the α_S coupling (at $\epsilon = 0$) to two loop order as

$$\mu \frac{d}{d\mu} \alpha_S(\mu) = \beta(\alpha_S(\mu)) = -\frac{\beta_0}{2\pi} \alpha_S(\mu)^2 - \frac{\beta_1}{8\pi^2} \alpha_S(\mu)^3 - \dots, \quad (\text{B.4})$$

where the beta constants are given explicitly as

$$\beta_0 = \frac{11}{3} C_2(A) - \frac{4}{3} T(F) n_f, \quad (\text{B.5})$$

$$\beta_1 = \frac{34}{3} C_2(A)^2 - \left(\frac{20}{3} C_2(A) - 4 C_2(F) \right) T(F) n_f. \quad (\text{B.6})$$

For the QCD gauge group $\text{SU}(3)$ with normalization $T(F) = 1/2$, the relevant Casimirs take the values $C_2(A) = 3$ and $C_2(F) = 4/3$ so that for n_f light quark flavours the beta constants are given by

$$\beta_0 = 11 - \frac{2}{3} n_f \quad \text{and} \quad \beta_1 = 102 - \frac{38}{3} n_f. \quad (\text{B.7})$$

Integrating the two loop beta function equation for the renormalized coupling

$$-\frac{1}{D} \int_{\alpha_s(\mu_0)}^{\alpha_s(\mu)} \frac{d\alpha}{\alpha^2 + C\alpha^3} = \int_{\mu_0}^{\mu} \frac{d\mu}{\mu} = \ln \frac{\mu}{\mu_0}, \quad (\text{B.8})$$

where we have let $C = \beta_1/(4\pi\beta_0)$ and $D = \beta_0/2\pi$, gives (by partial fractions):

$$\left[\frac{1}{\alpha} - C \ln \left(\frac{1}{C\alpha} + 1 \right) \right]_{\alpha_s(\mu_0)}^{\alpha_s(\mu)} = D \ln \frac{\mu}{\mu_0}. \quad (\text{B.9})$$

Because the fixed coupling $\alpha_s(\mu_0)$ depends on an arbitrary renormalization point μ_0 , a mass scale Λ may be defined by the condition

$$\ln \left(\frac{\mu_0}{\Lambda} \right) = \frac{1}{D} \left[\frac{1}{\alpha_s(\mu_0)} - C \ln \left(\frac{1}{C\alpha_s(\mu_0)} + 1 \right) \right], \quad (\text{B.10})$$

to completely remove the dependence on both parameters. We note that as $\mu_0 \rightarrow \Lambda$ the fixed coupling $\alpha_s(\mu_0) \rightarrow \infty$ such that Λ gives the position of the Landau pole. We then have

$$\frac{1}{\alpha_s(\mu)} = D \ln \left(\frac{\mu}{\Lambda} \right) + C \ln \left(\frac{1}{C\alpha_s(\mu)} + 1 \right). \quad (\text{B.11})$$

Letting $\alpha_s(\mu)$ be small, such that $\alpha_s(\mu)C \ll 1$, we may write

$$\frac{1}{\alpha_s(\mu)} = D \ln \left(\frac{\mu}{\Lambda} \right) + C \ln \left(\frac{1}{C\alpha_s(\mu)} \right) \quad (\text{B.12})$$

where by recursion

$$= D \ln \left(\frac{\mu}{\Lambda} \right) + C \ln \left(\frac{D}{C} \ln \left(\frac{\mu}{\Lambda} \right) + \dots \right). \quad (\text{B.13})$$

Solving for $\alpha_s(\mu)$ gives

$$\alpha_s(\mu) = \frac{1}{D \ln \left(\frac{\mu}{\Lambda} \right)} \left[\frac{1}{1 + \frac{C}{D} \ln \left(\frac{D}{C} \ln \left(\frac{\mu}{\Lambda} \right) \right) / \ln \left(\frac{\mu}{\Lambda} \right)} \right], \quad (\text{B.14})$$

where by the Taylor series expansion $1/(1+x) = 1 - x + O(x^2)$ (for small x) we find

$$\alpha_s(\mu) = \frac{1}{D \ln \left(\frac{\mu}{\Lambda} \right)} \left[1 - \frac{C \ln \left(\frac{D}{C} \ln \left(\frac{\mu}{\Lambda} \right) \right)}{D \ln \left(\frac{\mu}{\Lambda} \right)} + O \left(\ln \left(\frac{\mu}{\Lambda} \right)^{-2} \right) \right] \quad (\text{B.15})$$

$$= \frac{4\pi}{\beta_0 \ln(\mu^2/\Lambda^2)} - \frac{4\pi\beta_1}{\beta_0^3} \frac{1}{\ln(\mu^2/\Lambda^2)^2} \left[\ln \ln(\mu^2/\Lambda^2) + \ln \left(\frac{\beta_0^2}{\beta_1} \right) \right] + O \left(\ln \left(\frac{\mu}{\Lambda} \right)^{-3} \right), \quad (\text{B.16})$$

giving the final expression

$$\alpha_s(\mu) = \frac{4\pi}{\beta_0} \left[\frac{1}{\ln(\mu^2/\Lambda^2)} - \frac{\beta_1}{\beta_0^2} \cdot \frac{\ln \ln(\mu^2/\Lambda^2)}{\ln(\mu^2/\Lambda^2)^2} \right] + O\left(\ln(\mu^2/\Lambda^2)^{-2}\right). \quad (\text{B.17})$$

Note that instead of choosing the mass scale Λ to be located at the Landau pole, we could also have defined it as

$$\ln(\Lambda') = \ln(\Lambda) - \frac{C}{D} \ln\left(\frac{C}{D}\right), \quad (\text{B.18})$$

to give a convenient cancellation of the order $O\left(\ln(\mu^2/\Lambda^2)^{-2}\right)$ terms[36].

Bibliography

- [1] H. Baer and X. Tata, Weak Scale Supersymmetry: From Superfields to Scattering Events. Cambridge University Press, Cambridge, 2006.
- [2] S. P. Martin, “A Supersymmetry Primer,” arXiv:hep-ph/9709356.
- [3] G. D. Kribs, E. Poppitz, and N. Weiner, “Flavor in supersymmetry with an extended R-symmetry,” Phys. Rev. D **78** (2008) 055010, arXiv:0712.2039 [hep-ph].
- [4] E. Laenen, “Top quark in theory,” arXiv:0809.3158 [hep-ph].
- [5] L. Ryder, Quantum Field Theory, 2nd Ed. Cambridge University Press, 1985.
- [6] S. R. Coleman and J. Mandula, “All possible symmetries of the S matrix,” Phys. Rev. **159** (1967) 1251–1256.
- [7] R. Haag, J. T. Lopuszanski, and M. Sohnius, “All possible generators of supersymmetries of the s-matrix,” Nuclear Physics B **88** (1975) no. 2, 257 – 274. <http://www.sciencedirect.com/science/article/B6TVC-4718W97-YF/2/5b929365c64c0c0b36bf5a37c91c17f0>.
- [8] J. Wess and J. Bagger, Supersymmetry and Supergravity. Princeton University Press, New Jersey, USA, 1992.
- [9] H. E. Haber and G. L. Kane, “The search for supersymmetry: Probing physics beyond the standard model,” Physics Reports **117** (1985) no. 2-4, 75 – 263. <http://www.sciencedirect.com/science/article/B6TVP-46SWYSG-3V/2/50bf78d167cac42f6109d17f2d4ae8ef>.
- [10] A. Denner, H. Eck, O. Hahn, and J. Kblbeck, “Compact feynman rules for majorana fermions,” Physics Letters B **291** (1992) no. 3, 278 – 280. <http://www.sciencedirect.com/science/article/B6TVN-470FYDM-F/2/c7f0db24961ebef69034c5ad97a9bed6>.
- [11] L. J. Hall and L. Randall, “U(1)-R symmetric supersymmetry,” Nucl. Phys. **B352** (1991) 289–308.

- [12] G. D. Kribs, A. Martin, and T. S. Roy, “Squark Flavor Violation at the LHC,” JHEP **06** (2009) 042, arXiv:0901.4105 [hep-ph].
- [13] M. Ciuchini et al., “Delta M(K) and epsilon(K) in SUSY at the next-to-leading order,” JHEP **10** (1998) 008, arXiv:hep-ph/9808328.
- [14] P. J. Fox, A. E. Nelson, and N. Weiner, “Dirac gaugino masses and supersoft supersymmetry breaking,” JHEP **08** (2002) 035, arXiv:hep-ph/0206096.
- [15] G. Passarino and M. J. G. Veltman, “One Loop Corrections for e+ e- Annihilation Into mu+ mu- in the Weinberg Model,” Nucl. Phys. **B160** (1979) 151.
- [16] A. Denner, “Techniques for calculation of electroweak radiative corrections at the one loop level and results for W physics at LEP-200,” Fortschr. Phys. **41** (1993) 307–420, arXiv:0709.1075 [hep-ph].
- [17] T. Hahn and M. Perez-Victoria, “Automatized one-loop calculations in four and D dimensions,” Comput. Phys. Commun. **118** (1999) 153–165, arXiv:hep-ph/9807565.
- [18] T. Plehn and T. M. P. Tait, “Seeking Sgluons,” J. Phys. **G36** (2009) 075001, arXiv:0810.3919 [hep-ph].
- [19] S. Y. Choi et al., “Color-Octet Scalars of N=2 Supersymmetry at the LHC,” Phys. Lett. **B672** (2009) 246–252, arXiv:0812.3586 [hep-ph].
- [20] M. E. Peskin and D. V. Schroeder, An introduction to Quantum Field Theory. Westview Press, 1995.
- [21] G. 't Hooft and M. Veltman, “Scalar one-loop integrals,” Nuclear Physics B **153** (1979) 365–401.
- [22] B. D. Wit and J. Smith, Field Theory in Particle Physics. North Holland, 1986.
- [23] S. Weinzierl, “Introduction to Monte Carlo methods,” arXiv:hep-ph/0006269.
- [24] G. P. Lepage, “A New Algorithm for Adaptive Multidimensional Integration,” J. Comput. Phys. **27** (1978) 192.
- [25] G. P. Lepage, “VEGAS: an adaptive multidimensional integration program,” CLNS-80/447.
- [26] E. Lascaris, “Extensions of the Standard Model and their influence on single-top,” Master’s thesis (2006) .
- [27] T. Hahn, “FormCalc 6,” arXiv:0901.1528 [hep-ph].

- [28] T. Hahn, “Generating Feynman diagrams and amplitudes with FeynArts 3,” *Comput. Phys. Commun.* **140** (2001) 418–431, [arXiv:hep-ph/0012260](https://arxiv.org/abs/hep-ph/0012260).
- [29] J. A. M. Vermaseren, “The FORM project,” *Nucl. Phys. Proc. Suppl.* **183** (2008) 19–24, [arXiv:0806.4080](https://arxiv.org/abs/0806.4080) [hep-ph].
- [30] F. Maltoni and T. Stelzer, “MadEvent: Automatic event generation with MadGraph,” *JHEP* **02** (2003) 027, [arXiv:hep-ph/0208156](https://arxiv.org/abs/hep-ph/0208156).
- [31] J. Alwall, P. Demin, S. de Visscher, R. Frederix, M. Herquet, F. Maltoni, T. Plehn, D. L. Rainwater, and T. Stelzer, “Madgraph/madevent v4: The new web generation,” *JHEP0709* **028** (2007) .
<http://www.citebase.org/abstract?id=oai:arXiv.org:0706.2334>.
- [32] N. Ghodbane and H.-U. Martyn, “Compilation of SUSY particle spectra from Snowmass 2001 benchmark models,” [arXiv:hep-ph/0201233](https://arxiv.org/abs/hep-ph/0201233).
- [33] H. M. Georgi, S. L. Glashow, M. E. Machacek, and D. V. Nanopoulos, “Higgs bosons from two-gluon annihilation in proton-proton collisions,” *Phys. Rev. Lett.* **40** (Mar, 1978) 692–694.
- [34] CDF Collaboration, T. Aaltonen *et al.*, “First Observation of Electroweak Single Top Quark Production,” *Phys. Rev. Lett.* **103** (2009) 092002, [arXiv:0903.0885](https://arxiv.org/abs/0903.0885) [hep-ex].
- [35] D0 Collaboration, V. M. Abazov *et al.*, “Observation of Single Top-Quark Production,” *Phys. Rev. Lett.* **103** (2009) 092001, [arXiv:0903.0850](https://arxiv.org/abs/0903.0850) [hep-ex].
- [36] G. Sterman, *An introduction to Quantum Field Theory*. Cambridge University Press, 1993.